

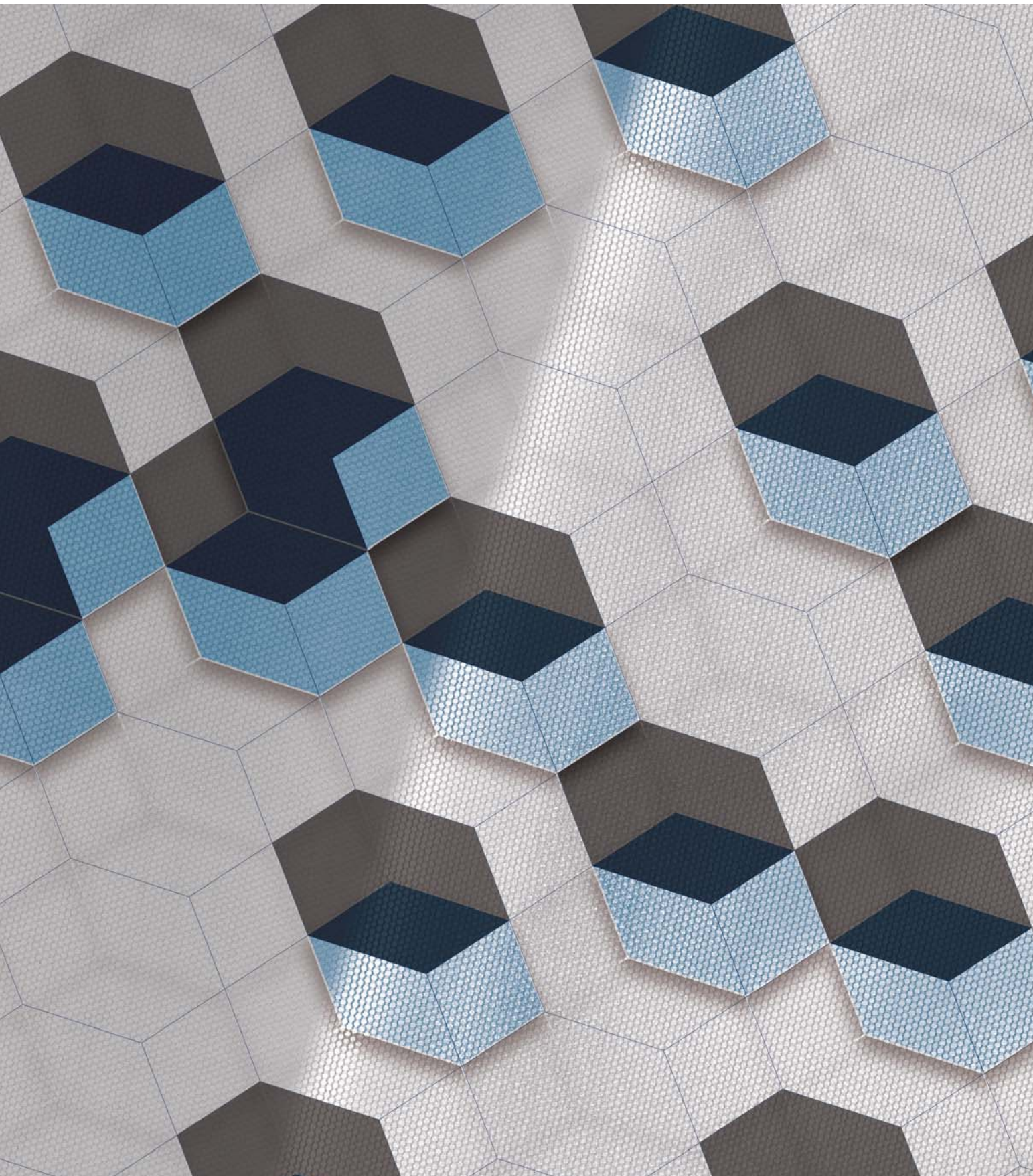
# tekstilec

1/2020 • vol. 63 • 1–76

ISSN 0351-3386 (tiskano/printed)

ISSN 2350 - 3696 (elektronsko/online)

UDK 677 + 687 (05)





<http://www.tekstilec.si>

Časopisni svet/*Publishing Council*  
**Barbara Simončič**, predsednica/*President*  
**Katja Burger**, Univerza v Ljubljani  
**Silvo Hribernik**, Univerza v Mariboru  
**Tatjana Kreže**, Univerza v Mariboru  
**Gasper Lesjak**, Predilnica Litija, d. o. o.  
**Nataša Peršuh**, Univerza v Ljubljani  
**Petra Prebil Bašin**, Gospodarska zbornica Slovenije  
**Melita Rebič**, Odeja, d. o. o.  
**Tatjana Rijavec**, Univerza v Ljubljani  
**Daniela Zavec Pavlinič**, ZITTS  
**Helena Zidarič Kožar**, Inplet pletiva d. o. o.  
**Vera Žlabravec**, Predilnica Litija, d. o. o.

Glavna in odgovorna urednica/  
*Editor-in-Chief*

**Tatjana Rijavec**

Namestnica glavne in odgovorne urednice/  
*Assistant Editor*

**Tatjana Kreže**

Področni uredniki/*Associate Editors*

**Matejka Bizjak, Katja Burger, Andrej Demšar, Alenka Pavko Čuden, Andreja Rudolf, Barbara Simončič, Sonja Šterman, Brigita Tomšič, Zoran Stjepanović**

Izvršna urednica za podatkovne baze/  
*Executive Editor for Databases*

**Irena Sajovic**

Mednarodni uredniški odbor/  
*International Editorial Board*

Arun Aneja, Greenville, US  
Andrea Ehrmann, Bielefeld, DE  
Aleš Hladnik, Ljubljana, SI  
Petra Forte Tavčer, Ljubljana, SI  
Darinka Fakin, Maribor, SI  
Jelka Geršak, Maribor, SI  
Karl Gotlih, Maribor, SI  
Memon Hafeezullah, Shanghai, CN  
Abu Naser Md. Ahsanul Haque, Daka, BD;  
Geelong, AU  
Ilda Kazani, Tirana, AL  
Svjetlana Janjić, Banja Luka, BA  
Igor Jordanov, Skopje, MK  
Petra Komarkova, Liberec, CZ  
Mirjana Kostić, Beograd, RS  
Manja Kurečić, Maribor, SI  
Rimvydas Milasius, Kaunas, LT  
Olga Paraska, Khmelnytskyi, UA  
Irena Petrinič, Maribor, SI  
Željko Penava, Zagreb, HR  
Tanja Pušić, Zagreb, HR  
Zenun Skenderi, Zagreb, HR  
Snežana Stanković, Beograd, RS  
Jovan Stepanović, Leskovac, RS  
Zoran Stjepanović, Maribor, SI  
Simona Strnad, Maribor, SI  
Jani Toroš, Ljubljana, SI  
Mariana Ursache, Iai, RO  
Antoneta Tomljenović, Zagreb, HR  
Dušan Trajković, Leskovac, RS  
Hidekazu Yasunaga, Kyoto, JP

**tekstilec** (ISSN: 0351-3386 tiskano, 2350-3696 elektronsko) je znanstvena revija, ki podaja temeljne in aplikativne znanstvene informacije v fizikalni, kemijski in tehnološki znanosti, vezani na tekstilno in oblačilno tehnologijo, oblikovanje in trženje tekstilij in oblačil. V prilogah so v slovenskem jeziku objavljeni strokovni članki in prispevki o novostih v tekstilni tehnologiji iz Slovenije in sveta, prispevki s področja oblikovanja tekstilij in oblačil, informacije o raziskovalnih projektih ipd.

**tekstilec** (ISSN: 0351-3386 printed, 2350-3696 online) the scientific journal gives fundamental and applied scientific information in the physical, chemical and engineering sciences related to the textile and clothing industry, design and marketing. In the appendices written in Slovene language, are published technical and short articles about the textile-technology novelties from Slovenia and the world, articles on textile and clothing design, information about research projects etc.

Dosegljivo na svetovnem spletu/*Available Online at*  
[www.tekstilec.si](http://www.tekstilec.si)



Tekstilec je indeksiran v naslednjih bazah/*Tekstilec is indexed in*  
Emerging Sources Citation Index – ESCI/Clarivate Analytics  
SCOPUS/Elsevier (2018: Q3, SJR 0.16, Cite Score 0.45, SNIP 0.612 – v sodelovanju *in cooperation with* Leiden University's Center for Science & Technology Studies)  
Ei Compendex  
DOAJ  
WTI Frankfurt/TEMA® Technology and Management/TOGA® Textile Database  
World Textiles/EBSCO Information Services  
Textile Technology Complete/EBSCO Information Services  
Textile Technology Index/EBSCO Information Services  
Chemical Abstracts/ACS  
ULRICHWEB – global serials directory  
LIBRARY OF THE TECHNICAL UNIVERSITY OF LODZ  
dLIB  
SICRIS: 1A3 (Z, A, A1/2)



# tekstilec

## Ustanovitelj / Founded by

- Zveza inženirjev in tehnikov tekstilcev Slovenije /  
*Association of Slovene Textile Engineers and Technicians*
- Gospodarska zbornica Slovenije – Združenje za tekstilno,  
oblačilno in usnjarsko predelovalno industrijo /  
*Chamber of Commerce and Industry of Slovenia – Textiles, Clothing and Leather  
Processing Association*

## Revijo sofinancirajo / Journal is Financially Supported

- Univerza v Ljubljani, Naravoslovnotehniška fakulteta / *University of Ljubljana,  
Faculty of Natural Sciences and Engineering*
- Univerza v Mariboru, Fakulteta za strojništvo /  
*University of Maribor, Faculty for Mechanical Engineering*
- Javna agencija za raziskovalno dejavnost Republike Slovenije /  
*Slovenian Research Agency*

## Izdajatelj / Publisher

Univerza v Ljubljani, Naravoslovnotehniška fakulteta /  
*University of Ljubljana, Faculty of Natural Sciences and Engineering*

## Sponzor / Sponsor

Predilnica Litija, d. o. o.

## Naslov uredništva/Editorial Office Address

Uredništvo Tekstilec, Snežniška 5, SI-1000 Ljubljana

Tel./Tel.: + 386 1 200 32 00, +386 1 200 32 24

Faks/Fax: + 386 1 200 32 70

E-pošta/E-mail: [tekstilec@ntf.uni-lj.si](mailto:tekstilec@ntf.uni-lj.si)

Spletni naslov/Internet page: <http://www.tekstilec.si>

Lektor za slovenščino / *Slovenian Language Editor* Barbara Luštek Preskar

Lektor za angleščino / *English Language Editor* Barbara Luštek Preskar,

Tina Kočevar Donkov, Glen David Champaigne

Oblikovanje platnice / *Design of the Cover* Tanja Nuša Kočevar

Oblikovanje / *Design* Vilma Zupan

Oblikovanje spletnih strani / *Website Design* Jure Ahtik

Tisk / *Printed by* PRIMITUS, d. o. o.

Copyright © 2020 by Univerza v Ljubljani, Naravoslovnotehniška fakulteta,

Oddelek za tekstilstvo, grafiko in oblikovanje

Noben del revije se ne sme reproducirati brez predhodnega pisnega dovoljenja

izdajatelja/No part of this publication may be reproduced without the prior written  
permission of the publisher.

Revija Tekstilec izhaja štirikrat letno / *Journal*

*Tekstilec appears quarterly*

Revija je pri Ministrstvu za kulturo vpisana v  
razvid medijev pod številko 583.

Letna naročnina za člane Društev inženirjev in  
tehnikov tekstilcev je vključena v članarino.

Letna naročnina za posameznike 38 € za  
študente 22 €

za mala podjetja 90 € za velika podjetja 180 €  
za tujino 110 €

Cena posamezne številke 10 €

Napodlagi Zakona o davku na dodano  
vrednost sodi revija Tekstilec med proizvode,  
od katerih se obračunava DDV po stopnji 5 %.

Transakcijski račun 01100-6030708186  
Bank Account No. SI56 01100-6030708186

Nova Ljubljanska banka d.d.,  
Trg Republike 2, SI-1000 Ljubljana,  
Slovenija, SWIFT Code: LJBA SI 2X.

SCIENTIFIC  
ARTICLES/  
*Znanstveni članki*

- 4** *Jana Filipič, Dominika Glažar, Špela Jerebic, Daša Kenda, Anja Modic, Barbara Roškar, Iris Vrhovski, Danaja Štular, Barbara Golja, Samo Smolej, Brigita Tomšič, Marija Gorjanc, Barbara Simončič*  
Tailoring of Antibacterial and UV-protective Cotton Fabric by an *in situ* Synthesis of Silver Particles in the Presence of a Sol-gel Matrix and Sumac Leaf Extract  
*Izdelava protibakterijske in UV zaščitne bombažne tkanine z in situ sintezo srebrvih delcev v prisotnosti sol-gel matrice in ekstrakta listov octovca*
- 14** *Sujit Kumar Sinha, P. Kanagasabapathi, Subhankar Maity*  
Performance of Natural Fibre Nonwoven for Oil Sorption from Sea Water  
*Zmogljivost vlaknovin iz naravnih vlaken za sorpcijo olj iz morske vode*
- 27** *Wu Hanbing, Hajo Haase, Boris Mahltig*  
Cationic Pretreatment for Reactive Dyeing of Cotton and its Simultaneous Antibacterial Functionalisation  
*Kationska predobdelava za reaktivno barvanje bombaža in sočasna protibakterijska funkcionalizacija*
- 38** *Elise Diestelhorst, Fjoralba Mance, Al Mamun, Andrea Ehrmann*  
Chemical and Morphological Modification of PAN Nanofibrous Mats with Addition of Casein after Electrospinning, Stabilisation and Carbonisation  
*Kemijska in morfološka modifikacija PAN nanovlaknatih kopren z dodanim kazeinom po elektropredenju, stabilizaciji in karbonizaciji*
- 50** *Darinka Fakin, Lavra Smoljanović, Alenka Ojstršek*  
Detection and Perception of Colour Regarding Gender and Age  
*Detekcija in zaznavanje barve glede na spol in starost*
- 60** *Desalegn Atalie, Rotich Gideon*  
Prediction of Psychological Comfort Properties of 100% Cotton Plain Woven Fabrics made from Yarns with Different Parameters  
*Napovedovanje psihološkega udobja 100-odstotnih bombažnih tkanin v vezavi platno, izdelanih iz prej z različnimi parametri*
- 68** *Sukhvir Singh, Niranjana Bhowmick, Anand Vaz*  
Theoretical Modelling of Can-spring Mechanism Using Bond Graph  
*Teoretično modeliranje mehanizma vzmeti v loncu z uporabo veznega grafa*

# Tailoring of Antibacterial and UV-protective Cotton Fabric by an *in situ* Synthesis of Silver Particles in the Presence of a Sol-gel Matrix and Sumac Leaf Extract

*Izdelava protibakterijske in UV zaščitne bombažne tkanine z in situ sintezo srebrvih delcev v prisotnosti sol-gel matrice in ekstrakta listov octovca*

## Original scientific article/Izvirni znanstveni članek

Received/Prispelo 10-2018 • Accepted/Sprejeto 12-2019

---

### Abstract

This research presents a new procedure for the chemical modification of cotton fabric, which included a "green" *in situ* synthesis of silver particles using an extract of sumac leaves as a reducing agent. To increase the adsorption ability of silver cations, a sol-gel matrix was previously created on cotton fabric using an organic-inorganic precursor sol-gel. The presence of silver particles on the cotton fabric was confirmed by scanning electron microscopy and energy-dispersive X-ray spectroscopy. The results showed that silver particles were created on the cotton fabric in the presence of the sumac leaf extract, which colored the fibers in brown. The presence of the sol-gel matrix increased the adsorption of silver cations and therefore the concentration of silver particles, which resulted in a deeper color yield. Silver particles provided antibacterial protection, with a 99–100% reduction of *E. coli* in *S. aureus* bacteria, while the sumac leaf extract provided excellent protection against ultraviolet radiation, with an ultraviolet protective factor equaling 66.54. The coating was also highly durable in terms of its washing fastness.

Keywords: silver particles, *in situ* synthesis, sumac leaves, cotton, sol-gel matrix, antibacterial activity, UV-protection

### Izvleček

V raziskavi je predstavljen nov postopek kemijske modifikacije bombažne tkanine, ki vključuje »zeleno« *in situ* sintezo srebrvih delcev z uporabo ekstrakta listov octovca kot reducenta. Za povečanje stopnje adsorpcije srebrvih kationov je bila na bombažni tkanini predhodno oblikovana sol-gel matrica z uporabo reaktivnega organskega-anorganskega hibridnega prekursorja. Vzorci bombažne tkanine so bili potopljeni v raztopno  $\text{AgNO}_3$  pri ustreznih pogojih, v njo pa je bil naknadno dodan ekstrakt octovca. Po obdelavi je bila tkanina večkrat prana. Prisotnost srebrvih delcev na bombažni tkanini je bila potrjena z vrstično elektronsko mikroskopijo z energijsko-disperzijsko spektroskopijo rentgenskih žarkov. Iz rezultatov raziskave je razvidno, da so se v prisotnosti ekstrakta listov octovca na bombažni tkanini oblikovali srebrovi delci, ki so vlakna obarvali v rjavem barvnem tonu. Prisotnost sol-gel matrice je povečala adsorpcijo srebrvih kationov ter s tem koncentracijo srebrvih delcev, kar se je odrazilo v temnejšem barvnem tonu. Srebrovi delci so podelili tkanini protibakterijsko zaščito z 99–100-odstotno redukcijo bakterij *E. coli* in *S. aureus*, prisotnost ekstrakta listov octovca pa je nudila odlično zaščito pred ultravijoličnim sevanjem z ultravijoličnim zaščitnim faktorjem enakim 66,54. Apretura je bila visoko pralno obstojna.

Ključne besede: srebrovi delci, *in situ* sinteza, listi octovca, bombaž, sol-gel matrica, protimikrobna aktivnost, UV zaščita

## 1 Introduction

In textiles, silver particles (Ag Ps) have been recognized as effective antimicrobial agents, with broad-spectrum activity against bacteria, fungi and viruses. Besides zinc oxide and titanium dioxide, Ag Ps are mostly used for the fabrication of medical and hygiene textiles. However, the antimicrobial mechanism of Ag Ps is not yet fully known, yet the activity has been attributed to silver cations ( $\text{Ag}^+$ ), which are released from the surface of Ag Ps, and to Ag Ps, if their size is within a nanometer scale (Ag NPs) [1, 2]. Both  $\text{Ag}^+$  and Ag NPs can interact with the bacterial cell wall, where their accumulation causes membrane damage. Furthermore,  $\text{Ag}^+$  and Ag NPs lower than 10 nm can penetrate the cell, where they hinder or deactivate its critical physiological functions and consequently destroy the cell. In the presence of oxygen,  $\text{Ag}^+$  and Ag NPs may also catalytically accelerate the formation of reactive oxygen species (ROS), which are highly toxic to microorganism cells [1, 2].

There are several classical and contemporary approaches for the application of Ag Ps to textile substrates, which include the application of pre-synthesized Ag Ps using an appropriate finishing method or an *in situ* synthesis of Ag Ps in the presence of a textile substrate [3–5]. An important advantage of the *in situ* generation of Ag Ps is that it enables the growth of Ag Ps inside the textile fibers, increases the homogeneity and uniformity of the particle distribution inside and on the fiber surface, and reduces the agglomeration of particles. In this process, no additional methods or chemicals are needed to enhance dispersibility of the *ex situ* synthesized Ag Ps and to achieve their stability against agglomeration. However, in both approaches, Ag Ps are formed in the chemical reduction of silver salt, where different environmentally harmful organic or inorganic reducing and stabilizing agents are usually used. To avoid toxic chemicals and perform the fabrication processes more sustainably, biological methods for the synthesis of Ag Ps, in which extracts of plants and microorganisms are used as reducing and stabilizing agents, have received increasing attention [6–8].

The *in situ* biosynthesis of Ag Ps represents a ‘green’ fabrication process of Ag-functionalized textile substrates. In this process,  $\text{AgNO}_3$ , as a silver precursor, and plant extracts, as reducing and stabilizing agents, have mostly been used simultaneously.

Namely, natural biomolecules with carbonyl and phenolic hydroxyl functional groups, including alkaloids, tannins, flavonoids, phenols, amino acids, and polysaccharides, have been extracted from leaves, seeds, peel, and fruits of different plants and introduced in the reduction of silver precursors to Ag Ps [9–17]. Among plant extracts, extracts from sumac (*Rhus* spp.) could be introduced as a promising reducing agent because of the variety of biological active compounds present in sumac’s bark, branches, roots, leaves, seeds and fruits [18, 19]. Sumac is native to the temperate regions of North America, but it has also been spread worldwide and developed as a sustainable non-traditional economic plant. While different parts of sumac have already been used in food and cosmetic industries, to the best of our knowledge, sumac has not yet been used for the production of the micro- and nanoparticles of metals or metal oxides.

Therefore, the aim of this research was to develop a novel process for the *in situ* synthesis of Ag Ps on cotton fibers using sumac leaf extracts. To increase the adsorption ability of silver cations, an organic–inorganic hybrid sol-gel precursor was applied to fibers to create a sol-gel matrix, prior the immersion of the fibers in  $\text{AgNO}_3$ . Namely, we assumed that the presence of a sol-gel matrix on cotton fibers will increase their concentration of Ag Ps, as well as enhance their coating durability in comparison to fibers with no sol-gel matrix. The chemically modified cotton fibers were characterized by scanning electron microscopy (SEM) and energy-dispersive X-ray spectroscopy (EDS). Their antibacterial properties were investigated against the Gram-positive *Staphylococcus aureus* and the Gram-negative *Escherichia coli* bacteria. Their ultraviolet (UV) protection properties were determined in terms of the ultraviolet protection factor (UPF). An important goal of the research was also to determine the washing fastness of the coating.

## 2 Experimental

### 2.1 Materials

Alkaline-scoured, bleached, and mercerized 100% cotton plain-weave fabric (Tekstina d.o.o., Ajdovščina, Slovenia), with a mass per unit area of 119 g/m<sup>2</sup>, was used for chemical modification. To create a sol-gel matrix on the cotton fabric, iSys MTX (CHT R.

Beitlich GmbH, Tübingen, Germany), a reactive organic–inorganic sol, which is miscible with water at every ratio, was used in combination with Kollasol CDO, an anti-foaming agent (CHT R. Beitlich GmbH, Tübingen, Germany). Silver nitrate ( $\text{AgNO}_3$ ; 99.98%, Sigma Aldrich) was used as a silver precursor. Fresh leaves of sumac were supplied by the public holding company, JP VOKA SNAGA d.o.o. All solutions were prepared in double-distilled water.

## 2.2 Preparation of the sumac leaf extract solution

First, 20 g of dried sumac leaves were crushed and poured with 1000 ml of water. The mixture was heated to 98 °C and let to boil for 20 min at a gentle boiling. Afterwards, the extract was filtered and cooled at room temperature.

## 2.3 Chemical modification of the cotton fabric

The modification of the cotton fabric samples was performed in a two-step procedure (Figure 1). Firstly, 15 g/l iSys MTX in the combination with 1 g/l Kollasol CDO were prepared in double-distilled water and applied to the cotton samples by a pad-dry-cure method, including full immersion at room temperature, a wet-pick-up of 80%, drying at 100 °C and curing for 3 min at 150 °C. The concentrations of the agents and the application conditions were those recommended by the producer. After the treatment, the samples were left for seven days under standard atmospheric conditions (65% ± 2% relative humidity and 20 °C ± 1 °C) to allow for a complete sol-gel matrix formation. In the second step, the samples without and the samples with the sol-gel matrix were immersed in a  $1.0 \times 10^{-3}$  M  $\text{AgNO}_3$  solution, at a liquor ratio of 1:25, and treated for 10 min at 60 °C under constant stirring in a Girowash machine (James Heal, GB). Then, the sumac leaf extract solution was added, until the liquor ratio was 1:50, and the samples were treated in the solution for 60 min under the same conditions. For comparison, the fabric samples were treated with the sumac leaf extract solution, without the previous application of  $\text{AgNO}_3$ . After the treatment, the samples were rinsed in cold distilled water, squeezed and dried at room temperature. The procedures of the chemical modifications of the fabric samples and the corresponding sample codes are summarized in Table 1.

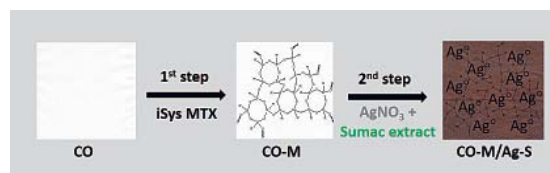


Figure 1: Schematic presentation of the procedure of cotton fabric chemical modification (Ag represents Ag P)

Table 1: Sample codes according to the chemical modification of the cotton fabric

| Sample code | Description of chemical modification  |
|-------------|---|
| CO          | No modification   |
| CO-M        | Application of iSys MTX in combination with Kollasol CDO  |
| CO/S        | Treatment of CO sample in sumac leaves extract solution without prior application of $\text{AgNO}_3$                |
| CO-M/S      | Treatment of CO-M sample in sumac leaves extract solution without prior application of $\text{AgNO}_3$              |
| CO/Ag-S     | Application of $\text{AgNO}_3$ to the CO sample followed by the sample treatment in sumac leaves extract solution   |
| CO-M/Ag-S   | Application of $\text{AgNO}_3$ to the CO-M sample followed by the sample treatment in sumac leaves extract solution |

## 2.4 Analyses and measurements

### 2.4.1 Scanning electron microscopy (SEM) and energy-dispersive X-ray spectroscopy (EDS)

Untreated and chemically modified cotton fabric samples were analyzed using a field emission scanning electron microscope, FEG-SEM Thermo Scientific Quattro S (ThermoFischer Scientific, USA). The sample analysis was performed using an Oxford Instruments Ultim Max 65 Energy-dispersive Detector (EDS) and AZtec software. The samples were coated with a thin layer of carbon before observation to provide conductivity and hence the quality of the images.

### 2.4.2 Antibacterial activity

The bacterial reduction on the functionalized samples was evaluated against the Gram-positive *Staphylococcus aureus* (ATCC 6538) and the Gram-negative



*Escherichia coli* (ATCC 25922) bacteria, according to the standard method, ASTM E 2149–01. The reduction in the number of bacteria,  $R$ , was calculated as follows [20]:

$$R = \frac{(B - A)}{B} \times 100 (\%) \quad (1),$$

where  $R$  is the bacterial reduction,  $A$  is the number of bacteria colony forming units per ml (CFU/ml) in a flask containing a chemically modified sample, after 1 hour of contact time, and  $B$  is the number of bacteria colony forming units per ml (CFU/ml) in a flask containing an unmodified reference sample, after 1 hour of contact time. Two parallel assessments with eight CFU counts were carried out for each functionalized sample and the  $R$  value was reported as the mean value and the standard error.

#### 2.4.3 UV protection properties

The UV protection properties of untreated and chemically modified cotton fabric samples, before and after repetitive washings, were determined according to the AATCC TM 183 standard. The measurements were performed using a Varian CARY 1E UV/Vis spectrophotometer (Varian, Australia), containing a DRA-CA-301 integration sphere and Solar Screen software. The transmission of the ultraviolet radiation through the samples were measured within the 280–400 nm spectral region, and the average transmittance ( $T$ ) at the wavelengths between 315 nm and 400 nm (UV-A), 280 nm and 315 nm (UV-B) and 280 nm and 400 nm (UV-R) were determined from the measurements. The ultraviolet protection factor ( $UPF$ ) was calculated as follows [21]:

$$UPF = \frac{\sum_{\lambda=280}^{400} E_{\lambda} \times S_{\lambda} \times \Delta\lambda}{\sum_{\lambda=290}^{400} E_{\lambda} \times S_{\lambda} \times T_{\lambda} \times \Delta\lambda} \quad (2),$$

where  $E_{\lambda}$  is the relative erythral spectral effectiveness,  $S_{\lambda}$  is the solar spectral irradiance,  $T_{\lambda}$  is the spectral transmittance of the specimen, and  $\Delta\lambda$  is the measured wavelength interval in nm. The higher the  $UPF$ , the higher the protection. The  $UPF$  rating and UVR protection categories were determined from the calculated  $UPF$  values, according to the Australian/New Zealand Standard: Sun protective clothing – Evaluation and classification [22]. Additionally, the transmission of the samples was measured within the 280–800 nm spectral region with

the use of the UV/Vis spectrophotometer Lambda 800 (Perkin Elmer, UK) equipped by the integrating sphere PELA-1000.

#### 2.4.4 Washing fastness

The fabric samples were washed once (1 W) and 5 times (5 W) in a Girowash machine (James Heal, GB), according to the ISO 105-C06 standard method. The washing cycles were performed in a SDC standard detergent solution, at a concentration of 4 g/l, at 40 °C for 45 min. After washing, the samples were rinsed in distilled water at 40 °C for 1 min, subsequently rinsed in tap water, and then dried in air at room temperature.

#### 2.4.5 Colour measurements

The CIELAB color coordinates of the untreated and chemically modified cotton samples, before and after repetitive washings and illumination, were determined using a Datacolor Spectraflash 600 PLUS-CT spectrophotometer. The measurements were performed with a 30-mm aperture under  $D_{65}$  illumination and an observation angle of 10°. The average of ten measurements was provided for each sample, and the color difference,  $\Delta E^*$ , was calculated using the following equation [23]:

$$\Delta E^*_{ab} = \sqrt{(\Delta L^*)^2 + (\Delta a^*)^2 + (\Delta b^*)^2} \quad (3),$$

where  $\Delta L^*$ ,  $\Delta a^*$  and  $\Delta b^*$  are differences between the color coordinates of the two samples.

## 3 Results and discussion

### 3.1 Sample characterization

The SEM/BSE images, shown in Figure 2, revealed numerous bright spots on the surface of the CO/Ag-S and CO-M/Ag-S samples, confirming that the presence of phenols, such as gallic acid, myricetin and quercetin derivatives, myricetin 3-rhamnoside, quercetin 3-glucoside as well as penta to decalloyl-glucosides in the sumac leaf extract [18, 19, 24], successfully converted  $Ag^+$  to  $Ag^0$  in the reduction reaction. The results also show that the application of a sol-gel matrix (CO-M sample) did not significantly change the fiber surface morphology, but it importantly influenced the adsorption ability of  $Ag^+$ . A comparison of CO/Ag-S and CO-M/Ag-S clearly showed that the amount of Ag was significantly

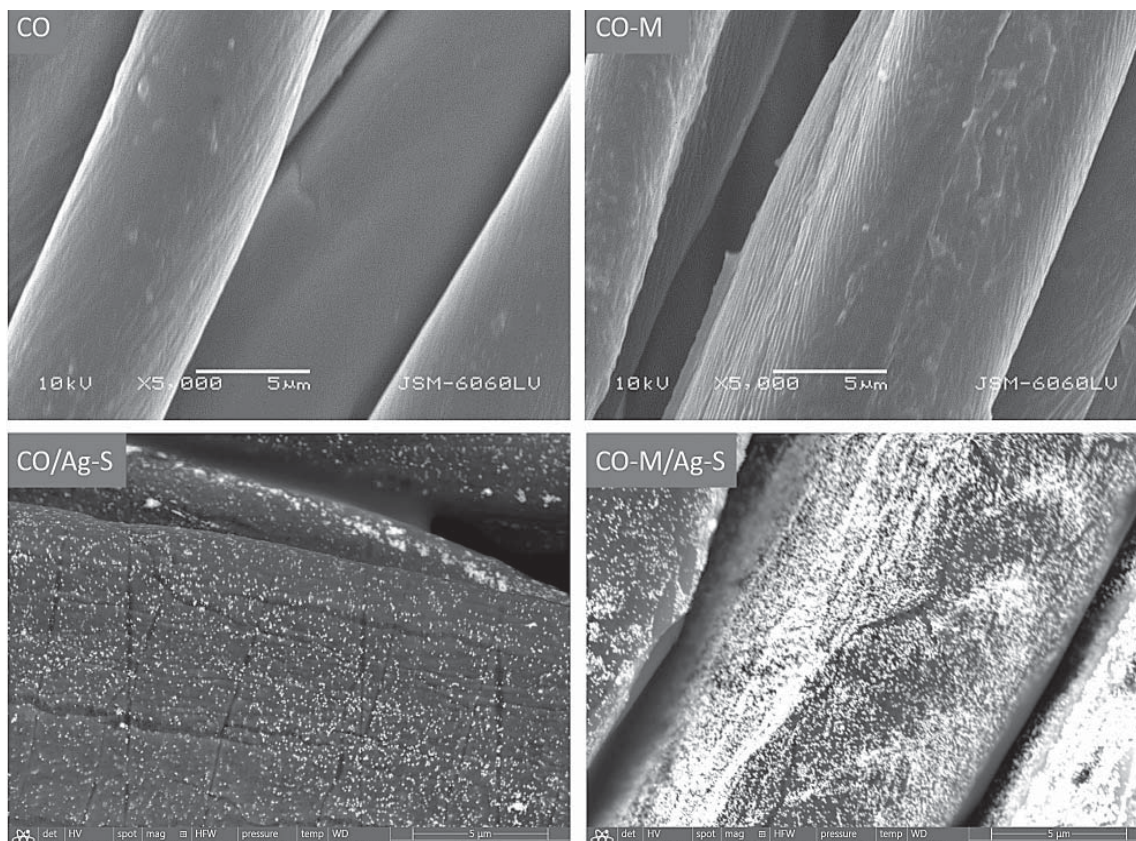


Figure 2: SEM/CBS images of CO, CO-M, CO/Ag-S and CO-M/Ag-S samples

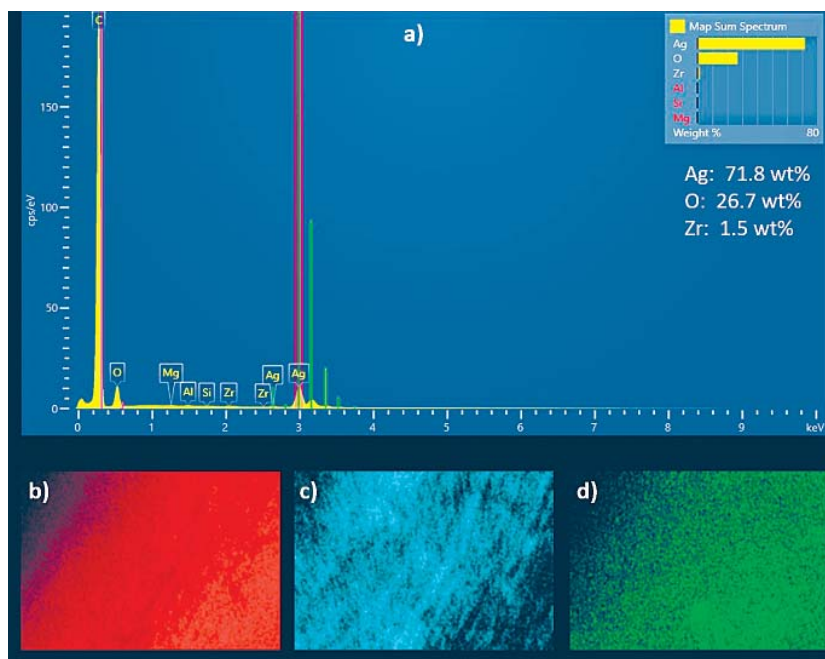


Figure 3: EDS spectrum acquired from Ag particles (a) and element mapping images of C (b), Ag (c) and O (d) on the CO-M/Ag-S sample

higher on the CO-M/Ag-S sample with the incorporated sol-gel matrix than on the CO/Ag-S sample without the sol-gel matrix.

The presence and distribution of the Ag element on the surface of the CO-M/Ag-S sample was confirmed by the EDS spectrum and element mapping images of C, Ag and O (Figure 3). The EDS spectrum showed a strong characteristic peak, corresponding to Ag at 2.984 keV. Furthermore, the element mapping images suggested that Ag was rather homogeneously distributed on the fiber surface, along with the intrinsic elements, C and O.

### 3.2 Functional properties of the chemically modified samples

The photo images of the untreated and chemically modified cotton fabric samples, shown in Figure 4, revealed that the application of the sol-gel matrix did not cause a visible color change in the cotton fibers, which generally remained white. In contrast, the treatment of cellulose fibers with sumac leaf extract colored the CO/S and CO-M/S samples in yellow (an increase in the positive value of the coordinate  $b^*$ ), which was slightly more yellow, if the sol-gel matrix

was present (CO-M/S sample). The *in situ* synthesis of Ag Ps in the presence of the sumac leaf extract converted the yellow color of the cotton fibers into a brown color, caused by a decrease in the values of the  $L^*$  and  $b^*$  coordinates, as well as a change of the  $a^*$  coordinate sign from negative to positive. The color change was more intense for the CO-M/Ag-S sample than for CO/Ag-S sample. These results clearly indicated that the presence of the sol-gel matrix increased the adsorption ability of the cotton fibers, for both the sumac leaf extract and  $AgNO_3$ , and that the reduction of  $Ag^+$  to  $Ag^0$  was accompanied by an intense color change. The latter was in accordance with the reports in the literature, in which the color change of the solution or of the textile substrates was chosen as the criteria for the formation of Ag Ps [25].

The antibacterial properties, presented in Figure 5, showed that not only Ag Ps (the CO-M/Ag-S sample), but also the sumac leaf extract (the CO-M/S sample) exhibited antibacterial activity. While the concentration of Ag on the cotton fibers was high enough to cause a 99–100% reduction of both *E. coli* and *S. aureus* bacteria, the phenolic compounds present in the water extract of the sumac leaves caused an excellent 99% growth reduction of *S. aureus*. On the other hand, the sumac leaf extract did not inhibit the growth of *E. coli*, but in contrast, it even promoted the bacterial growth which resulted in negative values of  $R$ . These findings were reasonable, since the substances in the sumac water and alcohol extracts are, in general, recognized as strong antibacterial agents against Gram-positive bacteria. The results also showed that the antibacterial activity of the CO-M/Ag-S sample was highly wash resistant, since a 100% bacterial reduction was obtained after five washings. This phenomenon was not observed

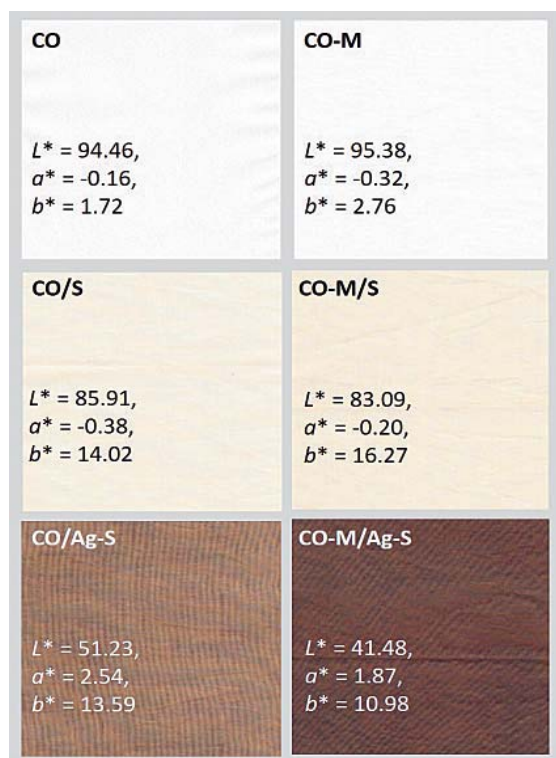


Figure 4: Photo images of the CO, CO-M, CO/S, CO-M/S, CO/Ag-S and CO-M/Ag-S samples

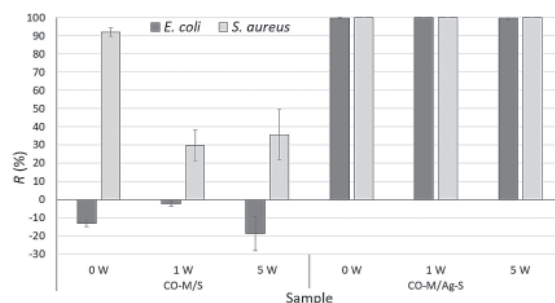


Figure 5: Reduction,  $R$ , of *E. coli* and *S. aureus* bacteria for the CO-M/S and CO-M/Ag-S samples, before (0 W) and after one (1 W) and five (5 W) consecutive washings



for the CO-M/S sample, where the antibacterial substances were partially desorbed from the cotton fibers during the washing of the sample. A desorption of the sumac extract during repetitive washing resulted in a lightening of the color, which is expressed by the values of  $\Delta E_{ab}^*$  in Figure 6. The lowest color change was determined for the CO-M/Ag-S sample, suggesting the durability of the chemical modification.

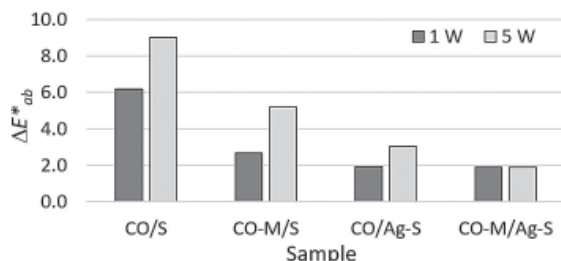


Figure 6: Color difference,  $\Delta E_{ab}^*$  of the CO/S, CO-M/S, CO/Ag-S and CO-M/Ag-S samples, unwashed and washed once (1W) and five (5W) times

The results in Figure 7 revealed that the presence of the sumac leaf extract (CO/S and CO-M/S samples) significantly decreased the transmission in the 280–400 nm spectral region in comparison to the CO and CO-M samples. This was attributed to the UV absorbing action of the aromatic phenolic compounds included in the sumac leaf extract. In the visible light spectrum (400–800 nm), the transmission of CO/S and CO-M/S samples gradually

increased with increasing wavelength and almost reached the values of 37–40 % in the 700–800 nm spectral region, which were characteristic for the CO and CO-M samples, respectively, in the whole visible spectrum. These results confirmed that lower wavelengths of visible light were absorbed by the yellow pigments of the sumac leaf extract. In contrast, the transmission of the CO/Ag-S and CO-M/Ag-S samples was very low in both UV and visible spectral region and it did not exceed 6 % even at 800 nm. This phenomenon implies that the brown colored Ag Ps successfully prevented the transmission in the whole measured spectral region.

The calculated UPF values summarized in Table 2 are in accordance with the results presented in Figure 7. Accordingly, the presence of the sumac leaf extract drastically increased the UPF, from 3.9 to 44.44, and this value was increased if the sol-gel matrix (the CO-M/S sample) and Ag Ps (the CO/Ag-S and CO-M/Ag-S samples) were present on the cotton fibers. These results clearly indicate the excellent UV-protection properties of the sumac leaf extract. While the UPF of the CO/S, CO-M/S, CO/Ag-S samples gradually decreased after subsequent washings (Figure 8) due to the sumac leaf extract desorption, the UPF of CO-M/Ag-S sample remained unchanged even after 5 washings, with a value of 66.5. This suggests that the interactions between the substances of the sumac leaf extract and Ag Ps, embedded in the sol-gel matrix, were strong

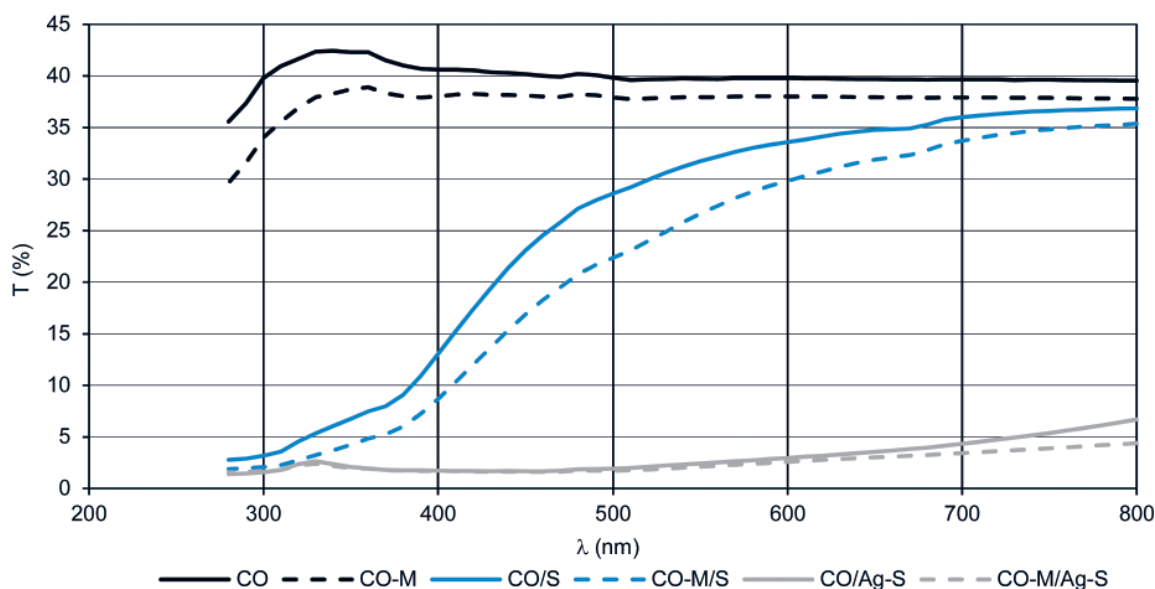


Figure 7: Transmission,  $T$ , versus wavelength,  $\lambda$ , for the CO, CO-M, CO/Ag-S and CO-M/Ag-S samples



Table 2: Mean ultraviolet protection factor, UPF, UPF rating and UVR protection categories for the untreated and differently coated samples

| Sample code | Mean UPF | T(UVA) (%) | T(UVB) (%) | T(UVR) (%) | UVA blocking (%) | UVB blocking (%) | UPF Rating | UVR protection category <sup>a)</sup> |
|-------------|----------|------------|------------|------------|------------------|------------------|------------|---------------------------------------|
| CO          | 3.90     | 29.06      | 24.78      | 27.75      | 70.62            | 75.12            | 4          | N                                     |
| CO-M        | 4.63     | 26.61      | 20.14      | 24.40      | 73.39            | 79.65            | 5          | N                                     |
| CO/S        | 44.44    | 5.10       | 1.79       | 4.12       | 94.89            | 98.18            | 40         | E                                     |
| CO-M/S      | 50.91    | 4.24       | 1.66       | 3.63       | 95.82            | 98.35            | 50         | E                                     |
| CO/Ag-S     | 66.1     | 2.06       | 1.35       | 1.73       | 97.96            | 98.69            | 70         | E                                     |
| CO-M/Ag-S   | 66.46    | 1.63       | 1.30       | 1.48       | 98.42            | 98.76            | 70         | E                                     |

<sup>a)</sup> N – non-rateable; E – excellent

enough to provide a durable coating. However, to be able to discuss this phenomenon in more detail, some additional investigations of the chemical compositions of the coating should be carried out.

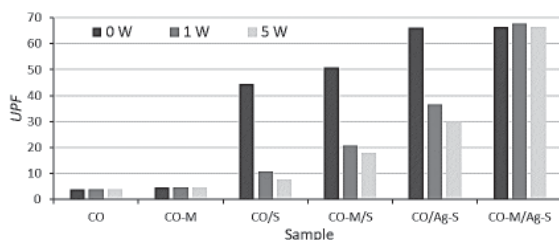


Figure 8: Ultraviolet protection factor, UPF, of the CO, CO-M, CO/S, CO-M/S, CO/Ag-S and CO-M/Ag-S samples before (0 W) and after one (1 W) and five (5 W) repetitive washings

## 4 Conclusion

In this research, we successfully created a highly durable antimicrobial and UV-protective coating on cellulose fibers by an in situ synthesis of Ag Ps in the presence of an extract of sumac leaves, which was used as a reducing agent. The results showed that:

- the sumac leaf extract colored the cellulose fibers in yellow, and the conversion of Ag cations to Ag Ps in the presence of the sumac leaf extract caused the fiber to be colored in brown;
- the concentration of Ag on the cotton fibers was high enough to cause a 99–100% reduction of both *E. coli* and *S. aureus* bacteria;
- the sumac leaf extract exhibited excellent antibacterial activity against *S. aureus* but did not inhibit the growth of *E. coli*;

- the sumac leaf extract provided high UV-protection, with a UPF value equal to 44.44, which was increased to 66.7, if Ag Ps were present on the cellulose fibers;
- the presence of the sol-gel matrix increased the adhesion ability of the cellulose fibers for the sumac leaf extract and Ag cations, resulting in an increased antibacterial activity and UV-protection properties of the chemically modified fibers, as well as their washing fastness.

## Acknowledgements

This research was carried out in the framework of the courses Advanced Finishing Processes and Chemical Functionalization of Textiles in the Master Study Programme, Textile and Clothing Planning. The research was cofounded by the EU project UIA02-228 AP-PLAUSE (Alien Plant Species from harmful to useful with citizens' led activities) and the Slovenian Research Agency (Program P2-0213, Infrastructural Centre RIC UL-NTF). The authors would like to thank Assoc Prof Dr. Raša Urbas for her help at the UV-Vis measurements.

## References

1. BEER, Christiane, FOLDBJERG, Rasmus, HAYASHI, Yuya, SUTHERLAND, Duncan S., AUTRUP, Herman. Toxicity of silver nanoparticles – nanoparticle or silver ion? *Toxicology Letters*, 2012, **208**(3), 286–292, doi: 10.1016/j.toxlet.2011.11.002.
2. LIAO, Chengzhu, LI, Yuchao, TJONG, Sie Chin. Bactericidal and cytotoxic properties of silver

- nanoparticles. *International Journal of Molecular Sciences*, 2019, **20**(2), 1–47, doi: 10.3390/ijms20020449.
3. ELSHAARAWY, Reda F. M., SEIF, Gelan A., EL-NAGGAR, Mehrez E., MOSTAFA, Tahia B., EL-SAWI, Emtithal A. *In-situ* and *ex-situ* synthesis of poly-(imidazolium vanillyl)-grafted chitosan/silver nanobiocomposites for safe antibacterial finishing of cotton fabrics. *European Polymer Journal*, 2019, **116**, 210–221, doi: 10.1016/j.eurpolymj.2019.04.013.
  4. CALHAN, Ebru, MAHLTIG, Boris. Microwave-assisted process for silver/silica sol application onto cotton fabrics. *Journal of Sol-Gel Science and Technology*, 2019, **92**(3), 607–617, doi: 10.1007/s10971-019-05149-2.
  5. MAHLTIG, Boris, FIEDLER, D., SIMON, P. Silver-containing sol-gel coatings on textiles: antimicrobial effect as a function of curing treatment. *Journal of the Textile Institute*, 2011, **102**(9), 739–745, doi: 10.1080/00405000.2010.515730.
  6. RAJAN, Ramachandran, CHANDRAN, Krishnaraj, HARPER, Stacey L., YUN, Soon-Il, KALAICHELVAN, P. Thangavel. Plant extract synthesized silver nanoparticles: an ongoing source of novel biocompatible materials. *Industrial Crops and Products*, 2015, **70**, 356–373, doi: 10.1016/j.indcrop.2015.03.015.
  7. ANSHU, Singh, SUJATA, Shekhar, SHRIVASTAVA, J. N. Biosynthesis of silver nanoparticles from various microbial and green resources: a review. *Research Journal of Biotechnology*, 2019, **14**(8), 120–130.
  8. SHAHEEN, Th. I., ABD EL ATY, Abeer A. *In-situ* green myco-synthesis of silver nanoparticles onto cotton fabrics for broad spectrum antimicrobial activity. *International Journal of Biological Macromolecules*, 2018, **118**(Part B), 2121–2130, doi: 10.1016/j.ijbiomac.2018.07.062.
  9. VANTI, Gulamnabi L., NARGUND, Vijendra B., BASAVESHA, K. N., VANARCHI, Rajinikanth, KURJOGI, Mahantesh, MULLA, Sikandar I., TUBAKI, Suresh, PATIL, Rajashekar R. Synthesis of *Gossypium hirsutum*-derived silver nanoparticles and their antibacterial efficacy against plant pathogens. *Applied Organometallic Chemistry*, 2019, **33**(1), 1–9, doi: 10.1002/aoc.4630.
  10. RAO, Amara Venkateswara, ASHOK, Basa, MAHESH, Mallavarapu Uma, SUBBAREDDY, Gopireddy Venkata, SEKHAR, Vatti Chandra, RAMANAMURTHY, Gollapudi Venkata, RAJULU, Anumakonda Varada. Antibacterial cotton fabrics with *in situ* generated silver and copper bimetallic nanoparticles using red sanders powder extract as reducing agent. *International Journal of Polymer Analysis and Characterization*, 2019, **24**(4), 346–354, doi: 10.1080/1023666X.2019.1598631.
  11. KARAMIAN, Roya, KAMALNEJAD, Jamalaldin. Green synthesis of silver nanoparticles using *Cuminum cyminum* leaf extract and evaluation of their biological activities. *Journal of Nanostructures*, 2019, **9**(1), 74–85, doi: 10.22052/JNS.2019.01.008.
  12. UL-ISLAM, Shahid, BUTOLA, B. S., VERMA, Deepali. Facile synthesis of chitosan-silver nanoparticles onto linen for antibacterial activity and free-radical scavenging textiles. *International Journal of Biological Macromolecules*, 2019, **133**, 1134–1141, doi: 10.1016/j.ijbiomac.2019.04.186.
  13. UL-ISLAM, Shahid, BUTOLA, B. S., GUPTA, Abhishek, ROY, Anasuya. Multifunctional finishing of cellulosic fabric via facile, rapid *in-situ* green synthesis of AgNPs using pomegranate peel extract biomolecules. *Sustainable Chemistry and Pharmacy*, 2019, **12**, 1–8, doi: 10.1016/j.scp.2019.100135.
  14. ABOUTORABI, S. Najmeh, NASIRIBORUMAND, Majid, MOHAMMADI, Pourya, SHEIBANI, Hassan, BARANI, Hossein. Biosynthesis of silver nanoparticles using Safflower flower: structural characterization, and its antibacterial activity on applied wool fabric. *Journal of Inorganic and Organometallic Polymers and Materials*, 2018, **28**(6), 2525–2532, doi: 10.1007/s10904-018-0925-5.
  15. SHAHRIARY, Marjan, VEISI, Hojat, HEKMATI, Malak, HEMMATI, Saba. *In situ* green synthesis of Ag nanoparticles on herbal tea extract (*Stachys lavandulifolia*)-modified magnetic iron oxide nanoparticles as antibacterial agent and their 4-nitrophenol catalytic reduction activity. *Materials Science & Engineering: C – Materials for Biological Applications*, 2018, **90**, 57–66, doi: 10.1016/j.msec.2018.04.044.
  16. SARAVANAKUMAR, Arthanari, PENG, Mei Mei, GANESH, Mani, JAYAPRAKASH, Jayabalan, MOHANKUMAR, Murugan, JANG, Hyun Tae. Low-cost and eco-friendly green synthesis

- of silver nanoparticles using *Prunus japonica* (Rosaceae) leaf extract and their antibacterial, antioxidant properties. *Artificial Cells Nanomedicine and Biotechnology*, 2017, **45**(6), 1165–1171, doi: 10.1080/21691401.2016.1203795.
17. ZHOU, Qingqing, LV, Jingchun, REN, Yu, CHEN, Jiayi, GAO, Dawei, LU, Zhenqian, WANG, Chunxia. A green in situ synthesis of silver nanoparticles on cotton fabrics using *Aloe vera* leaf extraction for durable ultraviolet protection and antibacterial activity. *Textile Research Journal*, 2017, **87**(19), 2407–2419, doi: 10.1177/0040517516671124.
18. RAYNE, Sierra, MAZZA, G. Biological activities of extracts from sumac (*Rhus* spp.): a review. *Plant Foods for Human Nutrition*, 2007, **62**(4), 165–175, doi: 10.1007/s11130-007-0058-4.
19. WANG, Sunan, ZHU, Fan. Chemical composition and biological activity of staghorn sumac (*Rhus typhina*). *Food Chemistry*, 2017, **237**, 431–443, doi: 10.1016/j.foodchem.2017.05.111.
20. ASTM E2149-01. *Standard Test Method for Determining the Antimicrobial Activity of Immobilized Antimicrobial Agents Under Dynamic Contact Conditions (Withdrawn 2010)*. West Conshohocken: ASTM International, 2001, 1–4.
21. LEE, Seungsin. Developing UV-protective textiles based on electrospun zinc oxide nanocomposite fibers. *Fibers and Polymers*, 2009, **10**, 295–301, doi: 10.1007/s12221-009-0295-2.
22. AS/NZS 4399:2017 *Sun Protective Clothing – Evaluation and Classification*. Sydney, Wellington: Standards Australia, Standards New Zealand, 2017, 1–8.
23. BERGER-SCHUNN, Anni. *Practical color measurement*. New York : John Wiley & Sons, 1994.
24. ROMEO, Flora V., BALLISTRERI, Gabriele, FABRONI, Simona, PANGALLO, Sonia, NICOSIA, Maria Giulia Li Destri, SCHENA, Leonardo, RAPISARDA, Paolo. Chemical characterization of different sumac and pomegranate extracts effective against *Botrytis cinerea* Rots. *Molecules*, 2015, **20**(7), 11941–11958, doi: 10.3390/molecules200711941.
25. MORALES-LUCKIE, Raul A., LOPEZFUENTES-RUIZ Adrian, Aldo, OLEA-MEJIA, Oscar F., LILIANA, Argueta-Figueroa, SANCHEZ-MENDIETA, Victor, BROSTOW, Witold, HINESTROZA, Juan P. Synthesis of silver nanoparticles using aqueous extracts of *Heterotheca inuloides* as reducing agent and natural fibers as templates: *Agave lechuguilla* and silk. *Materials Science & Engineering: C – Materials for Biological Applications*, 2016, **69**, 429–436, doi: 10.1016/j.msec.2016.06.066.

Sujit Kumar Sinha<sup>1</sup>, P. Kanagasabapathi<sup>1</sup>, Subhankar Maity<sup>2</sup>

<sup>1</sup> Dr. B. R. Ambedkar National Institute of Technology, Department of Textile Technology, Jalandhar 144011, Punjab, India

<sup>2</sup> Uttar Pradesh Textile Technology Institute, Department of Textile Technology, Kanpur, 208001, India

## Performance of Natural Fibre Nonwoven for Oil Sorption from Sea Water

### *Zmogljivost vlaknovin iz naravnih vlaken za sorpcijo olj iz morske vode*

Original scientific article/Izvirni znanstveni članek

Received/Prispelo 9-2019 • Accepted/Sprejeto 2-2020

#### Abstract

This work deals with the study of the oil sorption behaviour of needlepunched nonwoven fabrics produced from natural fibres such as cotton, cotton flat waste, cotton/kapok blend, and nettle fibres. Polypropylene nonwoven fabric, which is used as a commercial oil sorbent, was also prepared using the same needling parameters for comparison purposes. The effect of the type of fibre, oil, and fabric parameters on oil sorption and retention capacities was investigated. All of the fabrics displayed higher oil sorption capacities for engine oil (high viscosity) than diesel oil (low viscosity). Among natural fibre nonwovens, cotton and cotton/kapok nonwovens displayed higher oil sorption capacities than that of polypropylene nonwovens, while nettle fibre nonwoven fabric displayed poor oil sorption capacity. An increase in kapok content in cotton/kapok nonwovens led to an increase in oil sorption behaviour. More than 95% of the diesel oils adsorbed by the nonwoven fabrics could be recovered by simple compression. Oil sorption capacity of the nonwovens were reduced significantly during repetitive cycles of use due to higher thickness loss. This study indicated that cotton and cotton/kapok nonwovens displayed better oil sorption behaviour than polypropylene, and may be used as an alternative natural oil sorbent material.

Keywords: biodegradable oil sorbent, recovery of sea-water oil, sustainable textile, oleophilicity, oil spill

#### Izvleček

V članku je predstavljena študija učinkovitosti iglanih vlaknovin za sorpcijo olj, izdelanih iz naravnih vlaken, tj. bombaža, bombažnih odpadkov iz predilnic, mešanice bombaž/kapok in iz vlaken koprive. Pri enakih pogojih je bila za primerjavo izdelana tudi polipropilenska vlaknovina, saj so polipropilenske vlaknovine komercialni oljni sorbenti. Preučevan je bil vpliv vrste vlaken in olj ter parametri vlaknovin na sorpcijo in sposobnost zadrževanja olja. Vse vlaknovine so absorbirale večje količine motornega (visoka viskoznost) kot dizelskega olja (nizka viskoznost). Med vlaknovinami iz naravnih vlaken so večjo sorpcijo olja dosegle bombažne vlaknovine in vlaknovine iz mešanice bombaž/kapok kot polipropilenska vlaknovina. Pri tem pa je vlaknovina iz vlaken koprive dosegla najnižjo sorpcijo olja. Povečanje vsebnosti kapoka v vlaknovinah iz mešanice bombaž/kapok je vplivalo na povečanje sorpcije olja. Več kot 95 % dizelskih olj, ki so jih absorbirale vlaknovine, je bilo ponovno pridobljeno s preprostim stiskanjem. Pri ponovni uporabi vlaknovin so se zaradi zmanjšanja debeline njihove sorpcijske zmogljivosti zelo poslabšale. Raziskava dokazuje, da imajo vlaknovine iz bombaža in mešanice bombaž/kapok boljše sposobnosti sorpcije olja kot vlaknovina iz polipropilena in bi se zato lahko uporabljale kot alternativni naravni sorbenti.

*Ključne besede:* biorazgradljivi oljni sorbenti, zbiranje olja iz morske vode, hitrost sorpcije olja, trajnostni tekstil, oleofilnost, razlitje olja

Corresponding author/Korespondenčni avtor:

Subhankar Maity

E-mail: maity.textile@gmail.com

Tekstilec, 2020, 63(1), 14-26

DOI: 10.14502/Tekstilec2020.63.14-26



## 1 Introduction

Oil spills generally occur on the ocean's surface and also in nearby land areas due to tanker disasters, wars, operational failure, equipment failure, accidents and natural disasters during the production, transportation, storage and use of oil [1–3]. It is a serious problem that causes environmental and ecological imbalance, as well as financial loss. The immediate and effective decontamination and clean-up of spilled oils are necessary in order to protect the environment and human health [4]. Various methods are available for oil spill clean-up, such as mechanical recovery, dispersants, burning, etc. However, not a single system has been found to be completely effective. Oil spill clean-up through oil sorption using sorbents is one of the most efficient and economical methods [5–6].

Commercially, polypropylene is most widely used as oil sorbents due to its oleophilic and hydrophobic characteristics, but it is non-biodegradable [7–8]. This presents a great challenge in the disposal of the sorbent after usage [9]. The use of natural fibres such as milkweed, kapok, cotton, wool, flax, ramie, etc., as oil sorbents has been reported [10–16]. Cotton fibre was studied for oil sorption behaviour and reported to have higher oil sorption capacity than polypropylene fibre [17]. The crude oil sorption capacity of low-micronaire cotton is also significantly higher than that of high-micronaire cotton because it contains a higher number immature fibres [4, 18]. Milkweed and kapok fibres were reported to exhibit better oil sorption behaviour than the rest of the above-mentioned fibres. Higher surface waxes and non-collapsing lumens are believed to be the reason [9, 17]. Kapok/polypropylene blend needlepunched nonwovens were investigated as oil sorbents. It was reported that a 50/50 blend ratio of kapok and polypropylene demonstrated higher oil sorption [19]. Choi, Kwon, and Moreau investigated cotton/polypropylene blend needlepunched nonwovens as oil sorbents, and reported that an increase in cotton content increases oil sorption capacity [17]. Nettle fibre was also tested as another alternative material due to its hollow structure and the presence of surface waxes [20].

Loose fibres demonstrated a higher oil sorption capacity than structured fibrous assemblies due to a less effective or accessible fibre surface area [21]. The collection of fibres in loose form from a spill

area after use has been found to be a challenge. Hence, the nonwoven form is the best choice where the accessible fibre surface area is closer to loose fibres due to structural openness and the easy collection of nonwovens after use [9]. The oil sorbent characteristics of stitch-bonded, needlepunched and spunlaced nonwovens based on polypropylene were investigated. It was determined that porosity, pore size, and fibre fineness are important parameters for oil sorption [6]. However, the oil sorption behaviour of nonwovens does not depend on web forming technologies such as carding and air-laid techniques [9].

Based on literature review it is understood that as natural resources, immature cotton, kapok and nettle fibres may have great potential of oil sorption from seawater. Cotton flat waste has immature fibres in majority and may be a potential candidate for oil sorption. But it is not explored for this application. There is lack of information in literature on oil sorption capacity of needlepunched nonwovens made of cotton flat waste, cotton/kapok blend and nettle fibres.

Therefore, in this work, needlepunched nonwovens were produced from cotton, cotton flat waste, cotton/kapok blend of three different proportions, nettle and polypropylene fibres using the same needling parameters. Oil sorption behaviour, mechanical properties, and the re-usability of all these nonwoven specimens were tested and compared with polypropylene nonwoven to find a sustainable alternative of the same.

## 2 Experimental

### 2.1 Materials

The raw materials used for this work were cotton, cotton flat waste (collected from carding machine during spinning of the cotton fibre), kapok, nettle (*Girardinia diversifolia*) and polypropylene fibres. The African variety of cotton, its flat waste and virgin polypropylene fibres (3.33 dtex, 50 mm cut length) were collected from local industrial producers in Punjab, India. Properties of cotton, cotton flat waste and kapok were measured using a high volume instrument (HVI) and advanced fibre information system (AFIS) (Table 1). The nettle fibre (fineness 1.4 dtex and 50 mm cut length) was purchased from the Uttaranchal Bamboo and Fibre Development Board, India. The kapok was collected from

Table 1: Fibre properties measured by AFIS/HVI

| Fibre type        | Fibre properties (Measured by AFIS/HVI) |                              |                              |                    |                 |                       |
|-------------------|---|------------------------------|------------------------------|--------------------|-----------------|-----------------------|
|                   | 5% L(N) <sup>a)</sup><br>(mm)           | SFC (N) <sup>b)</sup><br>(%) | SFC (W) <sup>c)</sup><br>(%) | Fineness<br>(mtex) | Maturity<br>(%) | IFC <sup>d)</sup> (%) |
| Cotton            | 33.6                                    | 20.8                         | 7.1                          | 165                | 91              | 6.5                   |
| Cotton flat waste | 27.7                                    | 67.8                         | 37.0                         | 144                | 74              | 16.4                  |
| Kapok             | 19.7                                    | 67.1                         | 45.8                         | 125                | 78              | 12.6                  |

<sup>a)</sup> 5% AFIS fibre length, <sup>b)</sup> short fibre content by number, <sup>c)</sup> short fibre content by weight, <sup>d)</sup> immature fibre content

industrial producers in Coimbatore, India. Engine oil (high viscosity) and diesel (low viscosity) were used to conduct oil sorption testing. The specifications of the oils are given in Table 2.

Table 2: Specification of oils

| Oil type   | Viscosity at<br>40 °C (mm <sup>2</sup> /s) | Density at<br>15 °C (kg/dm <sup>3</sup> ) |
|------------|--|---|
| Engine oil | 121  | 0.95                                      |
| Diesel     | 2.5  | 0.82                                      |

## 2.2 Sample preparation

All needlepunched nonwoven samples were prepared using a DILO (Germany) needlepunching machine using a punch density of 50 punches/cm<sup>2</sup>, a needle depth penetration of 8 mm, and a mass per unit area of 200 g/m<sup>2</sup>. Parallel- and cross-laid nonwovens were prepared for 100% cotton fibre only. A cross lapper was used for the preparation of cross-laid nonwovens. The compositions of all prepared nonwoven samples are shown in Table 3.

Table 3: Composition of needlepunched nonwoven fabrics

| No. | Sample code | Sample description                               |
|-----|-------------|--|
| 1   | S1CP        | Nonwoven made of 100% cotton, parallel-laid      |
| 2   | S2CC        | Nonwoven made of 100% cotton, cross-laid         |
| 3   | S3FW        | Nonwoven made of 100% cotton flat waste          |
| 4   | S4C/K       | Nonwoven made of 30% cotton and 70 % kapok fibre |
| 5   | S5C/K       | Nonwoven made of 50% cotton and 50 % kapok fibre |
| 6   | S6C/K       | Nonwoven made of 70% cotton and 30 % kapok fibre |
| 7   | S7PP        | Nonwoven made of 100% polypropylene fibre        |
| 8   | S8NF        | Nonwoven made of 100% nettle fibre               |

## 2.3 Methods

### 2.3.1 Measurement of nonwoven properties

The mass per unit area of the nonwoven samples was determined according to the ASTM D6242-98 standard. The nonwoven fabric thickness was determined according to the ASTM D5729-97 standard at a pressure of 4.14 kPa. The bulk density (kg/m<sup>3</sup>) of nonwoven samples was calculated using equation 1.

$$\text{Bulk density} = \frac{W \times 10^3}{t} \quad (1)$$

where  $W$  is the mass per unit area of the sample (g/m<sup>2</sup>) and  $t$  is the thickness of the sample (m).

The porosity and pore size distribution of the nonwoven fabrics were measured using a capillary flow porometer (CFP-1100-AEHXL, PMI Inc.). The measurements were carried out in a dry-up/wet-up test mode using a Galwick solution (surface tension 15.9 mN/m) to saturate the samples after the dry test. The minimum, maximum, average pore diameters and pore size distribution of all samples were measured.

The tensile strength and breaking elongation in machine direction and in a cross direction of nonwoven fabrics was measured using a universal testing machine (Zwick) according to the ASTM D 5035-09 standard and the CRE principle, with a sample size of 20 cm × 10 cm, gauge length of 75 mm and testing speed of 300 mm/min.

### 2.3.2 Measurement of oil sorption capacity

The ASTM F716-82 (sorber performance of absorbents) and ASTM 726-81 (sorber performance of adsorbents) standards were followed for measurement of oil sorption capacity of the prepared nonwoven samples. The testing procedure of oil sorption capacity was classified in two ways: (a) oil sorption from oil in an artificial seawater bath; and (b) oil sorption from an oil bath. The artificial seawater bath was prepared according to the AATCC 106-8 standard.

#### a) Measurement of oil sorption from oil bath

To study the oil sorption capacity of oil sorbents without a water medium, a simple procedure was used. 60 g of sample oil was placed in a 1000 ml size glass beaker, and the dry nonwoven specimen was immersed in the oil for 10 minutes. As a result, the nonwoven specimen was soaked with the oil and the excess oil was allowed to drain by free hanging the soaked specimen vertically for 5 minutes. The specimen was then weighed. The oil sorption capacity of sorbents nonwoven was determined using equation 2.

$$\text{Oil sorption capacity} = \frac{W_{SO} - W_S}{W_S} = \frac{W_O}{W_S} \quad (2),$$

where  $W_S$  is the mass (g) of a dry and fresh nonwoven,  $W_{SO}$  is the mass (g) of the nonwoven saturated with oil and  $W_O$  is the mass (g) of oil soaked by the nonwoven.

#### b) Measurement of oil sorption from artificial sea water bath in static and dynamic conditions

One litre of artificial seawater was prepared by dissolving 30 g of sodium chloride and 5 g of magnesium chloride anhydride in 1000 ml of distilled water. 500 ml of this artificial seawater was poured in a 1000 ml size beaker and 50 g of sample oil was added to it and stirred with a digital magnetic stirrer (Cole Parmer) at 200 rpm, for 5 minutes to prepare an oil in a water emulsion.

A dry nonwoven specimen of known weight ( $m_o$ ) was immersed in the emulsion beaker for 10 min for

soaking in static condition. In case of dynamic condition of test, after immersing the dry sample into the emulsion beaker stirring was conducted using the same stirrer for 10 minutes at a frequency of 50 cycles/minute to simulate the actual ocean waves. After soaking, the specimen was taken out of the beaker and hanged vertically for 5 min so that excess solution can be drained out of the specimen. After that weight of the soaked specimen ( $m_f$ ) was taken for analysis.

The amount of sorbed solution was extracted from the soaked specimen by squeezing with a roller squeezer at a roller pressure of 1.5 kg/cm<sup>2</sup> and collected. The solution contained both oil and water, from which the water (mw) was separated using a separation funnel. Hence, the oil sorption capacity of sorber material was determined using equation 3.

$$\text{Oil sorption capacity} = \frac{m_f - (m_o + m_w)}{m_o} \quad (3),$$

where  $m_f$  is the mass (g) of the soaked specimen after draining,  $m_o$  is the initial dry mass (g) of the specimen and  $m_w$  is the water content (g) extracted from the specimen.

### 2.3.3 Theoretically defined oil sorption capacity

The oil sorption capacity of all nonwoven samples was also calculated theoretically and compared with experimental value. The theoretical oil sorption capacity of nonwovens indicates the maximum oil that a nonwoven fabric can adsorb. It is assumed that when all the pores in the nonwovens are filled with oils, the theoretical oil sorption capacity can be calculated using equation 4 [22].

$$\text{Theoretical oil sorption capacity} = \frac{v_p \times \rho_i}{v_f \times \rho_f} \quad (4),$$

where  $V_p$  and  $V_f$  indicate the volume of pores (equation 6) and fibres (equation 7) in the nonwovens, and  $\rho_i$  and  $\rho_f$  represent the density of oil and fibre respectively.

The volume of pores ( $V_p$ ) in a given fabric volume ( $V_F$ ) can be calculated from the porosity of the fabric (equation 5).

$$P = 1 - \frac{\rho_F}{\rho_f} \quad (5),$$

where  $\rho_F$  and  $\rho_f$  represent the bulk density of fabric and density of fibre respectively.

$$V_p = P \times V_F \quad (6)$$

$$V_f = (V_F - V_p) \quad (7)$$

### 2.3.4 Calculation of normalised oil sorption capacity

All nonwovens produced for this study had different levels of porosity with fibres of varying density. It was thus necessary to normalise the oil sorption capacity for comparison purposes. Normalised oil sorption capacities provide information about the effect of fibre characteristics (oleophilicity, contact angle and surface tension). The normalised oil sorption capacity can be expressed using equation 8 [9].

$$\text{Normalised oil sorption capacity} = \frac{\text{Experimental oil sorption capacity} (1 - \phi) \rho_f}{\phi \rho_i} \quad (8),$$

where  $\phi$  denotes the porosity,  $\rho_i$  and  $\rho_f$  represent the density of oil and fibre respectively.

### 2.3.5 Measurement of rate of oil release from sorbed nonwovens

Drainage/release of excess oil after soaking from oil bath by nonwoven specimens was measured by hanging the specimens freely in vertical manner so that loose oil can be drained automatically with time. The amount of oil releases from the specimens was calculated by measuring gradual weight loss of the soaked samples after various interval viz. 0, 1, 3, 5, 7, 10, 20 and 30 minutes. The amount of oil retained was determined by taking the difference between the initial weight of the soaked nonwoven specimen and the weight of the specimen after drainage for predetermined time.

### 2.3.6 Measurement of oil sorption rate

The sorption rate is defined as the amount of oil adsorbed by the nonwovens from oil bath over a period of time. An experimental setup was fabricated to measure the sorption rate of the nonwoven specimens. The experimental setup is shown in Figure 1. A reservoir with oil was placed over an electronic scale that was connected to a computer. The known weight of the specimen was placed over a mesh. The mesh was connected with a vertical rod that hung vertically from the wicking apparatus. The bottom surface of the specimen was then placed in contact with oil in the reservoir, as shown in Figure 1. The oil from the reservoir penetrated into the specimen due to wicking/capillary pressure. The change in weight of the reservoir was recorded over time and thus the sorption rate over time was calculated.

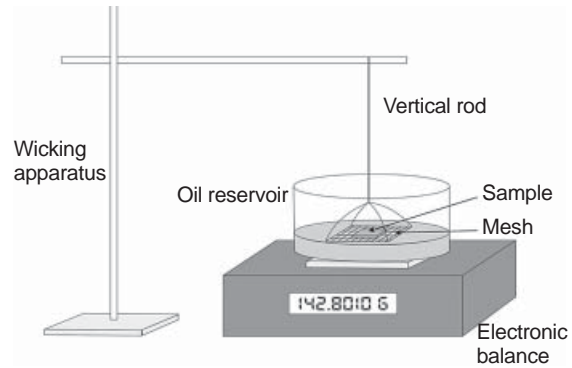


Figure 1: Instrumental setup for measurement of sorption rate

### 2.3.7 Measurement of recovery of absorbed oil

Oil recovery is defined as the ratio of the amount of oil recovered from a soaked specimen by mechanical squeezing to the total amount of oil soaked by the specimen. Squeezing of soaked specimens was conducted with the help of a squeezing roller keeping a roller pressure of 1.5 kg/cm<sup>2</sup>. This extracted amount of oil is recovered oil ( $W_r$ ). The amount of oil soaked by the specimen ( $W_o$ ) was measured by the method discussed in section 2.3.2 a). Then percentage recovery of oil was calculated by equation 9.

$$\text{Oil recovery} = \frac{W_r}{W_o} \times 100 \quad (9)$$

## 3 Results and discussion

### 3.1 Nonwovens properties

An engineered fibre structure needlepunched nonwovens are flexible thick sheets which are porous, thick, bulky, and strong. They are developed in such a way that they resemble a spongy low density fabrics, wherein textile fibres are loosely interlocked via fibre entanglement without disturbing the active surface area of fibres and capillary network between the fibres much. No external adhesive was employed for fibre bonding so that surface characteristics of fibres, pore structure and capillary network are not affected and the capillary network is responsible for absorbing oil from seawater. Performance of nonwoven structure for any application depend on its mass per unit area, thickness, tensile properties etc. Average values of mass per unit area, thickness, tensile strength and breaking elongation in machine and cross directions of prepared nonwoven samples are reported in Table 4.



Table 4: Structural properties of nonwovens

| Sample No. | Sample code | Sample description   | GSM <sup>a)</sup> (g/m <sup>2</sup> ) | t <sup>b)</sup> (mm) | Machine direction                   |                                   | Cross direction                     |                                   |
|------------|-------------|----------------------|---------------------------------------|----------------------|-------------------------------------|-----------------------------------|-------------------------------------|-----------------------------------|
|            |             |                      |                                       |                      | F <sub>br</sub> <sup>c)</sup> (N/m) | ε <sub>br</sub> <sup>d)</sup> (%) | F <sub>br</sub> <sup>c)</sup> (N/m) | ε <sub>br</sub> <sup>d)</sup> (%) |
| 1          | S1CP        | Cotton parallel-laid | 181.63                                | 4.33                 | 255.00                              | 71.98                             | 121.96                              | 118.58                            |
| 2          | S2CC        | Cotton cross-laid    | 187.35                                | 3.86                 | 117.52                              | 127.74                            | 265.20                              | 69.68                             |
| 3          | S3FW        | Cotton flat waste    | 187.18                                | 3.65                 | 119.48                              | 64.12                             | 55.92                               | 96.06                             |
| 4          | S4C/K       | Cotton/kapok (30/70) | 181.78                                | 5.33                 | 66.24                               | 50.42                             | 54.28                               | 92.16                             |
| 5          | S5C/K       | Cotton/kapok (50/50) | 181.60                                | 4.72                 | 141.56                              | 59.46                             | 80.16                               | 95.94                             |
| 6          | S6C/K       | Cotton/kapok (70/30) | 182.62                                | 4.22                 | 179.32                              | 75.74                             | 98.36                               | 102.14                            |
| 7          | S7PP        | Polypropylene        | 289.49                                | 7.30                 | 9496.00                             | 118.76                            | 4348.00                             | 130.80                            |
| 8          | S8NF        | Nettle               | 287.20                                | 2.43                 | 1206.00                             | 32.48                             | 585.20                              | 75.54                             |

<sup>a)</sup> mass per unit area, <sup>b)</sup> thickness, <sup>c)</sup> tensile strength, <sup>d)</sup> breaking elongation

The results depict that all nonwoven specimens are sufficient thick and strong for the application of oil spill clean-up from seawater.

### 3.2 Oil sorption capacity of nonwovens from oil bath

The oil sorption capacities of all nonwovens were determined for engine oil and diesel from oil baths. The results are graphically represented in Figure 2. All the nonwovens displayed higher oil sorption capacity for high viscosity oil (engine oil) than that of low viscosity oil (diesel).

It can be observed from Figure 2 that, among all types of nonwovens, the cotton/kapok blended nonwovens exhibited the highest oil sorption capacity. The oil sorption capacity increased with an increase in kapok content (samples S6–S4). This is due to the lower bulk density of kapok enriched nonwovens and oleophilic nature of the kapok fibres. Porosity and bulk density of all nonwovens are shown in Figure 3 and Figure 4 respectively. Good correlation has been observed between oil sorption capacity of the nonwovens and their porosity. Coefficients of correlation (*r*) between sorption capacity and porosity are found to be 0.92 and 0.97 for engine oil and diesel oil respectively. Kapok fibres are oleophilic in nature and have good affinity to oil. The oleophilicity is related to the surface waxes of fibres and kapok has higher surface waxes than cotton, that makes the kapok more oleophilic [25].

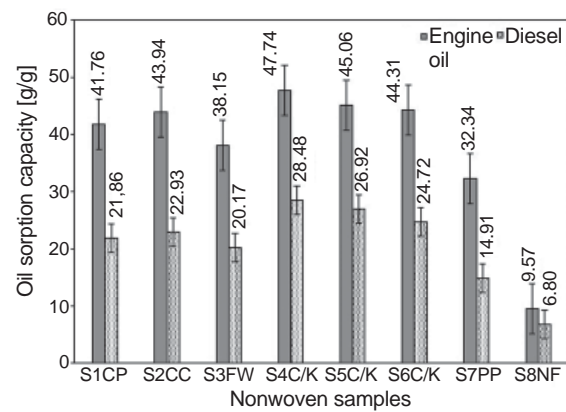


Figure 2: Oil sorption of different nonwovens from the oil bath

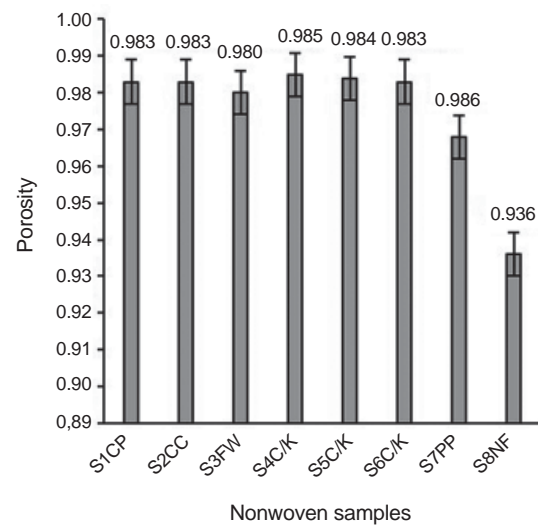


Figure 3: Porosity of nonwoven samples

All of the cotton nonwovens displayed an oil sorption capacity just below kapok blended nonwovens. The cotton flat waste nonwoven (S3FW) displayed significantly lower oil sorption than other cotton nonwovens for both engine and diesel oil because of the lower porosity and higher bulk density of the nonwovens, as shown in Figure 4. Good negative correlation has been observed between oil sorption capacity of the nonwovens and their bulk density. Coefficients of correlation ( $r$ ) between sorption capacity and bulk density are found to be -0.87 and -0.79 for engine oil and diesel oil respectively. The higher bulk density is attributed to the higher number of short fibres in cotton flat waste. The cotton cross-laid nonwovens (S2CC) displayed significantly higher oil sorption capacity than cotton parallel-laid (S1CP) nonwoven for high viscosity oil (engine oil). This might be due to difference in fibre orientation. For lower viscosity oil (diesel), both nonwovens displayed similar oil sorption capacity.

The polypropylene nonwoven (S7PP) displayed significantly lower oil sorption capacity than cotton and cotton/kapok blend nonwovens. This can be explained as follows. The oil sorption capacity of a nonwoven is generally influenced by the oleophilic nature of the fibre, fibre fineness and the structure of the nonwoven fabric prepared thereof. The oleophilic nature of the fibre was one of the important factors that favourably influenced oil sorption behaviour. A structure that facilitates capillary flow should be able to adsorb more liquids. The capillary flow through a structure depends on the number of pores and their size in the structure. A structure made of finer fibre should yield more pores but with a smaller size. Thus, a structure made of finer fibre is expected to have more oil retention capacity due to higher capillary pressure. If the pore size is higher, then capillary pressure will be lower. In the present experiment, the fineness of polypropylene was 3.33 dtex, which was coarser than all other fibres. Therefore, the nonwoven prepared by the polypropylene fibres had larger pores, which was experimentally verified by the measurement of mean pore diameters, as shown in Figure 5. Hence, oils drained more easily due to a higher gravitational force than capillary pressure on account of a larger pore size. As a result, polypropylene nonwoven fabric displayed a lower oil sorption capacity than that of the cotton and cotton/kapok nonwovens.

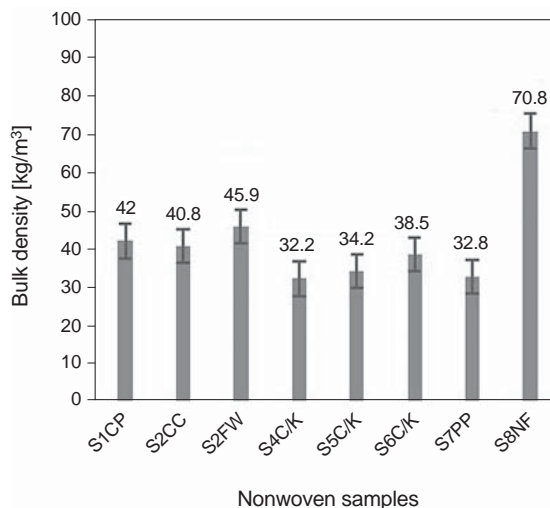


Figure 4: Bulk density of nonwovens

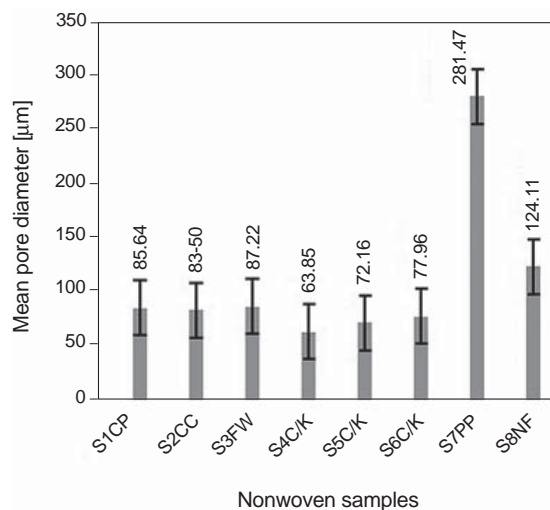


Figure 5: Mean pore diameter of nonwovens

### 3.3 Oil sorption of nonwovens from artificial sea water bath

Oil spills generally occur on the ocean's surface and in nearby land areas [1]. It was thus necessary to test the oil sorption capacities from oil in a water bath. The dynamic test conditions simulated the actual condition of ocean waves. The oil sorption capacities of all nonwovens from the artificial seawater bath for dynamic condition are shown in Figure 6 and on the Figure 7 the difference between oil sorption capacity from artificial seawater bath in static and dynamic condition is given.

For high viscosity oil (engine oil), all nonwovens displayed higher oil sorption under static conditions than

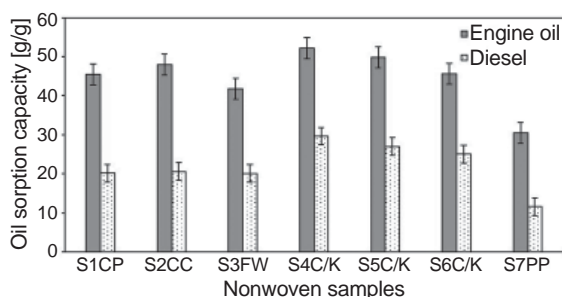


Figure 6: Oil sorption of nonwovens from artificial seawater bath under dynamic conditions

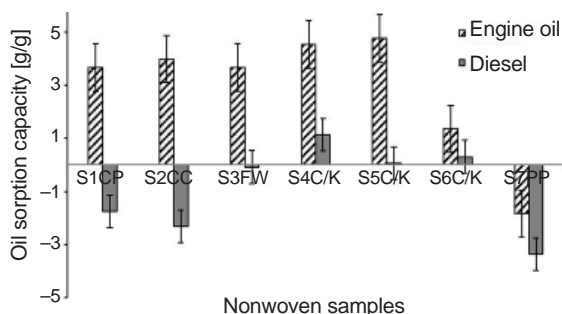


Figure 7: Difference between oil sorption of nonwovens from the static oil bath and dynamic oil in an artificial seawater bath

under dynamic conditions except polypropylene. In dynamic condition the agitation hampered the oil sorption mechanism. Polypropylene showed exceptional behaviour may be due to its hydrophobicity. For low viscosity oil (diesel), the cotton/kapok nonwovens (S4–S6) displayed higher oil sorption under static condition than that of dynamic condition due to the same reason as mentioned above. Exceptional behaviour observed in case of cotton nonwovens because agitation helps better penetration of oil inside these nonwoven structures which are relatively compact due to bulk density in higher side.

### 3.4 Difference between theoretical and measured oil sorption capacity of nonwovens

The oil sorption capacity of all nonwoven samples was calculated theoretically from equation 4 and then experimentally measured. The results of both theoretical and experimental sorption capacities for both high and low viscosity oil are represented in Figures 8 and 9.

It is evident from these figures that for engine oil, actual oil sorption capacity was higher than theoretical oil

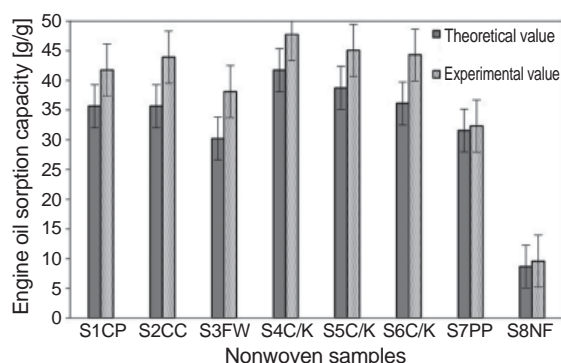


Figure 8: Theoretical and experimental oil sorption capacity of high viscosity liquid (engine oil)

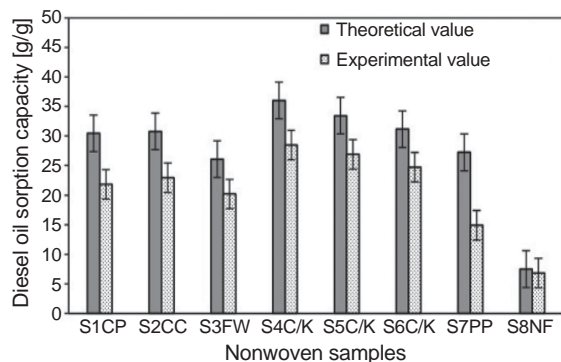


Figure 9: Theoretical and experimental oil sorption capacity of low viscosity liquid (diesel)

sorption capacity for all kinds of nonwovens whereas in case of diesel oil actual oil sorption was lower than that of theoretical. When oil is sorbed by a nonwoven structure the oil molecules are entered and occupied all pores in fibre interstices as well as attached over the surface of the nonwoven structure. As a result actual oil sorption should be higher than the theoretical value that actually happened in case of high viscosity engine oil. In case of low viscosity diesel oil due to poor surface tension there was weak bonding between diesel oil molecules and fibre surface and therefore diesel oil drain out easily from the nonwoven structure during vertical hanging and as a result actual sorption capacity become lower than that of theoretical value.

### 3.5 Normalised oil sorption capacity

All nonwovens produced for this study had different levels of porosity with fibres of varying density. Sorption capacity also depends on density of oil. For comparison purposes, it was thus necessary to normalise the oil sorption capacity of nonwovens to nullify the effect of density of sorbent fibres, sorbing oil and porosity of the nonwoven structure. The normalised

sorption capacities of all nonwovens are calculated as per equation (8) and shown in Figure 10.

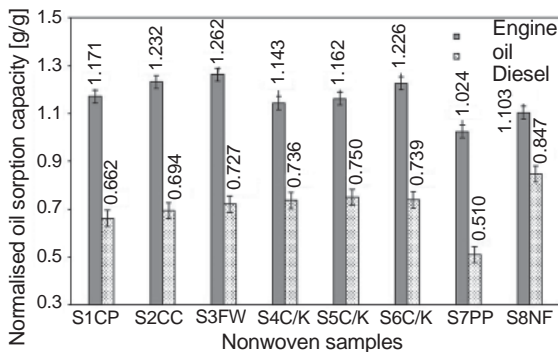


Figure 10: Normalised oil sorption capacity of nonwovens

Among cotton-based nonwovens (S1–S3), cotton flat waste nonwoven fabric (S3FW) showed the highest normalised oil sorption capacity. Though the nonwoven fabric made of cotton flat waste had more immature and shorter fibres resulting in lower porosity, a higher normalised oil sorption capacity was observed due to improved oleophilicity. An immature fibre generally contains higher surface waxes that improve its oleophilicity [23]. The sorption capacity of fibres is influenced by their oleophilic nature. In the case of cotton/kapok nonwovens (S4–S6), the normalised oil sorption capacities were found to be close to that of cotton-based nonwovens (S1–S3). This was due to both the oleophilic nature of kapok fibres and higher fabric porosity. Cotton/kapok nonwovens had a higher porosity because of poor compaction during needling on account of poor cohesiveness between kapok fibres [9, 18].

### 3.6 Oil sorption rate and rate of release of engine oil from the nonwovens

The oil sorption rate of the nonwovens was measured for engine oil, and the results are shown in Figure 11.

It is evident that all nonwovens adsorb engine oil more rapidly until 1 minute, followed by a slow-down in next two minutes till the nonwovens finally becomes saturated within 5 minutes. The initial steep rise in oil sorption was due to the porous structure of nonwovens that had small pores that exerted high capillary pressure. The next gradual rise in oil sorption might be attributed to larger pores. This can be explained in light of the Young-

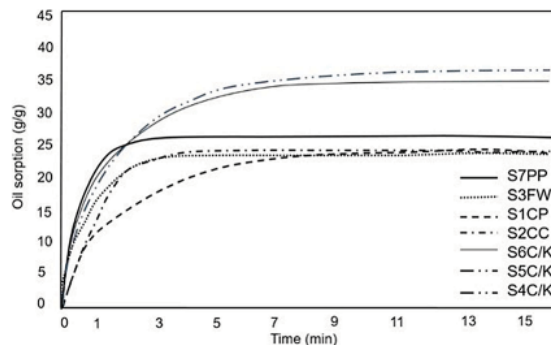


Figure 11: Engine oil sorption of nonwovens with time

Laplace equation of the relationship between capillary pressure and pore radius, as shown in equation 10 [1–2].

$$p = \frac{2 \gamma \cos \theta}{r_c} \quad (10)$$

where  $p$  indicates capillary pressure,  $r_c$  represents pore radius,  $\theta$  denotes the oil contact angle and  $\gamma$  indicates surface tension of oil.

Hence, the oil sorption rate depends on the capillary pressure, surface tension and contact angle of liquid, while capillary pressure depends on the size of the capillary. Therefore, the differences in the oil sorption rate among the nonwovens were due to the fibre-oil contact angle and mean pore diameter of the nonwovens. In the case of high viscosity oil, all cotton nonwovens displayed a similar oil sorption rate that was significantly lower than polypropylene nonwovens (S7PP). The cotton parallel-laid (S1CP) and cross-laid (S2CC) fabrics followed an almost similar pattern of oil sorption. It is clear that the difference in fibre orientation did not cause any significant difference in the oil sorption rate in the fabrics.

The release or draining-out of adsorbed oils from the nonwovens due to free vertical hanging is approximately an inverse phenomena of oil sorption. The oil release rate of all nonwovens for high viscosity engine oil is shown in Figures 12. Each oil release curve consists of three distinct phases. First phase is the initial stage of release that occurs within 1 minute. The rate of release is highest during this period. The second or transition phase occurs from 1 to 10 minutes. During this period, the rate of release decreased substantially. The third phase represents the steady-state period. In this period, the



nonwoven sorbent tended to begin a descent towards a steady state. High viscosity engine oil drained very slowly from nonwovens, and thus reached a steady-state after 10 minutes.

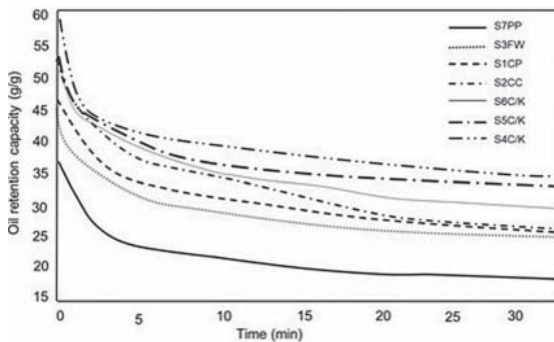


Figure 12: Release of engine oil from nonwovens with time

### 3.7 Oil sorption rate and retention capacity for diesel oil

The oil sorption rate of the nonwovens was measured for engine oil, and the results are shown in Figure 13. It is evident that nonwovens adsorb diesel oil very fast and reach saturation within 10 seconds. Low viscosity oil (diesel) would enter pores more quickly than high viscosity oil (engine oil), which leads to the quicker absorption of diesel oil. All nonwovens displayed a slightly higher oil sorption rate for lower viscosity oil (diesel) than high viscosity oil (engine oil). High viscosity oils were not able to adsorb upward through larger pores due to insufficient capillary pressure. The heavier oil (engine oil) would require a higher capillary pressure than lighter oil (diesel) to raise the oil to a particular height. The polypropylene nonwoven fabric (S7PP) displayed similar oil sorption rates for both engine and diesel oil, but the time taken to reach the saturation point is higher for high viscosity oil (engine oil). It was thus determined that the fibre type is a critical factor in determining the oil sorption rate.

The rate of release of diesel oil for all nonwovens is shown in a Figure 14. Each of these curves consists of two distinct phases. The first phase is the initial stage of release, which occurs within 1 minute. The rate of release is much high during this period. The second or transition zone lasts from 1 to 10 minutes. During this period, the rate of release was achieved a steady-state. Low viscosity oil (diesel) drained from nonwovens more rapidly and reached a steady-state quickly, i.e. within 1 minute.

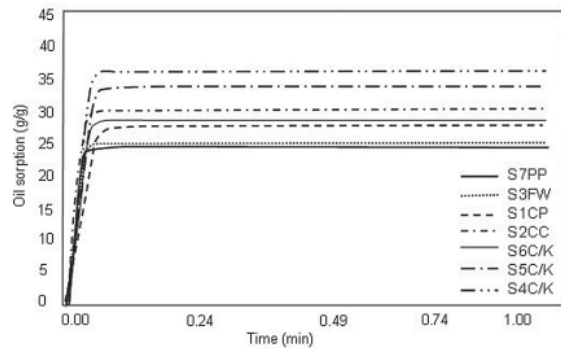


Figure 13: Sorption of diesel oil by the nonwovens with time

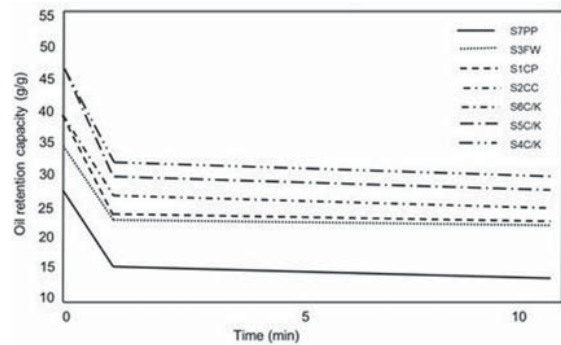


Figure 14: Release of diesel oil from nonwovens with time

The sorption of low viscosity oil (Figure 11) by all the nonwovens from the oil bath was quicker than that of the high viscosity oil (Figure 13). Also, low viscosity oil was found to drain away more rapidly during the draining period (1 minute) (Figure 12), while the draining of high viscosity oil was found to be slow (Figure 14). This is the reason for the ultimately higher oil sorption capacity for high viscosity oil exhibited by all kinds of nonwoven specimens.

### 3.8 Recovery of oil and reusability

The sorbed oil from nonwovens was recovered by compressing the nonwovens using a roller squeezer with a roller pressure of 1.5 kg/cm<sup>2</sup>. The percentage of recovered diesel oil from different nonwovens for consecutive four sorption cycles is shown in Figure 15. The recovery of diesel for PP nonwoven in the first cycle was observed to be around 94% which was found to be lowest among all nonwovens. The oil recovery showed a higher value in second cycle is attributed to the presence of residual oil inside nonwoven structure even after the squeezing in first cycle. This is the same reason due to which 100% recovery

cannot be achieved. It can be seen from Figure 15 that oil recovery did not deteriorate much after 4<sup>th</sup> cycle of test.

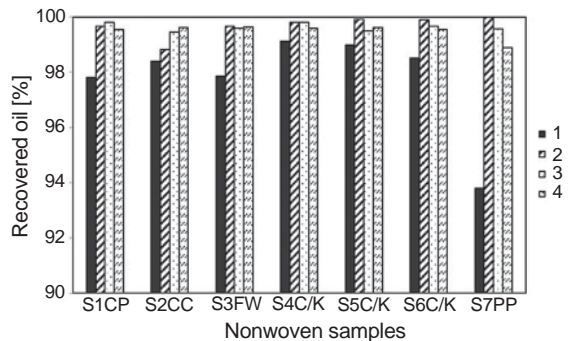


Figure 15: Percentage of diesel oil recovered from nonwovens after different cycles

An oil sorbent can be considered reusable if it can be easily compressed or squeezed to retain its original size and shape [12, 24]. Figure 16 shows the reusability of nonwovens for diesel oil. All nonwovens displayed a significant reduction in oil sorption capacities of around 50% (10 to 20 g/g) during the second cycle. The oil sorption depends on the porosity of the fabric, while the fabric porosity is in direct correlation with fabric thickness. Fabric thickness reduced after every cycle of padding, leading to a change in porosity and pore size. The flattening of pores was expected, which might result in the inability to hold much liquid. The thickness of the fabric was reduced due to padding after every cycle, which led to a reduction in oil sorption capacity. The percentage of thickness retained by nonwovens

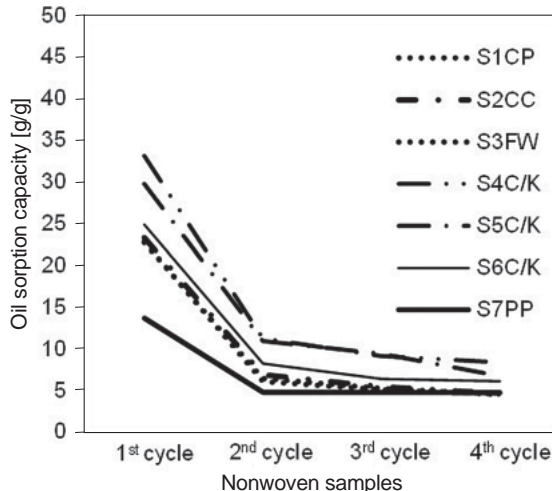


Figure 16: Reusability of nonwovens for diesel oil

after every cycle is given in Figure 17. The reduction in oil sorption capacities was much higher during the second cycle, while the reduction was not very significant during further successive cycles. During reuse, the reduction in oil sorption for polypropylene nonwoven fabric (S7PP) was found to be lower than in other nonwovens. The oil sorption capacity of polypropylene nonwoven fabric (S7PP), even after four cycles, was found to be lower than the nonwovens from natural fibres.

All nonwovens prepared from natural fibres displayed poor oil sorption capacity during reuse. Sorption is dependent on the availability of pores. Bulkier fabrics with similar mass per unit area should offer more oil retention sites. Nonwovens from natural fibres suffered more loss in thickness. This led

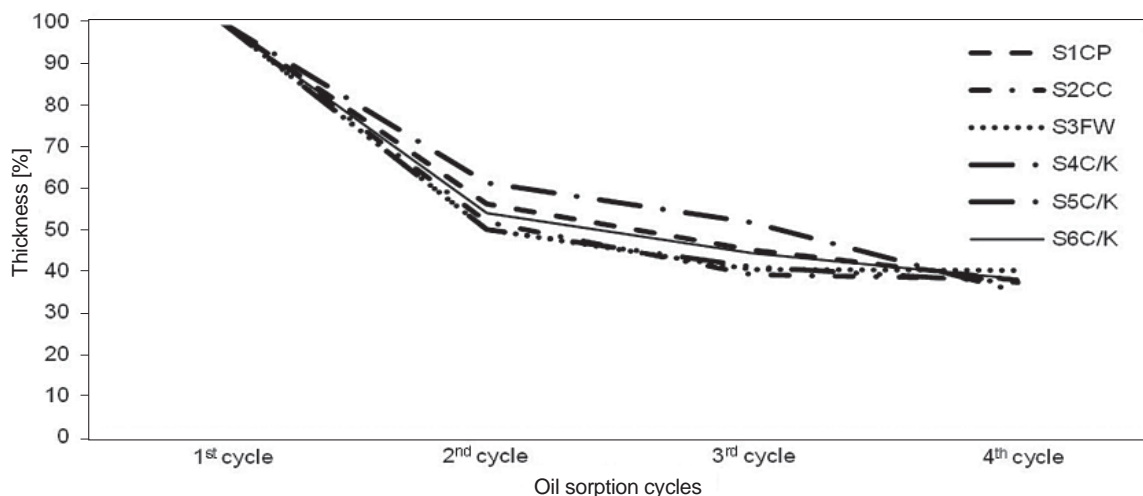


Figure 17: Percentage of thickness retained by nonwovens after every cycle of sorption

to a reduction in both porosity and the number of pores. Hence, the oil sorption capacity of nonwovens from natural fibres was lower during reuse. All nonwovens from natural fibres displayed poor compressional recovery, which needed to be improved.

## 4 Conclusion

All the studied nonwovens displayed significantly higher oil sorption capacity for high viscosity oil (engine oil) than that of the low viscosity oil (diesel). Nettle fibre nonwoven exhibited lowest oil sorption capacity and poor compressional recovery and therefore considered poor material for this application. Except nettle fibre nonwoven fabric (S8), all other natural fibre nonwovens (S1–S6) displayed higher oil sorption capacity than polypropylene nonwoven fabric (S7). Cotton/kapok blended nonwovens (S4–S6) were the best performer in terms of higher oil sorption and retention capacity, and oil sorption rate. An increase in kapok content in the cotton/kapok nonwoven led to a better oil sorption capacity. Even nonwovens prepared from cotton flat waste fibres exhibited very good normalised oil sorption capacity, which could open up a new door for sustainable usage of cotton waste. All these natural fibre nonwovens achieved a steady-state of sorption quickly, within 1 minute for low viscosity oil (diesel) and within 10 minutes for high viscosity oil (engine oil). In addition, more than 95% of the oils adsorbed by the nonwoven fabrics can be recovered through simple compression. During reuse, the oil sorption capacity of nonwovens gradually fell down due to thickness loss during compression. Thus, cotton/kapok fibres and cotton flat waste may be a sound choice as alternative materials to polypropylene as sea-water oil sorber in terms of low-cost, biodegradable and sustainable material.

## References

1. RENGASAMY, R.S., DAS, D., KARAN, C.P. Study of oil sorption behavior of filled and structured fiber assemblies made from polypropylene, kapok and milkweed fibers. *Journal of Hazardous Materials*, 2011, **186**(1), 526–532, doi: 10.1016/j.jhazmat.2010.11.031.
2. RENGASAMY, R.S., DAS, D., RENUKA S. Nonwoven oil sorbing pads from sustainable

- fibrous materials for marine oil spill removal. In *Proceedings of the 37th AMOP Technical Seminar on Environmental Contamination and Response*. Ottawa : Environment Canada, 2014.
3. SEDDIGHI, M., HEJAZI, S.M. Water-oil separation performance of technical textiles used for marine pollution disasters. *Marine Pollution Bulletin*, 2015, **96**(1–2), 286–293, doi: 10.1016/j.marpolbul.2015.05.011.
4. SINGH, V., JINKA, S., HAKE, K., PARAMESWARAN, S., KENDALL, R.J., RAMKUMAR, S. Novel natural sorbent for oil spill cleanup. *Industrial & Engineering Chemistry Research*, 2014, **53**(30), 11954–11961, doi: 10.1021/ie5019436.
5. CHOI, H.M., CLOUD, R.M. Natural sorbents in oil spill cleanup. *Environmental Science & Technology*, 1992, **26**(4), 772–776, doi: 10.1021/es00028a016.
6. CHOI, H.M., MOREAU, J.P. Oil sorption behavior of various sorbents studied by sorption capacity measurement and environmental scanning electron microscopy. *Microscopy Research and Technique*, 1993, **25**(5–6), 447–455, doi: 10.1002/jemt.1070250516.
7. WEI, Q.F., MATHER, R.R., FOTHERINGHAM, A.F., YANG, R.D. Evaluation of nonwoven polypropylene oil sorbents in marine oil-spill recovery. *Marine Pollution Bulletin*, 2003, **46**(6), 780–783, doi: 10.1016/S0025-326X(03)00042-0.
8. CHU, Z., FENG, Y., SEEGER, S. Oil/water separation with selective superantwetting/superwetting surface materials. *Angewandte Chemie International Edition*, 2015, **54**(8), 2328–2338, doi: 10.1002/anie.201405785.
9. RENUKA, S., RENGASAMY, R.S., DAS, D. Studies on needlepunched natural and polypropylene fiber nonwovens as oil sorbents. *Journal of Industrial Textiles*, 2016, **46**(4), 1121–1143, doi: 10.1177/1528083715613630.
10. RADETIĆ, M.M., JOCIĆ, D.M., JOVANČIĆ, P.M., PETROVIĆ, Z.L., THOMAS, H.F. Recycled wool-based nonwoven material as an oil sorbent. *Environmental Science & Technology*, 2003, **37**(5), 1008–1012, doi: 10.1021/es0201303.
11. GE, J., YE, Y.D., YAO, H.B., ZHU, X., WANG, X., WU, L., WANG, J.L., DING, H., YONG, N., HE, L.H., YU, S.H. Pumping through porous hydrophobic/oleophilic materials: an alternative technology for oil spill remediation. *Angewandte*

- Chemie International Edition*, 2014, **53**(14), 3612–3616, doi: 10.1002/anie.201310151.
12. LI, D., ZHU, F.Z., LI, J.Y., NA, P., WANG, N. Preparation and characterization of cellulose fibers from corn straw as natural oil sorbents. *Industrial & Engineering Chemistry Research*, 2012, **52**(1), 516–524, doi: 10.1021/ie302288k.
  13. HYUNG, Min Choi, RINN M. Cloud. Natural sorbents in oil spill cleanup. *Environmental Science & Technology*, 1992, **26**(4), 772–776, doi: 10.1021/es00028a016.
  14. HYUNG, Min Choi, JERRY, P. Moreau. Oil sorption behavior of various sorbents studied by sorption capacity measurement and environmental scanning electron microscopy. *Microscopy Research and Technique*, 1993, **25**(5–6), 447–455, doi: 10.1002/jemt.1070250516.
  15. HYUNG, Min Choi. Needlepunched cotton nonwovens and other natural fibers as oil cleanup sorbents. *Journal of Environmental Science & Health Part A*, 1996, **31**(6), 1441–1457, doi: 10.1080/10934529609376434.
  16. GE, J., ZHAO, H.Y., ZHU, H.W., HUANG, J., SHI, L.A., YU, S.H. Advanced sorbents for oil-spill cleanup: recent advances and future perspectives. *Advanced Materials*, 2016, **28**(47), 10459–10490, doi: 10.1002/adma.201601812.
  17. CHOI, H.M., KWON, H.J., MOREAU, J.P. Cotton nonwovens as oil spill cleanup sorbents. *Textile Research Journal*, 1993, **63**(4), 211–218, doi: 10.1177/004051759306300404.
  18. SINGH, V., KENDALL, R.J., HAKE, K. and RAMKUMAR, S. Crude oil sorption by raw cotton. *Industrial & Engineering Chemistry Research*, 2013, **52**(18), 6277–6281, doi: 10.1021/ie4005942.
  19. LEE, Y.H., KIM, J.S., KIM, D.H., SHIN, M.S., JUNG, Y.J., LEE, D.J., KIM, H.D. Effect of blend ratio of PP/kapok blend nonwoven fabrics on oil sorption capacity. *Environmental Technology*, 2013, **34**(24), 3169–3175, doi: 10.1080/09593330.2013.808242.
  20. HYUNG Min Choi, HYO-JUNG Kwon, JERRY P. Moreau. Cotton nonwovens as oil spill cleanup sorbents. *Textile Research Journal*, 1993, **63**(4), 211–218, doi: 10.1177/004051759306300404.
  21. ANSARI, Imtiyaz Ahmad, EAST, George C., JOHNSON, D. J. Structure-property relationships in natural cellulosic fibers: part III: flax-an oil sorbent. *Journal of the Textile Institute*, 2003, **94**(1–2), 1–15, doi: 10.1080/00405000308630590.
  22. HSIEH, Y.L. Liquid transport in fabric structures. *Textile Research Journal*, 1995, **65**(5), 299–307, doi: 10.1177/004051759506500508.
  23. PRICE, J. B., CUI, X., CALAMARI, T. A., MEREDITH Jr, W. R. Cotton wax and its relationship with fiber and yarn properties: part II: wax content and yarn properties. *Textile Research Journal*, 2002, **72**(7), 631–637, doi: 10.1177/004051750207200711.
  24. CHOI, H.M. Needlepunched cotton nonwovens and other natural fibers as oil cleanup sorbents. *Journal of Environmental Science and Health . Part A: Environmental Science and Engineering and Toxicology*, 1996, **31**(6), 1441–1457, doi: 10.1080/10934529609376434.
  25. LIM, T.T, HUANG, X. Evaluation of kapok (*Ceiba pentandra* (L.) Gaertn.) as a natural hollow hydrophobic–oleophilic fibrous sorbent for oil spill cleanup. *Chemosphere*, 2007, **66**(5), 955–963, doi: 10.1016/j.chemosphere.2006.05.062.



Wu Hanbing<sup>1</sup>, Hajo Haase<sup>2</sup>, Boris Mahltig<sup>1</sup>

<sup>1</sup> University of Applied Sciences Niederrhein, Faculty of Textile and Clothing Technology, Webschulstr. 31, 41065 Mönchengladbach, Germany

<sup>2</sup> Technische Universität Berlin, Institut für Lebensmitteltechnologie und Lebensmittelchemie, Gustav-Meyer Allee 25, 13355 Berlin, Germany

## Cationic Pretreatment for Reactive Dyeing of Cotton and its Simultaneous Antibacterial Functionalisation

### *Kationska predobdelava za reaktivno barvanje bombaža in sočasna protibakterijska funkcionalizacija*

Original scientific article/Izvirni znanstveni članek

Received/Prispelo 12-2019 • Accepted/Sprejeto 2-2020

#### Abstract

Reactive dyes are chemically bonded to a cotton fibre surface. The anchor groups of dye molecules initiate this covalent bonding. In addition to this anchor group, reactive dyes also contain charged functional groups that are often negatively charged sulphonate groups  $-SO_3^-$ . These negative groups are part of the dye to enable its solubility in water. In industrial applications, dyes are applied as part of a water-based dye bath. The aim of the presented study was to improve the dyeing of cotton through the cationic modification of the textile, supporting an attraction to negatively charged dye molecules. In this way, the dye up-take and achieved colour depth should be improved. The current study was performed with a vinyl sulfone reactive dye. Three different nitrogen containing cationic organic substances were used for cotton pretreatment. In addition to colour properties, the antibacterial properties of prepared textile samples were also studied because antibacterial properties are often related to compounds containing amino and ammonium groups. Finally, it was shown that the cationic pretreatment with two of the three studied agents increased the dye up-take of cotton fabric from the dye bath. At the same time, one cationic agent can introduce antibacterial properties to treat cotton fabrics against two different types of bacteria: *E. coli* and *S. warneri*. The simultaneous application of a functional property during an optimised dyeing process was demonstrated in this case and can serve as an example for further applications.

Keywords: Coloration, dyeing, antibacterial, cationic compounds

#### Izvleček

Reaktivna barvila so kemično vezana na površino bombažnih vlaken. Reaktivne skupine molekul barvila sprožijo kovalentno vezanje. Poleg te reaktivne skupine vsebujejo reaktivna barvila tudi funkcionalne skupine z nabojem, in sicer so to pogosto negativno nabite sulfonske skupine  $-SO_3^-$ , ki omogočajo topnost barvila v vodi. V industrijski rabi se barvila nanesejo kot del barvalne kopeli na vodni osnovi. Cilj predstavljene študije je izboljšati barvanje bombaža s kationsko modifikacijo tekstilije, ki temelji na privlačnosti negativno nabitih molekul barvila. Na ta način se izboljšata navzemanje barvila in globina barvnega tona. V raziskavi je bilo uporabljeno vinilsulfonsko reaktivno barvilo. Za predobdelavo bombaža so bila uporabljena tri različna sredstva kationskega značaja na osnovi dušika. Poleg barve so bile raziskane tudi protibakterijske lastnosti pripravljenih tekstilnih vzorcev, ki so pogosto vezane na spojine, ki vsebujejo amino in amonijeve skupine. Končne ugotovitve kažejo, da je kationska predobdelava z dvema od treh uporabljenih sredstev povečala vezanje barvila iz barvalne kopeli na bombažno tkanino. Hkrati lahko kationsko sredstvo podeli obdelani bombažni tkanini protibakterijsko zaščito pred dvema različnima vrstama bakterij, tj. *E. coli* in *S. warneri*. Raziskava prikazuje možnost funkcionalizacije tekstilij med optimizacijo postopka barvanja in lahko služi kot primer za nadaljnjo praktično uporabo.

Ključne besede: obarvanje, barvanje, protibakterijski, kationske spojine

Corresponding author/Korespondenčni avtor:

Prof dr. Boris Mahltig

E-mail: boris.mahltig@hs-niederrhein.de

Tel.: +49-2161-186-6128

ORCID: 0000-0002-2240-5581

Tekstilec, 2020, **63**(1), 27-37

DOI: 10.14502/Tekstilec2020.63.27-37

## 1 Introduction

The dyeing of cotton can be performed using various dyes from different dyestuff categories, i.e. as vat dyes, direct dyes or reactive dyes. Among all dyestuffs, reactive dyes are supposed to lead to the best wash fastness of coloration on cotton fabrics. However, it should be kept in mind that one problem of dyeing of cotton with reactive dyes is the hydrolysis of the reactive dye in the dye bath. In simple terms, a reactive dye can be understood as a dye molecule containing three parts with different functions. These are the chromophore, the reactive anchor and charged ionic groups. While the chromophore is responsible for coloration, the reactive anchor supports covalent bonding between dye molecules and the cotton fibre surface. The ionic groups result in solubility in a water-based dye bath. In acid dyes, anionic charged groups are also responsible for the attractive interaction between the acid dye and cationic wool or polyamide fibres. Wool and polyamide fibres contain a positive net charge due to the protonation of containing amino groups. Acid dyes contain a negative charge. For this reason, wool and polyamide fibres support a certain electrostatic attraction to the acid dye, thus supporting the dyeing process and dye fixation. The ionic attraction of anionic groups in reactive dyes to positively charged groups can be analogously used to improve the dyeing performance of reactive dyes [1]. For this purpose, cationic functional groups must be introduced to the cellulosic structure of the cotton fibre. A cotton fabric treated with cationic agents obtains positive charges on the cotton fibre surface. If a reactive dye containing anionic groups is then applied to this cationised cotton, the dyeing process can be supported analogously to the dyeing process of wool using an acid dye. In literature, many different procedures are described for the introduction of cationic groups to the cotton fibre surface.

Quaternary ammonium compounds are fixed to cotton using an epoxy anchor. For subsequent dyeing with acid dyes and reactive dyes, improved dyeing properties were observed [2]. In these experiments, the increased dye up-take was directly correlated to the amount of previously applied quaternary ammonium groups [3]. Instead of an epoxy anchor, the quaternary ammonium compound can also be anchored to cotton using a chlorine hydroxyl propyl group [4]. In this way, an

ionic attraction between dye molecules and cationised cotton was introduced. Improved colour-depth can be achieved for the application of different reactive dyes [4]. In addition, polymers with quaternary ammonium groups can be used for cotton pretreatment [5]. In an example by Blackburn et al., quaternary ammonium groups were part of an aliphatic ring system attached to the backbone of the polymer. Here, an increase in colour depth after dyeing with reactive dyes was also observed [5]. As a special cationic polymer, commercially available cationic starch can also be used for the modification of cotton [6, 7]. The application of this cationic polyelectrolyte improves the dye-fibre interaction. The improved dye up-take in this case is caused by the presence of cationic groups and the increased fibre roughness as the result of the applied starch [6]. In addition to these polymers with quaternary groups, polymers with amino groups can also be used for the modification of cotton. For this purpose, the chloride salt of polyvinylamine is used to improve the dyeing process of cotton with reactive dyes [8]. A cationic pretreatment is also used to improve the dyeability of cotton with natural dyes [9, 10]. If natural dyes contain negatively charged functional groups or groups that can gain a negative charge easily through deprotonation under moderate alkaline conditions, they probably show an electrostatic attraction to positively charged cationised cotton fibres, as well. For this reason, the dyeing process is improved. This phenomenon is probably the same for the application of a negatively charged reactive dye on cationised cotton textiles.

In addition to the influence of dyeing properties, quaternary ammonium containing cationic compounds are often mentioned for their antibacterial effects on textile substrates [11-15]. A special type of antibacterial active quaternary ammonium compounds is based on the cationically modified nitrogen component DABCO (1,4-Diazabicyclo(2.2.2)octan), which is a cyclic nitrogen compound [16]. For the achievement of antibacterial effects, not only the antibacterial effects of quaternary compounds have been reported; other nitrogen containing compounds such as PHMB (polyhexanid) have also been reported [11]. The antibacterial effect of PHMB is related to the presence of an amino group attached to the polymer structure. Another prominent antibacterial polymer containing amino groups is bio-based

chitosan [17-19]. The antibacterial activity in such cases is often related to the acidic conditions of the surrounding medium due to the necessary protonation of the containing amino group [20]. In addition to bio-based chitosan, synthetic polymers containing an amino group are also known for their antibacterial activity. A prominent example in this area are dendrimers with terminated amino groups [21].

Reactive dyes equipped with cationic groups can be used to introduce antibacterial properties to cellulosic fibres. In this reported application, coloration and antibacterial functions are achieved at once through the application of a single compound [22]. As an alternative to cationic nitrogen compounds, simple amino compounds can also be used to introduce antibacterial properties to textiles. An example is the application of polyvinylamine for the functionalisation of fabrics made from high-performance polyethylene [23].

With this background, the purpose of the presented study was to evaluate different cationic pretreatments for cotton with the aim of simultaneously improving dyeability with reactive dyes and achieving antibacterial properties. For the actual evaluation, three different commercially available cationic substances were chosen and applied in increasing concentrations onto cotton substrates. The dyeability of modified cotton was tested through the application of a vinyl sulfone reactive dye that contained two anionic groups. The antibacterial properties were tested against two different bacteria before and after the dyeing process. The achieved results were promising and showed that a cationic pretreatment can be used for simultaneous and different modifications of cotton fabrics.

## 2 Experimental section

### 2.1 Materials and sample preparation

For all sample preparations, a plain weaved cotton fabric with a weight of 150 g/m<sup>2</sup> was used. This cotton fabric was treated with three different cationic agents applied in three different concentrations to determine their influence on the subsequent application of a reactive dye. These cationic agents were RUCO-PUR SEC, supplied by Rudolf GmbH (Geretsried, Germany), RUCO BAC HSA, also supplied by Rudolf GmbH (Geretsried, Germany), and PERFIXAN F 5000, supplied by Textilchemie Dr Petry GmbH (Reutlingen, Germany). All these

chemicals were supplied as water-based solutions and further diluted with water as recommended by the suppliers. The aqueous cationic agent RUCO-PUR SEC was named the hydrophilic agent. It is cationically active and based on polyurethane and silicone compounds. This agent was further diluted with water to a concentration of 30, 45 or 60 g/L. The pH value was adjusted to 4.5 by adding acetic acid. The agent RUCO BAC HSA is an aqueous solution of the quaternary ammonium compound - dimethyl-tetradecyl (3-(trimethoxysilyl)propyl) ammonium chloride - and was distributed as the cationic antibacterial agent. This agent was further diluted with water to concentrations of 2, 11 or 20 g/L. The pH value was adjusted in the range of 4.5 to 5.0 by adding acetic acid. The agent PERFIXAN F 5000 is described as pre-cationising agent recommended for denim articles and for dyeing procedures with anionic dyes. It is an aqueous solution of a polyamine component containing a pH 2.5 to 3.5. For application, this agent was further diluted with water to a concentration of 20, 40 or 60 g/L. Of course, cotton fibres can be damaged under strong acidic conditions, but the agent used, PERFIXAN F 5000, was not applied as a pure substance. It was applied in concentrations of between 20 to 60 g/L after dilution with water. The acidity of the applied agent was decreased by this dilution, so potential damage to cotton fibres was minimised. The used concentrations for these studied cationic agents were based on the recommendation of the suppliers of these chemicals. All cationic agents were applied in an HFR 46292 padding machine supplied by Werner Mathis AG (Oberhasli, Switzerland). After application, drying was performed at 140 °C for 60 seconds using an OHE 4408787 lab dryer supplied by Werner Mathis AG. For the production of a reference sample, analogous treatment by padding the cotton fabric with pure water was carried out.

Dyeing was performed using the Reactive Black 5 (RemazolBlack B; CAS 17095-24-8) dye with the sum formula of C<sub>26</sub>H<sub>21</sub>N<sub>5</sub>Na<sub>4</sub>O<sub>19</sub>S<sub>6</sub> and a molecular weight of Mw 991.8 g/mol. The company Clariant (Frankfurt am Main, Germany) supplied this dye. The chemical structure of the dye is presented in Figure 1 and its full name is Tetrasodium 4-amino-5-hydroxy-3,6-bis[[4-[[2-(sulphonatooxy)ethyl]sulphonyl]phenyl]azo]naphthalene-2,7-disulphonate.

For dyeing purposes, an aqueous dye bath containing the following components was used: Reactive Black

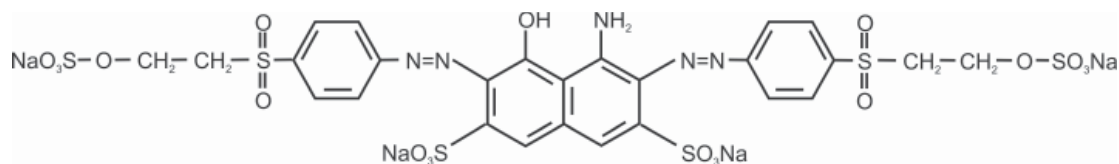


Figure 1: Chemical structure of the used Reactive Black 5 (Remazol BlackB) dye;  $C_{26}H_{21}N_5Na_4O_{19}S_6$

dye (5.3 g/L), NaOH (0.68 g/L),  $Na_2SO_4$  (65 g/L) and  $Na_2CO_3$  (25 g/L). To prepare the dye bath, 3 g of Reactive Black dye was first dissolved in 70 mL of hot water. After that, 65 g of  $Na_2SO_4$  was added and dissolved. Then 25 g of  $Na_2CO_3$  was added and dissolved. Finally, 0.68 g of NaOH was added and dissolved, and the vessel was filled with water until 1 L was reached. The bath ratio was set to 1:10 (1g fabric to 10 g dye bath). The concentration of the used reactive dye was 5.3 g/L or 0.53 weight-% in relation to the volume of the dye bath. In relation to the amount of treated cotton textile, the amount of dye was 5.3 weight-%. The dyeing process was performed in an Ahiba Polymat (model PM10) dyeing machine. The process temperature for dyeing was 60 °C, which was applied for 100 minutes, followed by heating for 10 minutes. After the dyeing procedure, the fabrics were rinsed with cold water, followed by a washing cycle at 95 °C for 5 minutes. That washing was performed in an S014.95 washing machine supplied by Werner Mathis AG. At the end, the fabrics were line-dried at room temperature.

## 2.2 Analytics

The remaining dye concentration in the dye bath after the dyeing process was determined. For this purpose, samples were taken from the dye bath after the dyeing process was completed. A total of 1.5 g of the remaining dye solution was taken and diluted with 8.5 g water. The absorption spectra of this solution were determined using a UV-2600 photo spectrometer from Shimadzu (Japan) in an arrangement of direct transmission. The coloration of prepared dyed textiles was studied using the same photo spectrometer with an integrated sphere and by measuring diffusive reflection. The colour properties were recorded as K/S-spectra. In order to determine K/S-spectra, the reflection spectrum was first measured in an arrangement of diffusive reflection. This reflection spectrum was transferred using the Kubelka-Munk function into a K/S-spectrum, which demonstrated the absorption of light for the studied textile sample as a function of the wavelength of light. A barium

sulphate plate was used as white reference material for these reflective measurements. In addition, the difference in the colour strength of the dyed fabrics with cationic pretreatment was determined using a Datacolor 400 colorimeter with a D65 light source (Datacolor, Luzern). For these measurements, the fabrics were folded into four layers. As a reference sample, the dyed cotton fabric without cationic pretreatment was used and set to a value of 100%. The FT-IR spectra of cotton samples were recorded using an Excalibur 3100 IR-spectrometer (Varian Inc.).

Bacterial viability was determined by using 3-(4,5-dimethylthiazol-2-yl)-2,5-diphenyltetrazolium bromide (MTT) as previously reported [24]. In brief, *E. coli* (strain BL21(D3)) and *S. warneri* (strain dsm-20316) were cultured in a Luria-Bertani (LB) medium or in a Trypticase Soy Yeast Extract (TYSE) medium, respectively. For the experiments, 200  $\mu$ l bacterial suspensions (1:250 dilution of an overnight culture) per cavity were seeded in sterile 96-multiwell cell culture plates (Techno Plastic Products AG, Trasadingen, Switzerland). Cells were grown in the presence of textile samples (circles with 5 mm diameter prepared using a conventional hole puncher) for 3 hours at 37 °C and rotated at 250 rpm in a PST-60-HL-4 orbital shaker (BioSan, Riga, Latvia). The cells were then incubated with MTT (final concentration 0.1 mg/l) in their respective culture media for 5 minutes, lysed in isopropanol for an additional 30 minutes, and their viability determined by measuring absorption at 570 nm with a reference wavelength of 700 nm on a Tecan M200 multiwell-plate reader (Tecan, Crailsheim, Germany). Control viability was measured in a test arrangement in the absence of any textile fabric, but otherwise identical to the other samples and set to 100%. The absorption determined with the same setup in the absence of bacteria was set to 0%. The antibacterial tests were repeated four times for each sample. The average of the repeated measurements was given as the remaining bacterial viability.



### 3 Results and discussion

#### 3.1 Preliminary investigations before dyeing

As preliminary experiments before dyeing, FT-IR spectroscopy and UV/Vis spectroscopy were performed on untreated cotton fabrics and on fabrics after application of the cationic agent. FT-IR spectroscopy was performed to determine whether the applied cationic agent can be detected on cotton fabrics. The measured FT-IR spectra are shown together in Figure 2. The determined spectrum from the untreated cotton fabric exhibited a similar shape compared to cotton spectra reported in literature [25]. The prominent peaks were from the stretch vibrations of the C-O bond, C-H bond and the O-H, with maxima at the wavenumbers  $1053\text{ cm}^{-1}$ ,  $2897\text{ cm}^{-1}$  and  $3329\text{ cm}^{-1}$ . The FT-IR spectra of samples after application of cationic agents were prepared for preparation with the highest applied concentration of these agents. For the RUCO BAC HSA agent, a nearly similar FT-IR spectrum compared to cotton was recorded. It is thus not possible to detect this agent on cotton using this spectroscopic method. The RUCO BAC HSA agent contained a quaternary ammonium group. This group was related to C-N bonds with stretch vibrations in the range of  $1020$  to  $1220\text{ cm}^{-1}$  [26]. However, an especially strong signal from the cotton substrate with the C-O vibration also appeared in this region. It is thus probable that the signal from the cotton substrate covered the signal of the added RUCO BAC HSA agent. For the RUCO-PUR SEC agent, a nearly similar FT-IR spectrum compared to cotton was recorded. Only one weak peak in the fingerprint area at  $779\text{ cm}^{-1}$  was

identified and not detected in the pure cotton fabric. According to literature, this peak can be caused by a Si-C vibration in an OSi-CH<sub>3</sub> group [26]. This result is in line with supplier information that this agent also contains silicone compounds.

For the PERFIXAN F 5000 agent, the peak at a wavenumber of  $1639\text{ cm}^{-1}$  exhibited an increased intensity, while a new peak with a weak intensity appeared at  $1543\text{ cm}^{-1}$ . This agent was based on polyvinylamine and contained amine groups that were related to C-N bonds with stretch vibrations in the range of  $1020$  to  $1220\text{ cm}^{-1}$  and N-H bonds with stretch vibrations close to  $3335\text{ cm}^{-1}$  [26]. However, both areas were covered by several strong vibration signals of the cotton substrates itself. The stronger signal at  $1639\text{ cm}^{-1}$  and the new signal at  $1543\text{ cm}^{-1}$  can be explained by the presence of amide groups in this agent. Polyvinylamine was prepared through the degradation of polyacrylamide [27, 28]. If this degradation is not complete, there would be remaining amide groups in this polymer that could be detected using IR-spectroscopy.

To evaluate the colour properties of textiles after the dyeing process, the K/S-UV/Vis spectra of undyed cotton fabrics with and without cationic treatment were determined (Figure 3). This measurement was done to determine whether the applied cationic agents can affect the colour properties of the treated cotton fabrics by themselves. All these undyed cotton fabrics exhibited low K/S-values in the range of visible light ( $400\text{ nm}$  to  $750\text{ nm}$ ) of only 0.1. These textiles were mainly uncoloured and the cationic treatment did not affect coloration. In the range of

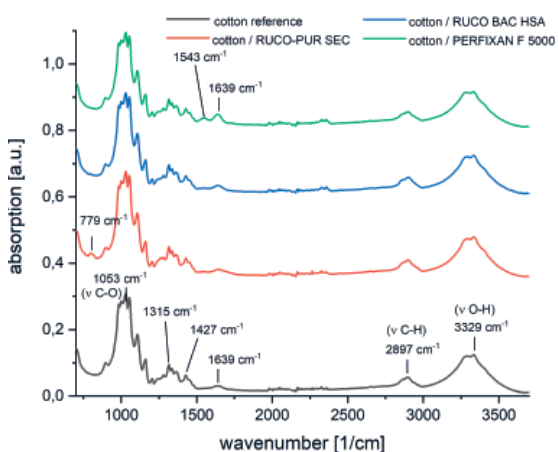


Figure 2: FT-IR spectra of cotton fabric before and after the application of cationic agents. Most prominent peaks are marked with related wavenumbers.

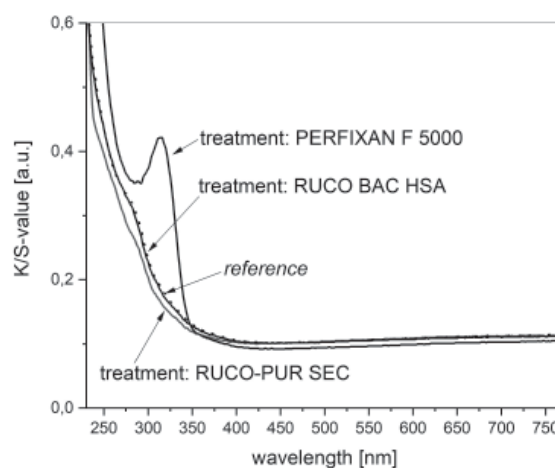


Figure 3: K/S-spectra of cotton fabrics before and after treatment with different cationic agents

UV-light, the cotton treated with PERFIXAN F 5000 exhibited a significant maximum at around 320 nm. This maximum was probable related to aromatic structures in the applied cationic component.

### 3.2 Dyeing properties and coloration results

Before determining the colour properties of dyed fabrics, the absorption spectra of the dye bath after the dyeing processes were measured (Figure 4). This measurement was taken to determine the remaining dye in the dye bath and for the dye not taken up by the dyed cotton fabric. The determined absorption spectra were compared with a reference spectrum achieved for an analogous dyeing procedure performed with the same cotton fabric, but without any cationic treatment. Absorption spectra with lower absorption values compared to this reference spectrum indicated an increased dye up-take from the dye bath by the cationised cotton. Different results were obtained for the three different types of cationic pretreatment (Figure 4). Treatment with the RUCO-PUR SEC agent led to a lower applied concentration of cationic agent and to higher absorption values in the remaining dye bath. Only in the case of the highest applied concentration of 60 g/L RUCO-PUR SEC was nearly the same absorption as the reference observed. For this reason, no improvement of dye up-take could be achieved in the applied dyeing procedure with RUCO-PUR SEC. In contrast, a significant decrease in dye concentration in the remaining dye bath was achieved with cotton pretreatment using RUCO BAC HSA (intermediate or high concentration) or using the PERFIXAN F 5000 (with all concentrations) agent. Here, it is probable that the up-take of dye by the cationic cotton increased. The up-take of the reactive dye was significantly affected by the type of cationic treatment performed on the cotton fabric in advance.

The colour properties of dyed cotton fabrics were determined as colour intensity (Figure 5) and K/S-spectra (Figure 6). The colour intensity was given as a percentage in relation to the coloration of cotton dyed without previous cationic treatment. This reference value was set to 100% (Figure 5). The determined colour intensity was seen as a function of the concentration of applied cationic agents. Treatment with the RUCO-PUR SEC agent led to the lower coloration of cotton fabric compared with the dyeing procedure using untreated cotton. Increasing

the concentration of RUCO-PUR SEC also led to an increase in colour intensity. However, even with the highest concentration for pretreatment with RUCO-PUR SEC, the same colour intensity as the reference untreated cotton sample could not be achieved. These results are in line with the remaining high dye concentration in the remaining dye bath. It can thus be said that this cationic agent cannot be used to improve the dyeing procedure for the studied reactive dye on cotton. In fact, this result is in some way surprising because the cationic active RUCO-PUR SEC agent should have improved the up-take of the applied reactive dye. A possible explanation could be that the number of cationic sides in this agent was not as high as the other studied additives. Thus, the effect on dyeing behaviour with the studied reactive dye is not strong.

In contrast, the coloration result of subsequent dyeing improved with pretreatment using the other two cationic agents. For both products, the colour intensity increased as a function of the concentration of the cationic component used for pretreatment. However, the type of increase was different (Figure 5). For the RUCO BAC HSA agent with the lowest concentration, an initial decrease in colour intensity was identified. The colour intensity was then continuously increased by increasing the concentration of this agent. For the PERFIXAN F 5000 agent, pretreatment with a medium to high concentration led to only a minor subsequent increase. A kind of plateau value could thus be estimated.

The evaluation of the K/S-spectra of the dyed samples completed this picture (Figure 6). The K/S-spectra for dyed samples after RUCO-PUR SEC pretreatment were very similar to the reference spectrum of a sample without any pretreatment. Here, almost no change in coloration was caused by the cationisation of cotton with this type of cationic compound. Using a pretreatment of RUCO BAC HSA, a significant increase in the K/S-values using the cationic treatment was observed. The reference sample exhibited a maximum K/S-value of 17.0 at 606 nm. The samples with RUCO BAC HSA pretreatment achieved a maximum K/S-value of 19.4 at 597 nm. Treatment with PERFIXAN F 5000 also resulted in a high K/S-value of 19.7. However, there was also a stronger significant shift in the position of the maximum to a wavelength of 590 nm. This shift indicated that not only colour intensity but also colour shade changed as the result of the applied cationic treatment.

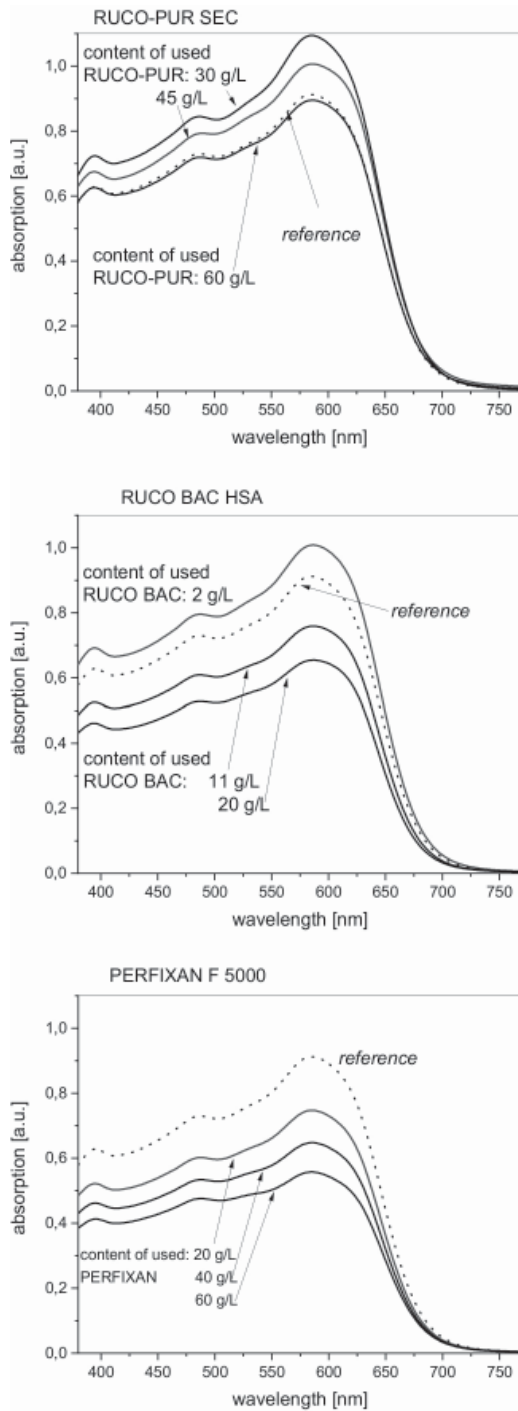


Figure 4: Absorption spectra of dye baths after the dyeing process. Compared are the spectra of dye baths after the dyeing of an untreated cotton reference and cationised cotton fabrics. The amount of applied cationic agent for the pretreatment of cotton is directly observable in the graphs. In order to record the spectra, the dye bath was diluted with water in a ratio of 15:85.

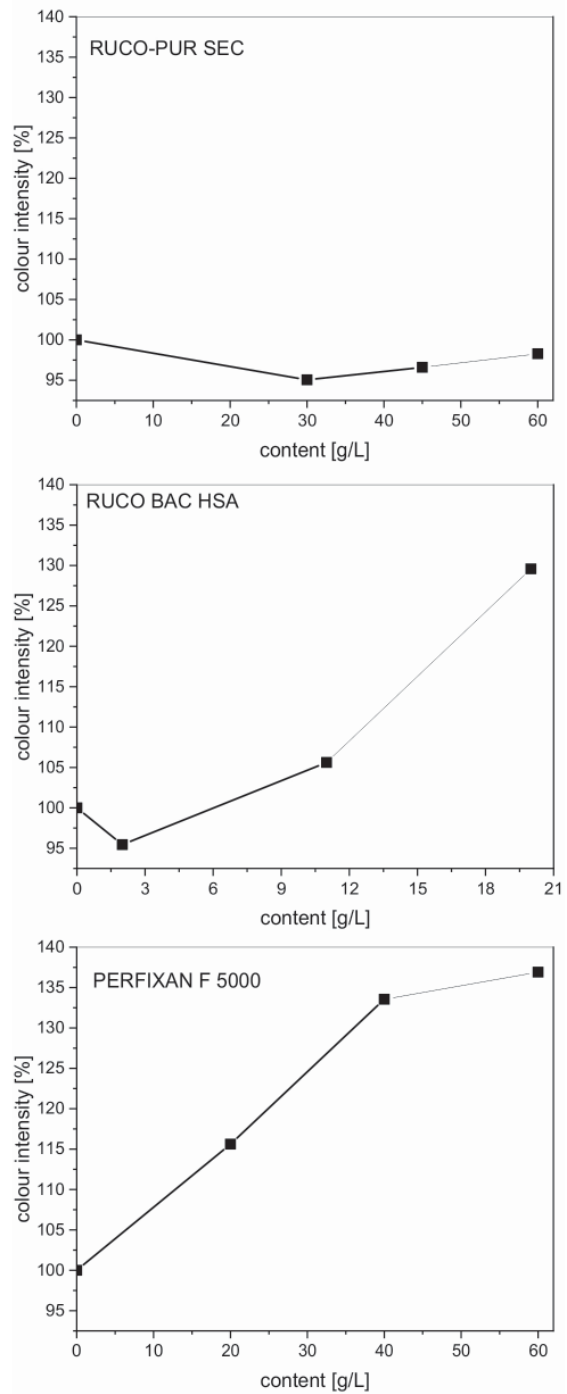


Figure 5: Colour intensity of dyed cotton fabrics with different pretreatments in relation to a reference cotton fabric dyed without any pretreatment. The colour intensity is shown as a function of the concentration of the cationic agent used for pretreatment.

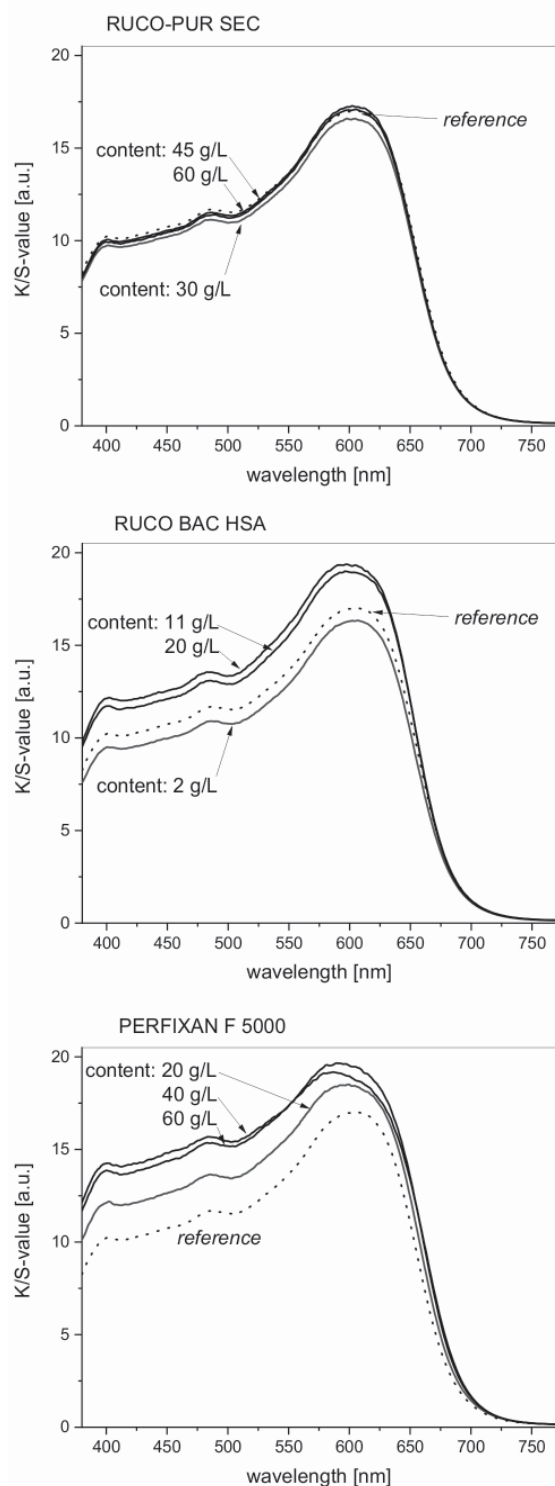


Figure 6: K/S-spectra of dyed cotton fabrics. The spectra are related to different pretreatments of the dyed cotton with different chemicals in increasing concentrations. The observed reference spectrum is for a cotton fabric without any cationic treatment.

### 3.3 Antibacterial properties

Antibacterial properties were studied against two types of bacteria: *E. coli* and *S. warneri* (Figure 6). The remaining bacterial viability was shown as a function of an increase in the concentration of the applied cationic agent. For all samples, bacterial viability was compared before and after the dyeing process (Figure 7). A value of 100% for bacterial viability represented the reference testing procedure without the addition of any textile sample.

In the presence of the pure cotton sample without any further treatment or dyeing, a remaining bacterial viability for *E. coli* of 79% and for *S. warneri* of 80% was determined. In the case of dyeing cotton without a cationic agent, values for the bacterial viability for *E. coli* of 75% and for *S. warneri* of 74% were observed. This small decrease in viability after dyeing was in the range of the standard deviation of this test arrangement. The applied dye thus had no probable antibacterial effect.

Compared with these reference measurements without a cationic agent, the effect achieved with cationic treatment was different, depending on the type of cationic agent applied (Figure 7). With the application of even the highest concentration of the PERFIXAN F 5000 agent, no decrease in bacterial viability was identified. This agent exhibited no clear antibacterial properties. According to supplier information, the Perfixan agent is related to the chemical structure of polyvinylamine. As a result, this agent is supposed to contain a large number of amino groups. Such amino group containing compounds often contain antibacterial properties. These antibacterial properties are related to an acidic medium leading to the protonation of the amino groups. However, the antibacterial tests were performed under neutral conditions. It should also be clear that amino containing compounds can be antibacterial, while not all chemicals containing amino groups are antibacterial. Good examples of amino containing groups without antibacterial properties are ordinary amino acids and proteins.

An effect against *S. warneri* was observed with the RUCO-PUR SEC agent at the highest applied concentration. In this case, a bacterial viability of only 27% was identified. That value then rose to 60% after the dyeing was performed. This antibacterial effect was clearly seen, but was not very strong. The loss in antibacterial activity after dyeing can



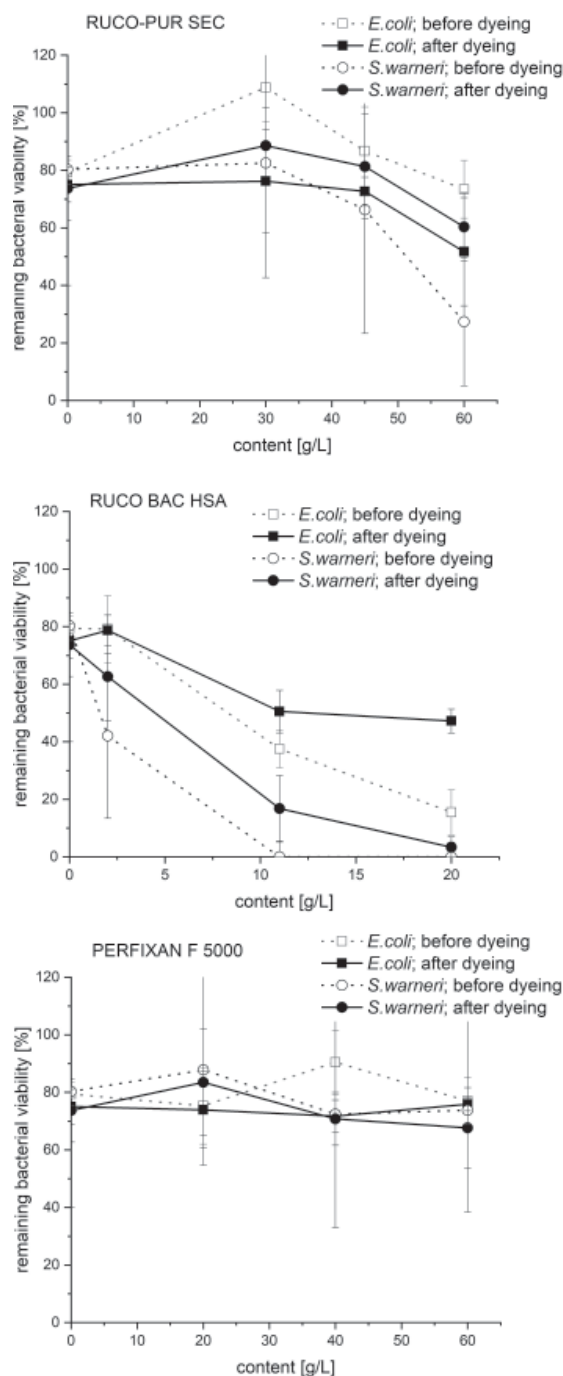


Figure 7: Antibacterial properties of differently pretreated cotton fabrics before and after the dyeing process. The antibacterial property is shown as the remaining bacterial viability as a function of the concentration of the cationic agent used for the treatment of cotton fabrics. The bacterial viability is shown as average of four independent measurements. The error bars indicate the standard deviation of this measurement.

be explained by the removal of some of the cationic agent during the dyeing process. If the RUCO-PUR SEC agent was applied in the lowest concentration of 30 g/L, a small increase in bacterial viability for the bacteria *S. warneri* was observed. This small increase in bacterial viability with the lowest RUCO-PUR SEC concentration was in the range of standard variation for this measurement and did not indicate that this agent could support the growth of bacteria in low concentrations.

In the presence of the cationic RUCO BAC HSA agent, the antibacterial effect was significant against both tested bacteria types: *E. coli* and *S. warneri* (Figure 7). That activity was particularly strong against *S. warneri*. This was shown by a remaining bacterial viability of less than 0.5%. This strong effect should be expected because this agent is promoted by the supplier as antibacterial finishing agent. The antibacterial effect decreased when the dyeing process was performed. However, the effect is still excellent, even after the dyeing procedure, especially against *S. warneri*. Such a decrease in antibacterial activity after dyeing can be explained by an insufficient fixation of the cationic agent on the cotton surface. For this reason, the RUCO BAC HSA agent is probably removed in part from the cotton samples during the dyeing process, resulting in a decrease in antibacterial activity.

With these results, it can be said that these cationic agents can be used to achieve two effects with only one application. It is possible to simultaneously improve the dyeability of cotton for reactive dyes and to achieve antibacterial properties on the same cotton fabric.

## 4 Conclusion

In conclusion, it can be said that it is possible to introduce two advantageous properties to cotton in one step through pretreatment with cationic agents. Improved dyeability and an antibacterial activity can be achieved together through this simple application. It was also shown, however, that not all cationic agents are useful for improving dyeability or antibacterial effectivity. The simultaneous application of a functional property during an optimised dyeing process was carried out and could serve as an example for further applications.

### Acknowledgements

For helpful discussions and advice in the finishing laboratory, the authors would like to thank Thomas Heistermann (Hochschule Niederrhein, Mönchengladbach, Germany). All product and company names mentioned in this chapter may be trademarks of their respective owners, even without labelling.

### References

1. RISTIĆ, Nebojša, RISTIĆ, Ivanka. Cationic modification of cotton fabrics and reactive dyeing characteristics. *Journal of Engineered Fibers and Fabrics*, 2012, **7**(4), 113–121, doi: 10.1177/155892501200700408.
2. HAUSER, Peter J., TABBA, Adham H. Improving the environmental and economic aspects of cotton dyeing using a cationised cotton. *Coloration Technology*, 2001, **117**(5), 282–288, doi: 10.1111/j.1478-4408.2001.tb00076.x.
3. EL-SHISHTAWY, Reda M., NASSAR, S. H. Cationic pretreatment of cotton fabric for anionic dye and pigment printing with better fastness properties. *Coloration Technology*, 2002, **118**(3), 115–118, doi: 10.1111/j.1478-4408.2002.tb00367.x.
4. MONTAZER, M., MALEK, R.M.A., RAHIMI A. Salt free reactive dyeing of cationized cotton. *Fibers and Polymers*, 2007, **8**(6), 608–612, doi: 10.1007/BF02875997.
5. BLACKBURN, Richard S., BURKINSHAW, Stephen M. Treatment of cellulose with cationic, nucleophilic polymers to enable reactive dyeing at neutral pH without electrolyte addition. *Journal of Applied Polymer Science*, 2003, **89**(4), 1026–1031, doi: 10.1002/app.12226.
6. ALI, Shamshad, MUGHAL, Mohsin Ali, SHOUKAT, Umair, BALOCH, Mansoor Ali, KIM, Seong Hun. Cationic starch (Q-TAC) pre-treatment of cotton fabric: influence on dyeing with reactive dye. *Carbohydrate Polymers*, 2015, **117**, 271–278, doi: 10.1016/j.carbpol.2014.09.064.
7. ZHANG, Shufen, MA, Wei, JU, Benzhi, DANG, Nanyan, ZHANG, Min, WU, Suli, YANG, Jinzong. Continuous dyeing of cationised cotton with reactive dyes. *Coloration Technology*, 2005, **121**(4), 183–186, doi: 10.1111/j.1478-4408.2005.tb00270.x.
8. MA, Wei, ZHANG, Shufen, TANG, Bingtao, YANG, Jinzong. Pretreatment of cotton with poly(vinylamine chloride) for salt-free dyeing with reactive dyes. *Coloration Technology*, 2005, **121**(4), 193–197, doi: 10.1111/j.1478-4408.2005.tb00272.x.
9. TOPIČ, Taja, GORJANC, Marija, KERT, Mateja. The influence of the treatment process on the dyeability of cotton fabric using goldenrod dye. *Tekstilec*, 2018, **61**(3), 192–200, doi: 10.14502/Tekstilec2018.61.192-200.
10. GORJANC, Marija, KERT, Mateja, MUJADZIC, Amra, SIMONČIČ, Barbara, FORTE-TAVČER, Petra, TOMŠIČ, Brigita, KOSTAJNŠEK, Klara. Cationic pretreatment of cotton dyeing with *Fallopia Japonica* leaves. *Tekstilec*, 2019, **62**(3), 181–186, doi: 10.14502/Tekstilec2019.62.181-186.
11. GAO, Yuan, CRANSTON, Robin. Recent advances in antimicrobial treatments of textiles. *Textile Research Journal*, 2008, **78**(1), 60–72, doi: 10.1177/0040517507082332.
12. SIMONČIČ, Barbara, TOMŠIČ, Brigita. Structures of novel antimicrobial agents for textiles – a review. *Textile Research Journal*, 2010, **80**(16), 1721–1737, doi: 10.1177/0040517510363193.
13. ZHU, Ping, SUN, Gang. Antimicrobial finishing of wool fabrics using quaternary ammonium salts. *Journal of Applied Polymer Science*, 2004, **93**(3), 1037–1041, doi: 10.1002/app.20563.
14. MAHLTIG, Boris, FIEDLER, Dirk, BÖTTCHER, Horst. Antimicrobial sol-gel coatings. *J. Sol-Gel Sci. Technol.*, 2004, **32**(1–3), 219–222, doi: 10.1007/s10971-004-5791-7.
15. VASILJEVIĆ, Jelena, TOMŠIČ, Brigita, JERMAN, Ivan, SIMONČIČ, Barbara. Organofunctional trialkoxysilane sol-gel precursors for chemical modifications of textile fibres. *Tekstilec*, 2017, **60**(3), 198–213, doi: 10.14502/Tekstilec2017.60.198-213.
16. DIZMAN, Bekir, ELASRI, Mohamed O., MATHIAS, Lon J. Synthesis and antimicrobial activities of new water-soluble bis-quaternary ammonium methacrylate polymers. *Journal of Applied Polymer Science*, 2004, **94**(2), 635–642, doi: 10.1002/app.20872.
17. ZHANG, Zitao, CHEN, Liang, JI, Jinmin, HUANG, Yanliu, CHEN, Donghui. Antibacterial properties of cotton fabrics treated with chitosan. *Textile Research Journal*, 2003, **73**(12), 1103–1106, doi: 10.1177/004051750307301213.

18. CHUNG, Ying-Chien, CHEN, Chih-Yu. Antibacterial characteristics and activity of acid-soluble chitosan. *Bioresource Technology*, 2008, **99**(8), 2806–2814, doi: 10.1016/j.biortech.2007.06.044.
19. RAHMAN BHUIYAN, M.A., HOSSAIN, M.A., ZAKARIA, M., ISLAM, M.N., ZULHASH UD-DIN, M. Chitosan coated cotton fiber: physical and antimicrobial properties for apparel use. *Journal of Polymers and the Environment*, 2017, **25**(2), 334–342, doi: 10.1007/s10924-016-0815-2.
20. SAHARIAH, Priyanka, MASSON, Mar. Antimicrobial chitosan and chitosan derivatives: a review of the structure-activity relationship. *Biomacromolecules*, 2017, **18**(11), 3846–3868, doi: 10.1021/acs.biomac.7b01058.
21. CLABRETTA, Michelle K., KUMAR, Amit, MC-DERMOTT, Alison M., CAI, Chengzhi. Antibacterial activities of poly(amidoamine) dendrimers terminated with amino and poly(ethylene glycol) groups. *Biomacromolecules*, 2007, **8**(6), 1807–1811, doi: 10.1021/bm0701088.
22. ZHAO, Tao, SUN, Gang, SONG, Xinyuan. An antimicrobial cationic reactive dye: synthesis and applications on cellulosic fibers. *Journal of Applied Polymer Science*, 2008, **108**(3), 1917–1923, doi: 10.1002/app.27859.
23. NATARAJAN, HariharaSudan, HAASE, Hajo, MAHLTIG, Boris. Polyvinylamine application for functionalization of polyethylene fiber materials. *Journal of the Textile Institute*, 2017, **108**(4), 615–621, doi: 10.1080/00405000.2016.1177246.
24. HAASE, Hajo, JORDAN, Lisa, KEITEL, Laura, KEIL, Claudia, MAHLTIG, Boris. Comparison of methods for determining the effectiveness of antibacterial functionalized textiles. *PLoS ONE*, 2017, **12**(11), e0188304, 1–16, doi: 10.1371/journal.pone.0188304.
25. FLESNER, Jessica, MAHLTIG, Boris. Fibers from natural resources. In *Handbook of Composites from Renewable Materials. Vol. 4: Functionalization*. Edited by V. K. Thakur, M. K. Thakur and M. R. Kessler. Beverly : Scrivener Publishing, 2017, pp. 287–310, doi: 10.1002/9781119441632.ch73.
26. GÜNZLER, Helmut, GREMLICH, Hans-Ulrich. *IR Spectroscopy*. Weinheim : Wiley, 2002.
27. TANAKA, Hiroo, SENJU, Ryoichi. Preparation of polyvinylamine by the homann degradation of polyacrylamide. *Bulletin of the Chemical Society of Japan*, 1976, **49**(10), 2821–2823, doi: 10.1246/bcsj.49.2821.
28. EL ACHARI, Ahmida, COQUERET, Xavier, LABLACHE-COMBIER, Alain, LOUCHEUX, Claude. Preparation of polyvinylamine from polyacrylamide. *Die Makromolekulare Chemie*, 1993, **194**(7), 1879–1891, doi: 10.1002/macp.1993.021940703.

Elise Diestelhorst<sup>1</sup>, Fjoralba Mance<sup>2</sup>, Al Mamun<sup>1</sup>, Andrea Ehrmann<sup>1</sup>

<sup>1</sup> Bielefeld University of Applied Sciences, Faculty of Engineering and Mathematics, Interaktion 1, 33619 Bielefeld, Germany

<sup>2</sup> Polytechnic University of Tirana, Faculty of Mechanical Engineering, Textile and Fashion Department, Tirana, Albania

---

# Chemical and Morphological Modification of PAN Nanofibrous Mats with Addition of Casein after Electrospinning, Stabilisation and Carbonisation

*Kemijska in morfološka modifikacija PAN nanovlaknatih kopren z dodanim kazeinom po elektrospedenju, stabilizaciji in karbonizaciji*

Original scientific article/Izvirni znanstveni članek

Received/Prispelo 12-2019 • Accepted/Sprejeto 2-2020

---

## Abstract

Electrospun polyacrylonitrile (PAN) nanofibrous mats belong to typical precursor materials of carbon nanofibres. They have, however, the problem that they need to be fixed or even stretched during stabilisation and ideally also during carbonisation in order to avoid undesired conglutinations and deformations of the original nanofibre morphology, resulting in brittle behaviour of the macroscopic nanofibrous mat, which impedes several applications. In an earlier investigation, blending PAN with ZnO was shown to increase fibre diameters and lead to unproblematic stabilisation and carbonisation of nanofibrous mats. ZnO, on the other hand, may have a negative impact on biotechnological applications such as tissue engineering. Here, we thus report on the morphological and chemical modifications due to blending PAN electrospinning solutions with different amounts of casein. By optimising the PAN : casein ratio, relatively thick, straight nanofibres are obtained, which can be stabilised and carbonised unambiguously, without the well-known negative impact on cell adhesion due to the addition of ZnO.

Keywords: electrospinning, polyacrylonitrile (PAN), casein, nanofibrous mat, stabilisation, carbonisation, tissue engineering

## Izvleček

*Elektrospedene nanovlaknate koprene iz poliakrilonitrila (PAN) predstavljajo tipične prekurzorje za izdelavo ogljikovih nanovlaken. Med stabilizacijo in po možnosti tudi med karbonizacijo morajo biti pritrjene, da bi lahko preprečili neželjeno zlepljenje in deformacijo prvotne nanovlaknate oblike, ki vodi v krhkost makroskopske nanovlaknate koprene in zmanjša možnosti njene uporabe. V predhodni raziskavi je bilo ugotovljeno, da mešanje PAN z ZnO vpliva na povečanje premera vlaken in omogoči stabilizacijo ter karbonizacijo nanovlaknatih kopren. ZnO pa lahko po drugi strani negativno vpliva na biotehnoške aplikacije, kot je tkivni inženiring. V članku so zato predstavljene morfološke in kemijske modifikacije, ki so bile dosežene z uporabo predilnih raztopin za elektrospedenje PAN z dodatkom različnih količin kazeina. Z optimizacijo razmerja PAN : kazein dobimo relativno debela, ravna nanovlakna, ki jih je moč stabilizirati in karbonizirati, brez da bi zaradi dodatka ZnO prišlo do dobro znanega negativnega vpliva na celično adhezijo.*

*Ključne besede: elektrospedenje, poliakrilonitril (PAN), kazein, nanovlaknata koprena, stabilizacija, karbonizacija, tkivni inženiring*

---

Corresponding author/Korespondenčna avtorica:

Prof. Dr. Dr. Andrea Ehrmann

E-mail: andrea.ehrmann@fh-bielefeld

Tekstilec, 2020, **63**(1), 38-49

DOI: 10.14502/Tekstilec2020.63.38-49



## 1 Introduction

Electrospinning can be used to prepare nanofibrous mats with fibre diameters between some ten and several hundred nanometres up to few micrometres [1, 2]. Different technologies exist, from needle-based processes using a syringe to press a polymer through the needle into an electric field to coated high-voltage electrodes in the shape of wires or rotating cylinders to free surface electrospinning [3–5]. Diverse polymers can be electrospun, e.g. biopolymers such as poly(ethylene oxide) [4], gelatine [6] or chitosan [7], but also other polymers such as polycaprolactone [8], poly(vinyl alcohol) [9] or polyacrylonitrile (PAN) [10], as well as blends with different polymers and non-polymeric nanoparticles [11].

PAN is of high interest for electrospinning not only as it can be electrospun from the low-toxic solvent dimethyl sulfoxide (DMSO), but also as it is a typical precursor for carbon nanofibres [12–14]. Such carbon nanofibres can be used as fillers in composites, but due to their conductive properties also as parts of batteries, supercapacitors or dye sensitized solar cells [13, 15–17].

To prepare carbon nanofibres from electrospun PAN nanofibres, it is necessary to firstly stabilise the nanofibrous mat in air, resulting in cyclisation, oxidation, crosslinking and dehydrogenation [18–20]. While diverse heating rates and stabilisation temperatures are discussed in the literature, this process always presents the problem of dimensional changes of nanofibrous mats and fibres themselves. Conglutinations between neighbouring fibres can occur depending on the stabilisation process parameters [21–23]. In addition, the shape of fibres can be strongly deformed from thin, straight nanofibres to thicker, shorter and meandering fibres [24, 25].

Typically, this problem is solved with mechanical solutions [13, 25–27]. In previous research, PAN/ZnO nanofibrous mats resulted in significantly thicker fibres which were nearly unmodified by stabilisation and carbonisation without any mechanical fixing [28], while a similar amount of TiO<sub>2</sub> in the PAN spinning solution did not significantly modify the nanofibres after electrospinning and thermal post-treatments [24]. PAN/gelatine nanofibres, on the other hand, were again much thicker after electrospinning and allowed for stabilisation without mechanical fixing [25].

Here, we report on another blend of PAN and a biopolymer, i.e. casein, for electrospinning. Casein was chosen since it can simply be gained from waste milk and is thus abundantly available [29]. In addition, casein is known to be electrospinnable with different materials as spinning agents [30–32]. Nevertheless, only few reports on PAN/casein electrospun nanofibres can be found in the scientific literature [11]. It is thus of technological interest whether casein can be used to modify PAN nanofibrous mats. We showed that carefully optimising the PAN : casein ratio results in straight, relatively thick nanofibres which can be unambiguously stabilised and carbonised, offering another route to prepare carbon nanofibres, or desired dimensions and morphology. While this effect could also be reached with PAN/ZnO and PAN/gelatine blends [25, 28], the second aim of our study was to find new blends without the cytotoxicity of ZnO to prepare new substrates for tissue engineering or generally cell growth besides PAN/gelatine, which is partly molten during sterilisation by autoclaving at 121 °C [33]. Casein is relatively stable in this temperature range [34] and may thus be an interesting blend for PAN, possibly supporting cell growth similar to gelatine [33] without losing the nanofibrous structure. Combined with the aforementioned material-related approach, another aim was using sufficiently mechanically stable carbon nanofibrous mats as conductive substrates for tissue engineering, which has often been reported in the literature as advantageous for diverse cell types [35].

## 2 Materials and methods

The wire-based electrospinning machine “Nanospider Lab” (Elmarco Ltd., Liberec, Czech Republic) was used to prepare nanofibrous mats with the following spinning parameters: voltage 80 kV, nozzle diameter 0.8 mm, carriage speed 100 mm/s, bottom electrode/substrate distance 240 mm, ground electrode/substrate distance 50 mm, temperature in the chamber 22–23 °C, and 32–33% of relative humidity in the chamber. A polypropylene (PP) nonwoven was used as the substrate to catch the nanofibres approaching the grounded upper wire.

The spinning solutions of 10 mg overall mass contained PAN (X-PAN, Dralon GmbH, Lingen, Germany), partly casein (according to Hammarsten, purchased from VWR Chemicals, Radnor, Pennsylvania,

USA) and DMSO as solvent (DMSO, min. 99.9%, purchased from S3 Chemicals, Bad Oeynhausen, Germany). Two different amounts of PAN (i.e. 1.6 g and 1.38 g) were combined with four different amounts of casein (i.e. 0 g, 0.1 g, 0.2 g, 0.4 g), overall resulting in eight spinning solutions, of which the combination of 1.6 g PAN and 0.4 g casein could not be electrospun due to its high viscosity. The amounts of PAN were chosen in the range that is typical of the pure material, i.e. between approximately 14% and 16%, while lower concentrations of pure PAN usually result in beads along the fibres [36].

Parts of all samples were afterwards stabilised in a muffle oven B150 (Nabertherm, Lilienthal, Germany), approaching the typical stabilisation temperature of 280 °C with the heating rate of 1 K/min [14, 24, 25]. Parts of the stabilised samples were afterwards carbonised at 500 °C or 800°, respectively, approached with the heating rate of 10 K/min in a furnace (Carbolite Gero, Neuhausen, Germany) under the nitrogen flow of 150 mL/min (STP). Both isothermal treatments were performed for 1 h each. Carbonisation is of high interest for cell growth experiments on a conductive surface, allowing the application of small voltage to support cell orientation. All samples were afterwards investigated by confocal laser scanning microscopy (CLSM), using a VK-8710 (Keyence, Neu-Isenburg, Germany), and by Fourier transform infrared (FTIR) spectroscopy with an Excalibur 3100 (Varian Inc., Palo Alto, CA, USA).

### 3 Results and discussion

Figure 1 shows CLSM images of nanofibrous mat surfaces after electrospinning. Generally, no large differences were visible between nanofibrous mats electrospun with 1.38 g PAN or 1.6 g PAN, respectively. As expected, without casein and with only 0.1 g casein, the latter showed a more homogenous nanofibrous mat with less beads and membrane-like areas [36].

The addition of 0.1 g casein to both amounts of PAN did not lead to significant modifications of the nanofibrous mat morphology. This finding abruptly changed with the addition of 0.2 g casein or even 0.4 g casein. In both cases, the nanofibrous mats showed much thicker fibres, sometimes above 1 µm, i.e. were no longer nanofibres. At the same time, standard deviations increased strongly (cf. insets in

Figure 1), i.e. fibre diameters showed a broader distribution. This effect is already known from PAN/gelatine nanofibres [25] and other PAN blends [24], and has been reported several times, while a physical explanation could not be found in the literature. In addition, 0.2 g or more casein led to large membrane-like areas, indicating an incomplete mixture of PAN and casein, with the casein apparently not being solely spinnable, as shown before [11]. It should be mentioned that in the previous study of diverse biopolymers and biopolymer blends, other PAN and casein were used, making the test results not completely comparable.

After stabilisation, the nanofibrous mat colours and morphologies partly changed (cf. Figure 2). Starting with the samples without casein, the typical brown colour of stabilised PAN was visible, which was also the case for PAN 1.6 g + casein 0.1 g. However, for a smaller amount of PAN, the addition of 0.1 g casein was already sufficient to result in silvery areas, indicating molten casein, which did not contribute to the carbonisation process similar to the biopolymer component in stabilized PAN/gelatine nanofibrous mats [25]. These silvery areas became more prominent at larger amounts of casein. It should be mentioned, however, that due to the small area visible in CLSM images, these can always depict only exemplary results which may differ for other areas under examination.

Most interestingly, the combination of PAN 1.6 g + casein 0.2 g led to relatively regular, long, straight fibres, again with the diameters of a few microns, as already visible after electrospinning (cf. Figure 1), which may be promising for the carbonisation process.

Comparing the fibre diameters with those after electrospinning, the diameter distributions stayed relatively similar for the samples prepared with 1.6 g PAN and 0.1 g casein as well as for both samples with 0.2 g casein. This finding suggests that the fibre morphologies were not significantly influenced by the stabilisation process, opposite to pure PAN samples.

The results of carbonisation at 500 °C and 800 °C are shown in Figures 3 and 4, respectively. Firstly, it should be mentioned that nanofibrous mats with smaller amounts of casein in combination with a larger amount of PAN still showed a brownish colour after the carbonisation at 500 °C, indicating that the treatment temperature or duration were not sufficient.

Besides this finding, smaller amounts of casein (0.0 g or 0.1 g, respectively) resulted in relatively fine fibres

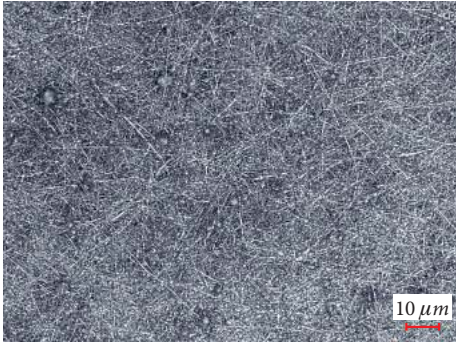
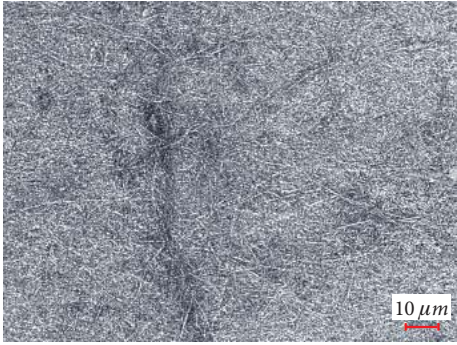
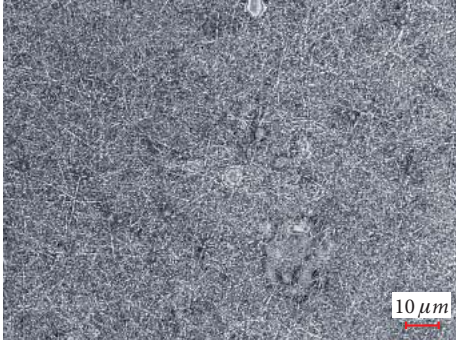
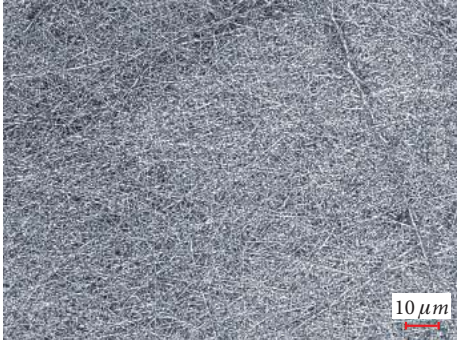
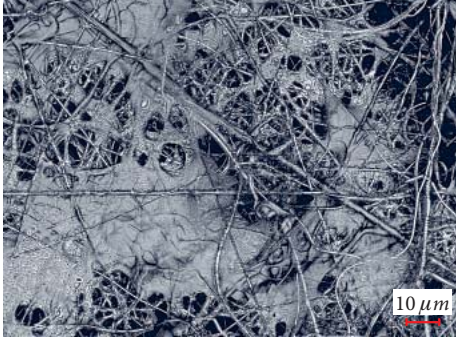
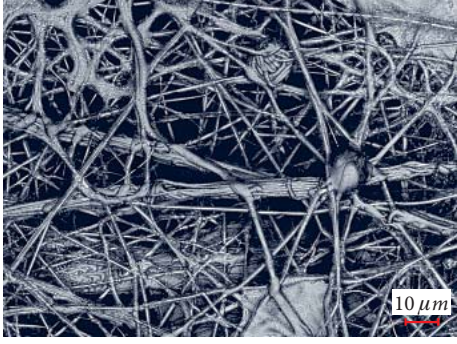
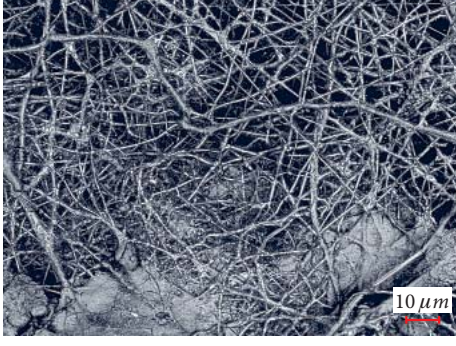
|                 | PAN 1.38 g  | PAN 1.6 g  |
|-----------------|---|--|
| Casein<br>0.0 g |  <p>(230 ± 70) nm</p>    |  <p>(280 ± 70) nm</p>    |
| Casein<br>0.1 g |  <p>(270 ± 80) nm</p>    |  <p>(330 ± 100) nm</p>   |
| Casein<br>0.2 g |  <p>(470 ± 250) nm</p> |  <p>(550 ± 280) nm</p> |
| Casein<br>0.4 g |  <p>(460 ± 180) nm</p> |  |

Figure 1: Nanofibrous mats with different amounts of PAN and casein after electrospinning (scale bars indicate 10 μm, fibre diameters are given as insets)



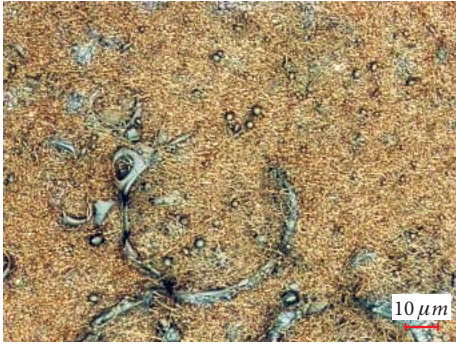
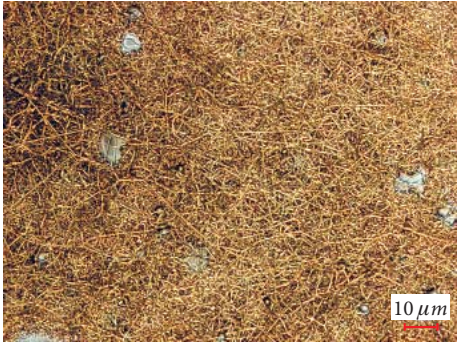
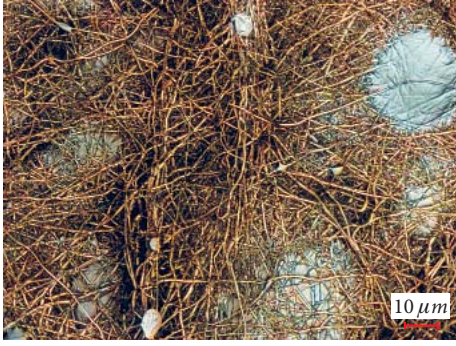


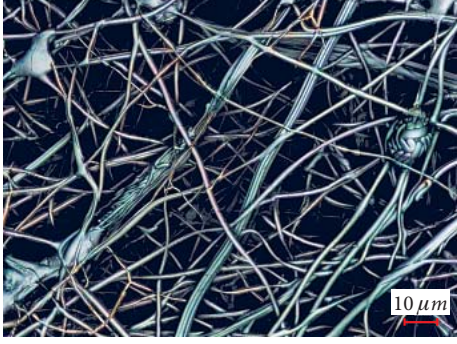

|                 | PAN 1.38 g  | PAN 1.6 g  |
|-----------------|---|--|
| Casein<br>0.0 g |  <p>(310 ± 100) nm</p>   |  <p>(320 ± 80) nm</p>    |
| Casein<br>0.1 g |  <p>(410 ± 120) nm</p>   |  <p>(360 ± 110) nm</p>   |
| Casein<br>0.2 g |  <p>(450 ± 140) nm</p> |  <p>(630 ± 240) nm</p> |
| Casein<br>0.4 g |  <p>(680 ± 370) nm</p> |  |

Figure 2: Nanofibrous mats with different amounts of PAN and casein after stabilisation (scale bars indicate 10  $\mu$ m, fibre diameters are given as insets)



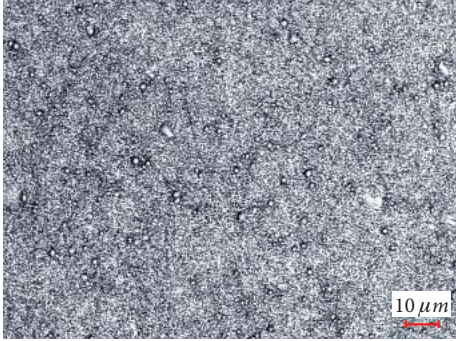
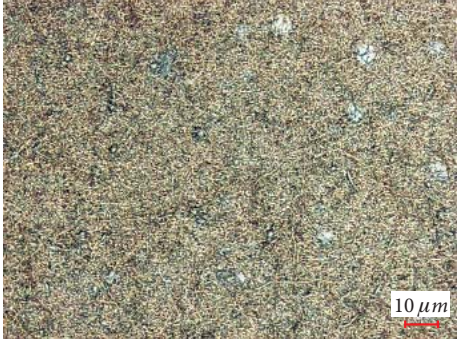
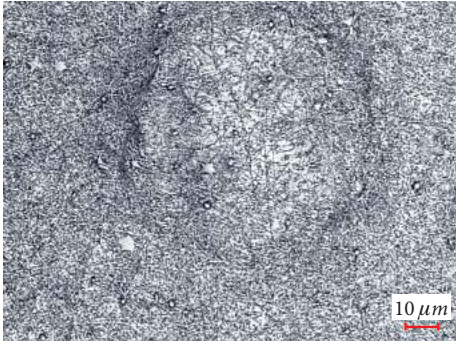

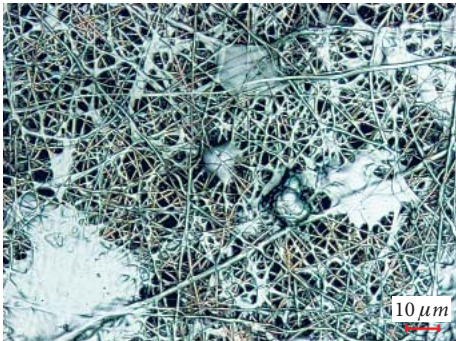
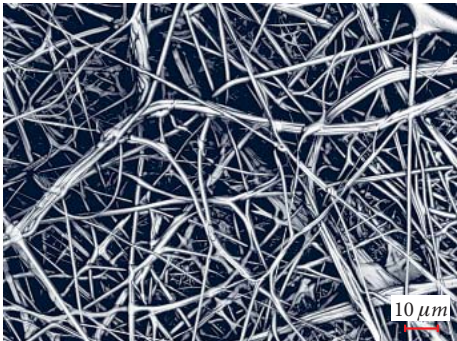

|                 | PAN 1.38 g  | PAN 1.6 g  |
|-----------------|---|--|
| Casein<br>0.0 g |  <p>(370 ± 130) nm</p>   |  <p>(360 ± 90) nm</p>    |
| Casein<br>0.1 g |  <p>(370 ± 110) nm</p>   |  <p>(330 ± 80) nm</p>    |
| Casein<br>0.2 g |  <p>(470 ± 190) nm</p> |  <p>(630 ± 320) nm</p> |
| Casein<br>0.4 g |  <p>(780 ± 650) nm</p> |  |

Figure 3: Nanofibrous mats with different amounts of PAN and casein after carbonisation at 500 °C (scale bars indicate 10 µm, fibre diameters are given as insets)



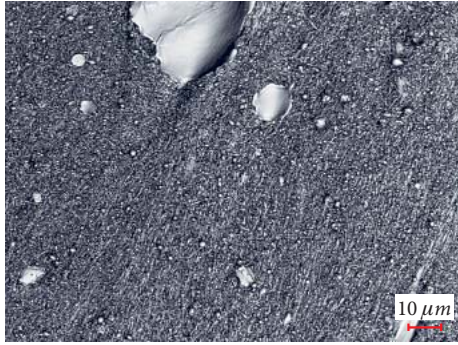
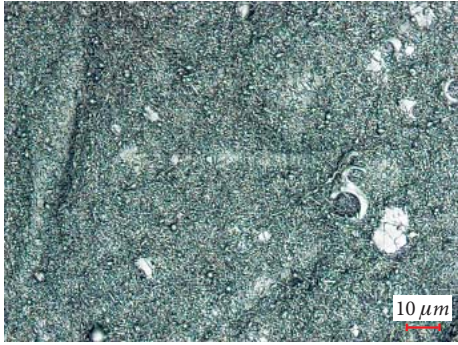



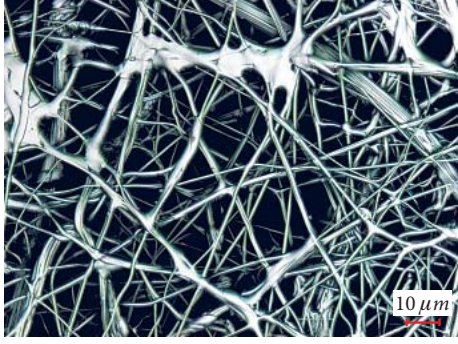

|                 | PAN 1.38 g  | PAN 1.6 g  |
|-----------------|---|--|
| Casein<br>0.0 g |  <p>(410 ± 80) nm</p>    |  <p>(380 ± 90) nm</p>    |
| Casein<br>0.1 g |  <p>(400 ± 80) nm</p>    |  <p>(360 ± 110) nm</p>   |
| Casein<br>0.2 g |  <p>(480 ± 130) nm</p> |  <p>(820 ± 430) nm</p> |
| Casein<br>0.4 g |  <p>(450 ± 130) nm</p> |  |

Figure 4: Nanofibrous mats with different amounts of PAN and casein after carbonisation at 800 °C (scale bars indicate 10 µm, fibre diameters are given as insets)

after the carbonisation at 500 °C or 800 °C. Similarly to stabilised nanofibrous mats, the combinations of 1.38 g PAN with 0.2 g or 0.4 g casein again showed a combination of fibrous and membrane-like areas, hinting at casein/PAN agglomerations. The combination of 1.6 g PAN with 0.2 g casein, on the other hand, again showed relatively thick, straight fibres, the diameters of which remained similar to those of original fibres.

Macroscopically, a strongly increased mechanical stability of PAN/casein nanofibre mats was recognized. While the samples without casein or with 0.1 g casein were brittle after the carbonisation at 500 °C or 800 °C (cf. Figure 5b), the sample with 1.6 g PAN and 0.2 g casein was touchable without problems and even bendable to a certain degree without being destroyed (cf. Figure 5a) even after the carbonisation at 800 °C. Other samples were less brittle than pure PAN after carbonisation, but less elastic than the sample with 1.6 g PAN and 0.2 g casein. Nevertheless, it must be mentioned that further research is necessary to investigate how stable this effect is, whether small deviations from this material ratio or slightly different electrospinning conditions would retain similar results or modify them significantly. The very broad fibre diameter distribution suggests that the thicker fibres in the micrometre range would possibly remain intact, while the thinnest fibres may be more prone to breaking. This is going to be investigated in more detail in a follow-up study, using a defined bending process.

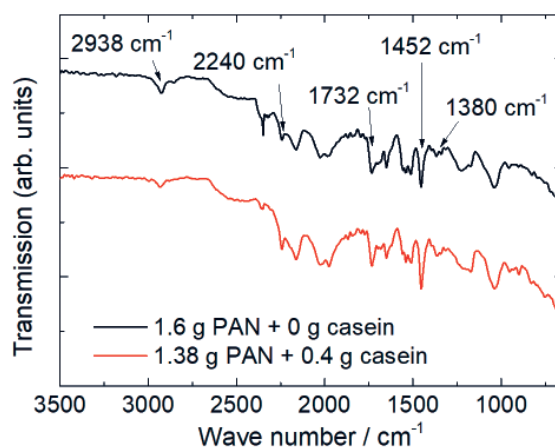


Figure 6: FTIR graphs of PAN and PAN/casein nanofibrous mats after electrospinning

Next, FTIR investigations were performed to investigate the influence of casein on the electrospun PAN nanofibrous mats (cf. Figure 6).

A few typical peaks which can be expected for pure PAN are stretching vibration of the C≡N nitrile functional group at 2240 cm<sup>-1</sup>, the carbonyl (C=O) stretching peak at 1732 cm<sup>-1</sup>, and the bending and stretching vibrations of CH<sub>2</sub> at 2938 cm<sup>-1</sup>, 1452 cm<sup>-1</sup> and 1380 cm<sup>-1</sup> [37].

Casein should show amide bands at around 1659 cm<sup>-1</sup> and 1539 cm<sup>-1</sup>, respectively [38], which are here hidden in the PAN bands. Dong and Gu also reported about the missing amide bands for PAN/casein blends [39]. The measurements of stabilised and carbonised samples look similar to those visible



Figure 5: (a) Bending sample carbonised at 500 °C, electrospun from 1.6 g PAN and 0.2 g casein; (b) broken residues after the same bending test, performed on carbonised (500 °C) sample electrospun from 1.6 g PAN without casein



in Figure 5 for the pure PAN nanofibrous mats, with the signals being slightly smaller, possibly due to slightly thinner fabrics.

Figure 7 shows a pure PAN nanofibrous mat after electrospinning, stabilisation and carbonisation at 500 °C and 800 °C, respectively, for comparison.

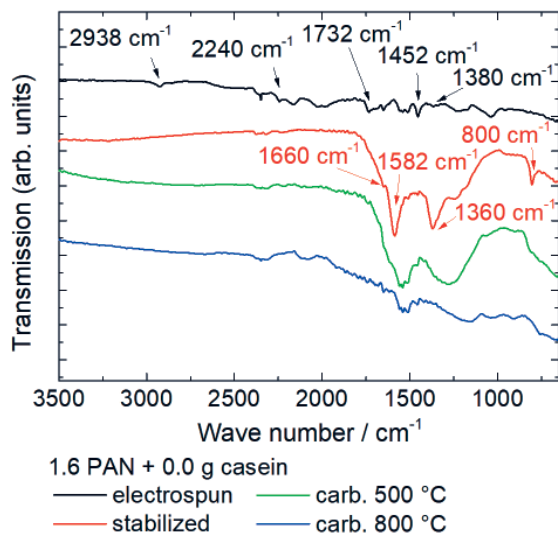


Figure 7: FTIR graphs of nanofibrous mats, electrospun from pure PAN, stabilised and carbonised at different temperatures

After the stabilisation, a new peak near 800  $\text{cm}^{-1}$  becomes visible due to aromatic C–H vibrations [40] as well as large peaks of C=N stretching vibrations at 1582  $\text{cm}^{-1}$  and C=C stretching vibrations at 1660  $\text{cm}^{-1}$  [37]. The second large peak at around 1360  $\text{cm}^{-1}$  can be explained by C–H bending and C–H<sub>2</sub> wagging [41].

After full carbonisation at 800 °C, typically only very few peaks are left due to the high absorbance of carbon [42]. The carbonisation at 500 °C, however, resulted in a spectrum between the stabilised and fully carbonised state, as it could be expected due to the relatively low temperature.

Finally, Figure 8 shows the results of FTIR investigations of the nanofibrous mats with the highest amount of casein. A comparison between Figures 8 and 7 shows that the general chemical process is apparently nearly identical with the one found for pure PAN, indicating that the increased fibre diameter does not influence the stabilisation and carbonisation process. Different peak heights may be attributed to different nanofibrous mat thicknesses.

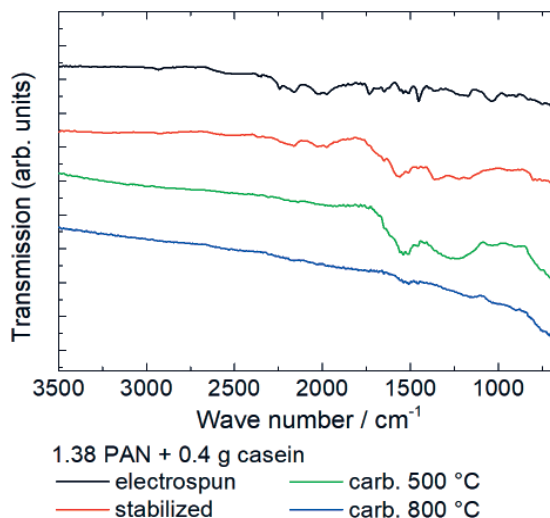


Figure 8: FTIR graphs of nanofibrous mats, electrospun from PAN with maximum amount of casein, stabilised and carbonised at different temperatures

## 4 Conclusion and outlook

Adding the biopolymer casein to a PAN electrospinning solution prepared in DMSO can be used to modify the nanofibrous mat morphology. By carefully tailoring the PAN : casein ratio, relatively thick fibres can be created, and unambiguously stabilised and carbonised. In this way, a new path may be offered to prepare PAN/casein or conductive carbon nanofibrous substrates for future cell growth experiments.

### Acknowledgments

The project was partly funded by the HiF funds of Bielefeld University of Applied Sciences, the programme Erasmus+ of the European Union and the internal PhD funds of Bielefeld University of Applied Sciences.

## References

1. SUBBIAH, Thandavamoorthy, BHAT, G. S., TOCK, R. W., PARAMESWARAN, S., RAMKUMAR, S. S. Electrospinning of nanofibers. *Journal of Applied Polymer Science*, 2005, **96**(2), 557–569, doi: 10.1002/app.21481.
2. GREINER, Andreas, WENDORFF, Joachim H. Electrospinning: a fascinating method for the



- preparation of ultrathin fibers. *Angewandte Chemie International Edition*, 2007, **46**(30), 5670–5703, doi: 10.1002/anie.200604646.
3. JAHAN, Israt, JADHAV, Amit, WANG, Lijing, WANG, Xin. Electrospinning from a convex needle with multiple jet toward better controlling and enhanced production rate. *Journal of Applied Polymer Science*, 2019, **136**(40), 48014, doi: 10.1002/app.48014.
  4. GROTHE, Timo, GROßERHODE, Christina, HAUSER, Thomas, KERN, Philip, STUTE, Kai, EHRMANN, Andrea. Needleless electrospinning of PEO nanofiber mats. In *Second International Conference on Mechanics, Materials and Structural Engineering (ICMMSE 2017)*. (*Advances in Engineering Research*). Edited by D.K. Kim, J.W. Hu, J.K. Ahn. Paris : Atlantis Press, 2017, 54–58, doi: 10.2991/icmmse-17.2017.9.
  5. ALI, Usman, NIU, Haitao, KHURSHID, Muhammad Furqan, ABBAS, Amir, LIN, Tong. Electrospinning behavior of needleless spinneret with a popular mace shape. *Journal of the Textile Institute*, 2019, **110**(3), 349–357, doi: 10.1080/00405000.2018.1480456.
  6. BANNER, Jana, DAUTZENBERG, Maria, FELDHANS, Theresa, HOFMANN, Julia, PLÜMER, Pia, EHRMANN, Andrea. Water resistance and morphology of electrospun gelatine blended with citric acid and coconut oil. *Tekstiles*, 2018, **61**(2), 129–135, doi: 10.14502/Tekstiles2018.61.129-135.
  7. SANDRI, Giuseppina, ROSSI, Silvia, BONFERONI, Maria Cristina, MIELE, Dalila, FACENDINI, Angela, DEL FAVERO, Elena, DI COLA, Emanuela, CORNAGLIA, Antonia Icaro, BOSELLI, Cinzia, LXBACHER, Thomas, MALAVASI, Lorenzo, CANTU, Laura, FERRARI, Franca. Chitosan/glycosaminoglycan scaffolds for skin reparation. *Carbohydrate Polymers*, 2019, **220**, 219–227, doi: 10.1016/j.carbpol.2019.05.069.
  8. SCHNELL, Eva, KLINKHAMMER, Kristina, BALZER, Simone, BROOK, Gary, KLEE, Doris, DALTON, Paul, MEY, Jörg. Guidance of glial cell migration and axonal growth on electrospun nanofibers of poly- $\epsilon$ -caprolactone and a collagen/poly- $\epsilon$ -caprolactone blend. *Biomaterials*, 2007, **28**(19), 3012–3025, doi: 10.1016/j.biomaterials.2007.03.009.
  9. QIN, Xiao-Hong, WANG, Shan-Yuan. Electrospun nanofibers from crosslinked poly(vinyl alcohol) and its filtration efficiency. *Appl. Polym. Sci.*, 2008, **109**(2), 951–956, doi: 10.1002/app.28003.
  10. ROCHE, Roche, YALCINKAYA, Fatma. Electrospun polyacrylonitrile nanofibrous membranes for point-of-use water and air cleaning. *ChemistryOpen*, 2019, **8**(1), 97–103, doi: 10.1002/open.201800267.
  11. WEHLAGE, Daria, BÖTTJER, Robin, GROTHE, Timo, EHRMANN, Andrea. Electrospinning water-soluble/insoluble polymer blends. *AIMS Materials Science*, 2018, **5**(2), 190–200, doi: 10.3934/matricsci.2018.2.190.
  12. DE OLIVEIRA, Juliana Bovi, MÜLLER GUERRINI, Lilia, DOS SANTOS CONEJO, Luiza, REZENDE, Mirabel Cerqueira, BOTELHO, Edson Cocchieri. Viscoelastic evaluation of epoxy nanocomposite based on carbon nanofiber obtained from electrospinning processing. *Polymer Bulletin*, 2019, **76**(12), 6063–6076, doi: 10.1007/s00289-019-02707-0.
  13. LIU, Hua, SONG, Weiguo, XING, Aihua. *In situ* K<sub>2</sub>S activated electrospun carbon nanofibers with hierarchical meso/microporous structures for supercapacitors. *RSC Advances*, 2019, **9**(57), 33539–33548, doi: 10.1039/c9ra06847c.
  14. SABANTINA, Lilia, RODRÍGUEZ-CANO, Miguel Ángel, KLÖCKER, Michaela, GARCÍA-MATEOS, Francisco José, TERNERO-HIDALGO, Juan José, MAMUN, Al, BEERMANN, Friederike, SCHWAKENBERG, Mona, VOIGT, Anna-Lena, RODRÍGUEZ-MIRASOL, José, CORDERO, Tomás, EHRMANN, Andrea. Fixing PAN nanofiber mats during stabilization for carbonization and creating novel metal/carbon composites. *Polymers*, 2018, **10**(7), 735-1–735-11, doi: 10.3390/polym10070735.
  15. BARZOKI, P. Kheirkhah, REZADOUST, A. M., LATIFI, M., SAGHAFI, H., MINAK, G. Effect of nanofiber diameter and arrangement on fracture toughness of out of autoclave glass/phenolic composites – Experimental and numerical study. *Thin-Walled Structures*, 2019, **143**, 106251, doi: 10.1016/j.tws.2019.106251.
  16. KIAI, Maryann Sadat, EROGLU, Omer, KIZIL, Huseyin. Electrospun nanofiber polyacrylonitrile coated separators to suppress the shuttle effect for long-life lithium-sulfur battery. *Journal*

- of *Applied Polymer Science*, 2019, **137**(17), 48606 doi: 10.1002/app.48606.
17. SARANYA, K., SUBRAMANIA, A., SIVASANKAR, N., BHARGAVA, P. *In-situ* growth of cos nanoparticles onto electrospun graphitized carbon nanofibers as an efficient counter electrode for dye-sensitized solar cells. *Journal of Nanoscience and Nanotechnology*, 2017, **17**(1), 398–404, doi: 10.1166/jnn.2017.12542.
  18. BASHIR, Z. A critical review of the stabilization of polyacrylonitrile. *Carbon*, 1991, **29**(8), 1081–1090, doi: 10.1016/0008-6223(91)90024-D.
  19. DALTON, Stephen, HEATLEY, Frank, BUDD, Peter M. Thermal stabilization of polyacrylonitrile fibres. *Polymer*, 1999, **40**(20), 5531–5543, doi: 10.1016/S0032-3861(98)00778-2.
  20. ISMAR, Ezgi, SARAC, A. Sezai. Oxidation of polyacrylonitrile nanofiber webs as a precursor for carbon nanofiber: aligned and non-aligned nanofibers. *Polymer Bulletin*, 2018, **75**, 485–499, doi: 10.1007/s00289-017-2043-x.
  21. ALARIFI, Ibrahim, M., ALHARBI, Abdulaziz, KHAN, Waseem S., SWINDLE, Andrew, ASMATULU, Ramazan. Thermal, electrical and surface hydrophobic properties of electrospun polyacrylonitrile nanofibers for structural health monitoring. *Materials*, 2015, **8**, 7017–7031, doi: 10.3390/ma8105356.
  22. ARBAB, Shahram, TEIMOURY, Arash, MIRBAHA, Hamideh, ADOLPHE, Dominique C., NOROOZI, Babak, NOURPANAH, Parviz. Optimum stabilization processing parameters for polyacrylonitrile-based carbon nanofibers and their difference with carbon (micro) fibers. *Polymer Degradation and Stability*, 2017, **142**, 198–208, doi: 10.1016/j.polymdegradstab.2017.06.026.
  23. DHAKATE, Sanjay R., GUPTA, Ashish, CHAUDHARI, Anurag, TAWALE, Jai, MATHUR, Rakesh B. Morphology and thermal properties of PAN copolymer based electrospun nanofibers. *Synthetic Metals*, 2011, **161**(5–6), 411–419, doi: 10.1016/j.synthmet.2010.12.019.
  24. SABANTINA, Lilia, BÖTTJER, Robin, WEHLAGE, Daria, GROTHE, Timo, KLÖCKER, Michaela, GARCÍA-MATEOS, Francisco José, RODRÍGUEZ-MIRASOL, José, CORDERO, Tomás, EHRMANN, Andrea. Morphological study of stabilization and carbonization of polyacrylonitrile/TiO<sub>2</sub> nanofiber mats. *Journal of Engineered Fibers and Fabrics*, 2019, **14**, 1558925019862242, doi: 10.1177/1558925019862242.
  25. SABANTINA, Lilia, Wehlage, Daria, Klöcker, Michaela, Mamun, Al, Grothe, Timo, GARCÍA-MATEOS, Francisco José, RODRÍGUEZ-MIRASOL, José, CORDERO, Tomás, FINSTERBUSCH, Karin, EHRMANN, Andrea. Stabilization of electrospun PAN/gelatin nanofiber mats for carbonization. *Journal of Nanomaterials*, 2018, **2018**, 6131085, doi: 10.1155/2018/6131085.
  26. WU, Meiyu, WANG, Qiaoying, LI, Kaina, WU, Yiqiong, LIU, Haiqing. Optimization of stabilization conditions for electrospun polyacrylonitrile nanofibers. *Polymer Degradation and Stability*, 2012, **97**(8), 1511–1519, doi: 10.1016/j.polymdegradstab.2012.05.001.
  27. SANTOS DE OLIVEIRA JUNIOR, Mauro, MANZOLLI RODRIGUES, Bruno Vinícius, MARCUZZO, Jossano Saldanha, MÜLLER GUERINI, Lília, RIBEIRO BALDAN, Maurício, REZENDE, Mirabel Cerqueira. A statistical approach to evaluate the oxidative process of electrospun polyacrylonitrile ultrathin fibers. *Journal of Applied Polymer Science*, 2017, **134**(43), 42458, doi: 10.1002/app.45458.
  28. TRABELSI, Marah, MAMUN, Al, KLÖCKER, Michaela, SABANTINA, Lilia, GROßERHODE, Christina, BLACHOWICZ, Tomasz, EHRMANN, Andrea. Increased mechanical properties of carbon nanofiber mats for possible medical applications. *Fibers*, 2019, **7**(11), 98, doi: 10.3390/fib7110098.
  29. BIER, M. C., KOHN, S., STIERAND, A., GRIMMELSMANN, N., HOMBURG, S. V., RATTENHOLL, A., Ehrmann, A. Investigation of eco-friendly casein fibre production methods. *IOP Conf. Series: Materials Science and Engineering*, 2017, **254**, 192004, doi: 10.1088/1757-899X/254/19/192004.
  30. DONG, Qingzhi, GU, Lixia. Synthesis of AN-g-casein copolymer in concentrated aqueous solution of sodium thiocyanate and AN-g-casein fiber's structure and property. *European Polymer Journal*, 2002, **38**(3), 511–519, doi: 10.1016/S0014-3057(01)00214-2.
  31. TOMASULA, P. M., SOUSA, A. M. M., LIOU, S.-C., LI, R., BONNAILLIE, L. M., LIU, L. S. Short communication: Electrospinning of casein/pullulan blends for food-grade application.

- Journal of Dairy Science*, 2016, **99**(3), 1837–1845, doi: 10.3168/jds.2015-10374.
32. GROTHE, Timo, GRIMMELSMANN, Nils, HOMBURG, Sarah Vanessa, EHRMANN, Andrea. Possible applications of nano-spun fabrics and materials. *Materialstoday: Proceedings*, 2017, **4**(2), S154–S159, doi: 10.1016/j.matpr.2017.09.180.
  33. WEHLAGE, Daria, BLATTNER, Hannah, SABANTINA, Lilia, BÖTTJER, Robin, GROTHE, Timo, RATTENHOLL, Anke, GUDERMANN, Frank, LÜTKEMEYER, Dirk, EHRMANN, Andrea. Sterilization of PAN/gelatin nanofibrous mats for cell growth. *Tekstilec*, 2019, **62**(2), 78–88, doi: 10.14502/Tekstilec2019.62.78-88.
  34. MOCANU, Anca Mihaela, MOLDOVEANU, C., ODOCHIAN, Lucia, PAIUS, Cristina Maria, APOSTOLESCU, N., NECULAU, R. Study on the thermal behavior of casein under nitrogen and air atmosphere by means of the TG-FTIR technique. *Thermochimica Acta*, 2012, **546**, 120–126, doi: 10.1016/j.tca.2012.07.031.
  35. BLACHOWICZ, Tomasz, EHRMANN, Andrea. Conductive electrospun nanofiber mats. *Materials*, 2020, **13**(1), 152, doi: 10.3390/ma13010152.
  36. SABANTINA, Lilia, RODRÍGUEZ-MIRASOL, José, CORDERO, Tomás, FINSTERBUSCH, Karin, EHRMANN, Andrea. Investigation of needleless electrospun PAN nanofiber mats. *AIP Conference Proceedings*, 2018, **1952**(1), 020085, doi: 10.1063/1.5032047.
  37. MOLNÁR, Kolos, SZOLNOKI, Beáte, TOLDY, Andrea, VAS, Lázló Mihály. Thermochemical stabilization and analysis of continuously electrospun nanofibers. *Journal of Thermal Analysis and Calorimetry*, 2014, **117**, 1123–1135, doi: 10.1007/s10973-014-3880-6.
  38. SZYK-WARSZYNSKA, Lilianna, RASZKA, Katarzyna, WARSZYNSKI, Piotr. Interactions of casein and polypeptides in multilayer films studied by FTIR and molecular dynamics. *Polymers*, 2019, **11**(5), 920, doi: 10.3390/polym11050920.
  39. DONG, Qingzhi, GU, Lixia. Synthesis of AN-g-casein copolymer in concentrated aqueous solution of sodium thiocyanate and AN-g-casein fiber's structure and property. *European Polymer Journal*, 2002, **38**(3), 511–519, doi: 10.1016/S0014-3057(01)00214-2.
  40. GERGIN, Ilknur, ISMAR, Ezgi, SARAC, A. Sezai. Oxidative stabilization of polyacrylonitrile nanofibers and carbon nanofibers containing graphene oxide (GO): a spectroscopic and electrochemical study. *Beilstein J. Nanotechnol.*, 2017, **8**, 1616–1628, doi: 10.3762/bjnano.8.161
  41. CIPRIANI, E., ZANETTI, M., BRACCO, P., BRUNELLA, V., LUDA, M. P., COSTA, L. Crosslinking and carbonization processes in PAN films and nanofibers. *Polymer Degradation and Stability*, 2016, **123**, 178–188, doi: 10.1016/j.polymdegradstab.2015.11.008.
  42. ARSHAD, Salman N., NARAGHI, Mohammad, CHASIOTIS, Ioannis. Strong carbon nanofibers from electrospun polyacrylonitrile. *Carbon*, 2011, **49**(5), 1710–1719, doi: 10.1016/j.carbon.2010.12.056.

Darinka Fakin<sup>1</sup>, Lavra Smoljanović, Alenka Ojstršek<sup>1,2</sup>

<sup>1</sup> University of Maribor, Faculty of Mechanical Engineering, Institute for Engineering Materials and Design, Smetanova 17, 2000 Maribor, Slovenia

<sup>2</sup> University of Maribor, Faculty of Electrical Engineering and Computer Science, Institute of Automation, Koroška cesta 46, 2000 Maribor, Slovenia

---

# Detection and Perception of Colour Regarding Gender and Age

## *Detekcija in zaznavanje barve glede na spol in starost*

Original scientific article/Izvirni znanstveni članek

Received/Prispelo 12-2019 • Accepted/Sprejeto 2-2020

---

### Abstract

People have been accompanied by colours throughout the history and through all periods of life. In different eras, colours were also associated with status symbols of different social classes or mythological beliefs. We are often addressed emotionally by colour combinations, since colour perception is always and exclusively a sensorial experience. Various colour combinations can have a pleasant effect on us or leave us cold as well as in a state of shock. All of the above, presented the starting point of this research. Detection and perception of sensations through colour was accomplished by preparing a questionnaire related to 12 selected colours. The research included 302 participants from Slovenia, of both sexes and different ages, born from 1940 to 2004. From the obtained results, it could be concluded how popular a certain colour is in a material, design and spiritual sense. Moreover, the results were validated and compared regarding the gender and age of participants, and further compared with the results of previous studies.

Keywords: colour perception, survey, colour popularity, colour of joy, colour of clothes, colour of sleeping area

### Izvleček

Barve spremljajo človeka skozi vso zgodovino in skozi vsa življenjska obdobja. V različnih obdobjih so bile tudi statusni simboli socialnih slojev ali mitoloških prepričanj. Barvne kombinacije, ki jih srečamo, nas čustveno nagovorijo, kajti doživetje barve je vedno in izključno samo čutno doživetje. Različne barvne kombinacije lahko na nas delujejo prijetno, lahko pa nas pustijo hladne ali se nas celo neprijetno dotaknejo. Slednje je bilo izhodišče za našo raziskavo. Z izbranimi dvanajstimi barvnimi otenki in pripravljenim anketnim vprašalnikom smo opravili raziskavo o zaznavanju in doživetju barv. V raziskavi je zajet vzorec populacije 302 ljudi iz Slovenije, ki zajema tako ženske kot moške različnih generacij, leto rojstva od 1940 do 2004. Iz raziskave je mogoče ugotoviti priljubljenost posameznih barv tako v materialnem, oblikovalskem, kot tudi duhovnem smislu. Rezultati raziskave so ovrednoteni in primerjani glede na starostna obdobja in spol udeležencev, saj se ti med seboj razlikujejo, narejena je tudi primerjava s preteklimi raziskavami.

Ključne besede: zaznavanje barve, vprašalnik, popularnost barve, barva veselja, barva oblačil, barva spalnega prostora

---

## 1 Introduction

Colour is a subjective sensorial perception that depends on the physicochemical composition of the observed object, type of light, and physiological and

psychological abilities of the observer [1, 2]. The physical aspect of Colour Science, which is an interdisciplinary discipline, deals with light and its interaction. The chemical aspect covers the chemical properties of substances – colourants, which can under

Corresponding author/Korespondenčna avtorica:

Prof. Dr. Darinka Fakin

ORCID: 0000-0002-4251-8655

Telephone: +386 2 220 7637

E-mail: darinka.fakin@um.si

Tekstilec, 2020, **63**(1), 50-59

DOI: 10.14502/Tekstilec2020.63.50-59



the influence of visible light absorb or reflect light of different spectral wavelengths. The psychological aspect of colours considers the visual system of the observer, dealing with its influence on the well-being, consciousness and perception of colours.

The most important aspect of colour in daily life is probably the one that is least defined and most variable. It involves aesthetic and psychological responses to colour, and influences art, fashion, commerce, and even physical and emotional sensations [3]. However, detection and perception of colour is not isolated from other sensory elements, but is related closely to: (i) Perception of space and movement (dark colours seem closer, light makes things farther away), (ii) Weight perception (dark colours appear heavy, light lighter), (iii) Thermal sensations (red, orange, yellow and brown hues are “warm”, while blue, green and grey are “cold”), (iv) Touch sensations (velvety are “soft” colours and metallic are “hard”), (v) Odour, (vi) Taste and (vii) Acoustic sensing [4]. Furthermore, red, orange and yellow hues are said to induce excitement, cheerfulness, stimulation and aggression; blues and greens security, calm and peace; and browns, greys and blacks sadness, depression and melancholy [3]. How we perceive colours depends also on our character, mood, past experiences (memory colour effect) [5], gender, age and cultural conditions – place and historical period to which we belong [6]. In addition, mental health is one of the very important factors influencing colour perception, i.e. schizophrenics have been reported to have abnormal colour perception. Also, specific colours can have a therapeutic effect on physical and mental disabilities [3].

Many authors have been dealing with colours in history, although, the studies are mainly related to the psychology of colours and their impact on the well-being, mood and health. A study similar to our research was published by A. Trstenjak in [10] and later by M. Tušak in [8], which summarised the research by M. Pfister [11], Gibson J. J. [12], H. Frieling [13] and others.

The aim of this study was to investigate the perception of sensations through colour, regarding gender and age, by preparing a survey together with 12 selected colours, representing the whole colour circle. The survey included questions about the (un)popularity of colours, the association of colours with joy, favourite colours of clothing and preferred colours of the sleeping area.

## 2 Experimental

### 2.1 Participants

In the presented study, 302 persons participated in total, 195 females and 107 males, from whom 5 persons (1 female and 4 males) had different colour perception disorders (self-proclaimed). In order to compare the obtained results, three groups were generated according to the year of birth, i.e. 1<sup>st</sup> group 1940–1970 (47 females and 19 males), 2<sup>nd</sup> group 1971–1990 (60 females and 46 males), and 3<sup>rd</sup> group 1991–2004 (88 females and 42 males). The percentages of participants included in the study regarding the year of birth and gender are disclosed in Figure 1.

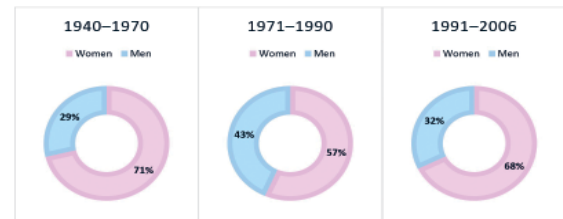














Figure 1: Participants included in study

### 2.2 Test samples and survey

For the purpose of this research, a survey was prepared with nine questions. The first three questions were related to gender, year of birth and the colour vision disorder of participants included in the research, whereas the other six questions were connected to the perception of sensations through colour. Firstly, participants had to sort the 12 selected colours (cf. Table 1) regarding their popularity by creating a personal scale, from the most popular to the least popular colour. The next question was related to the perception of joy through colour, i.e. selection of the most and the least joyful colours. In addition, participants needed to select the colour of clothing they prefer to wear and finally, what colour they favour for their sleeping room. The collected answers were calculated as a percentage of the total number of participants in each group (gender and date of birth).

Together with the survey, 12 selected colour samples (i.e. black, grey, white, pink, purple, blue, turquoise, green, yellow, orange, red, brown) were prepared according to the RAL colour system, measured using a UV-VIS SF 600 Plus (Datacolor) spectrophotometer (cf. Table 1) and positioned in the CIE  $a^*b^*$  colour space (cf. Figure 2). The survey was conducted in July and August 2018 in a physical form, for all participants to be able to evaluate

Table 1: Selected colours according to RAL [7] and CIE  $L^*a^*b^*$  measured values

| Colour pattern  | RAL mark  | Naming colour | Measured CIE $L^*a^*b^*$ colour value |        |        |       |        |
|---|-----------|---------------|---------------------------------------|--------|--------|-------|--------|
|   |           |               | $L^*$                                 | $a^*$  | $b^*$  | $C^*$ | $h$    |
|  | 15 00     | black         | 27.42                                 | 0.21   | -0.42  | 0.47  | 296.53 |
|  | 270 70 10 | grey          | 71.56                                 | -0.21  | -9.41  | 9.42  | 268.74 |
|  | 290 90 05 | white         | 90.31                                 | 0.94   | -2.47  | 2.65  | 290.80 |
|  | 340 70 30 | pink          | 70.36                                 | 27.58  | -9.92  | 29.31 | 340.22 |
|  | 300 60 35 | purple        | 60.77                                 | 16.84  | -28.56 | 33.16 | 300.53 |
|  | 250 50 40 | blue          | 52.70                                 | -12.75 | 34.52  | 36.80 | 249.73 |
|  | 180 70 25 | turquoise     | 70.66                                 | -24.42 | 0.17   | 24.42 | 179.56 |
|  | 120 70 50 | green         | 70.92                                 | -23.90 | 40.93  | 47.40 | 120.28 |
|  | 090 90 60 | yellow        | 89.19                                 | 0.18   | 57.06  | 57.06 | 89.82  |
|  | 050 60 70 | orange        | 60.92                                 | 42.83  | 44.65  | 61.88 | 46.19  |
|  | 030 40 60 | red           | 44.35                                 | 44.60  | 21.28  | 49.41 | 25.51  |
|  | 060 40 40 | brown         | 45.04                                 | 17.00  | 25.35  | 30.53 | 56.15  |

the same colour patterns, which could not be possible through a social network survey (different screens, screen settings, devices etc.).

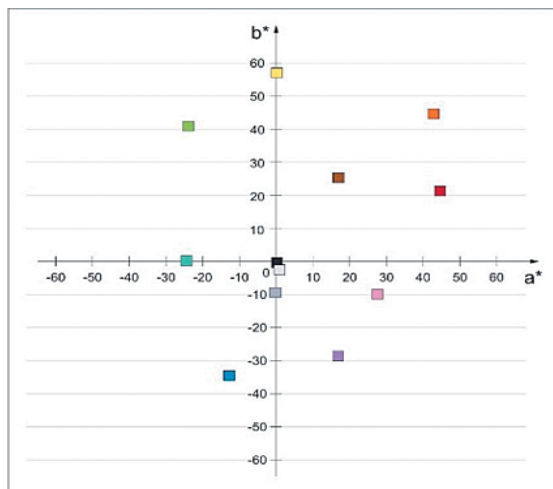


Figure 2: Position of colour samples in CIE  $a^*b^*$  diagram

### 3 Results and discussion

#### 3.1 Popularity and unpopularity of colours in general

The first objective of the presented study was to determine the popularity scale of the 12 selected colours, regarding gender and year of birth (Figure 3 – females and Figure 4 – males). The diagrams

capture the data of the whole scale; thus, a full picture is given of the colour range. The favourite colours are shown as a positive proportion of colours (+) above indifferent colours (less than 5%), and unpopular colours are shown at the bottom of the scale as a negative share (-).

From Figure 3, it can be observed that the favourite colour for females born between 1940 and 1970 was blue (19.6%), followed by red, green and turquoise. The least popular was brown (30.4%), followed by grey, black and finally, pink. Other colours were of minor interest. The second female group (1971–1990) preferred red (14%), blue and green, and refused brown (40%), grey and pink. The youngest females preferred black (13.3%), blue and white, and refused brown (39.9%), orange and purple.

In general, the least popular colour in all three groups was brown and the central position on all scales was reserved for turquoise, with ca. 4–6% of popularity. Orange, which was popular in the eldest population (8%), proved to be a less popular colour for the youngest participating group, with almost the same share (-8.2%). In contrast, black was shifted from less popular (-10%) by the oldest generation to the most popular colour (13.3%) by younger females.

Figure 4 shows the popularity of colours in male groups, from which less difference could be perceived in comparison with female groups, i.e. the most popular colour was blue (up to 34.5%), the

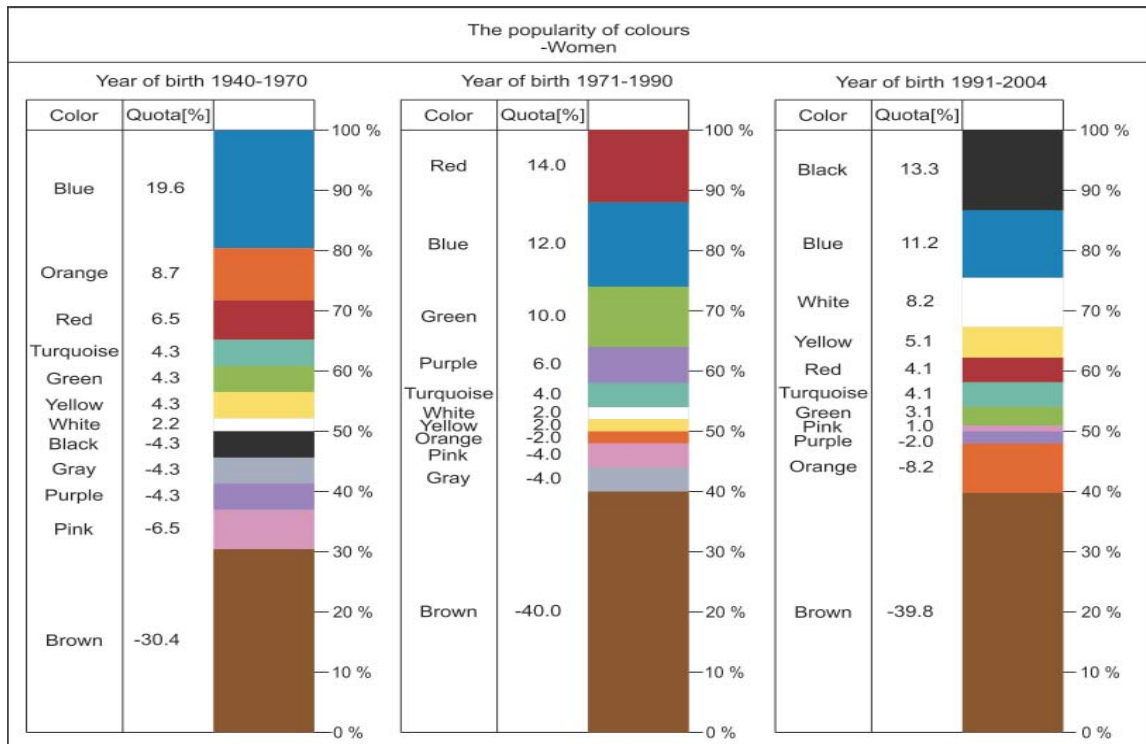


Figure 3: Colour popularity among female participants

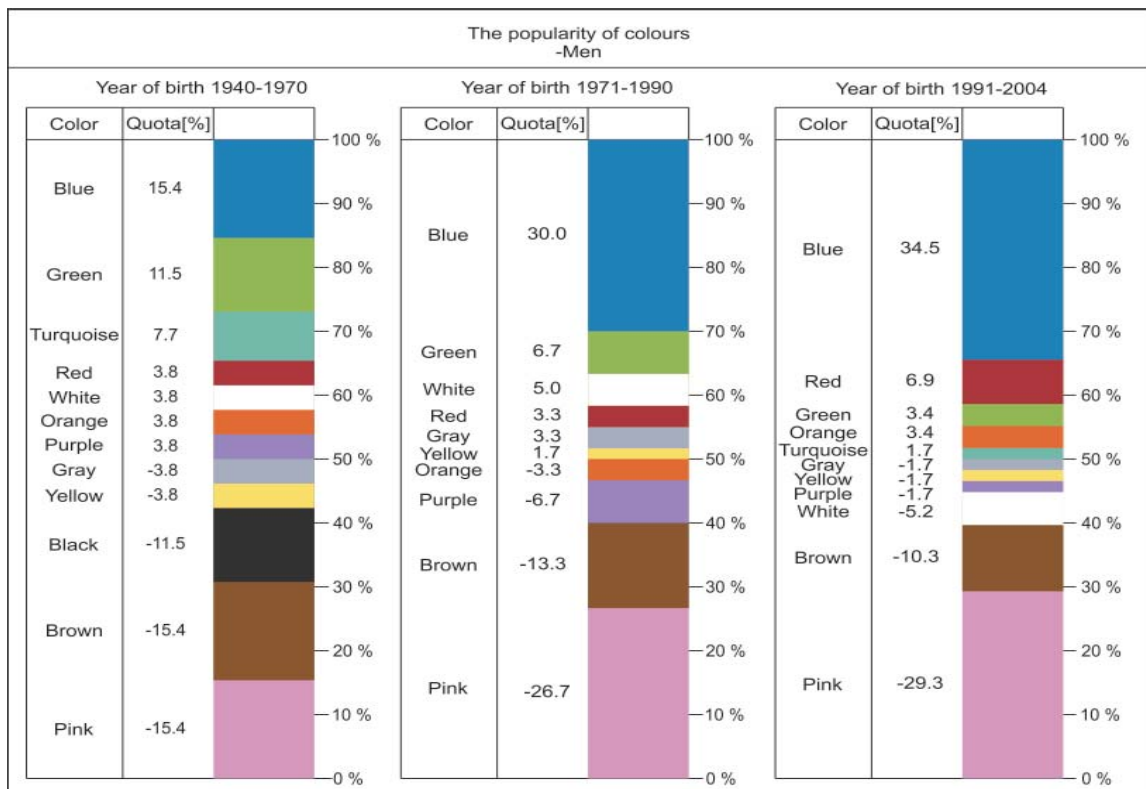


Figure 4: Colour popularity among male participants

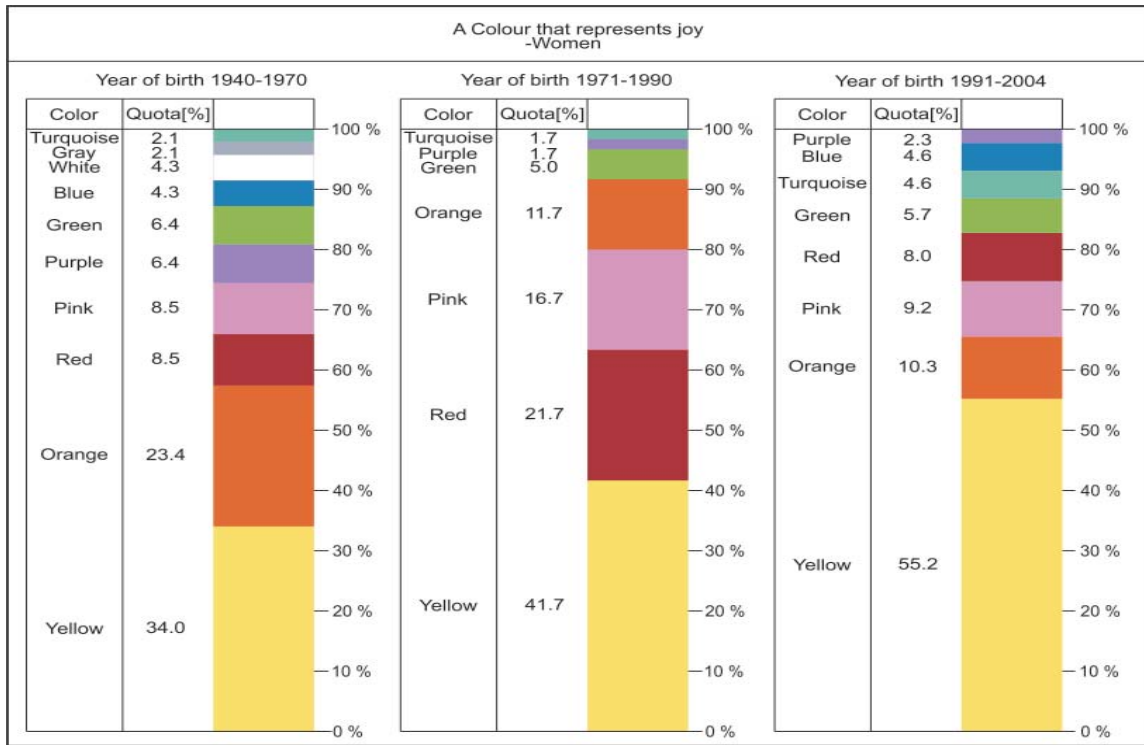


Figure 5: Colours of joy for females

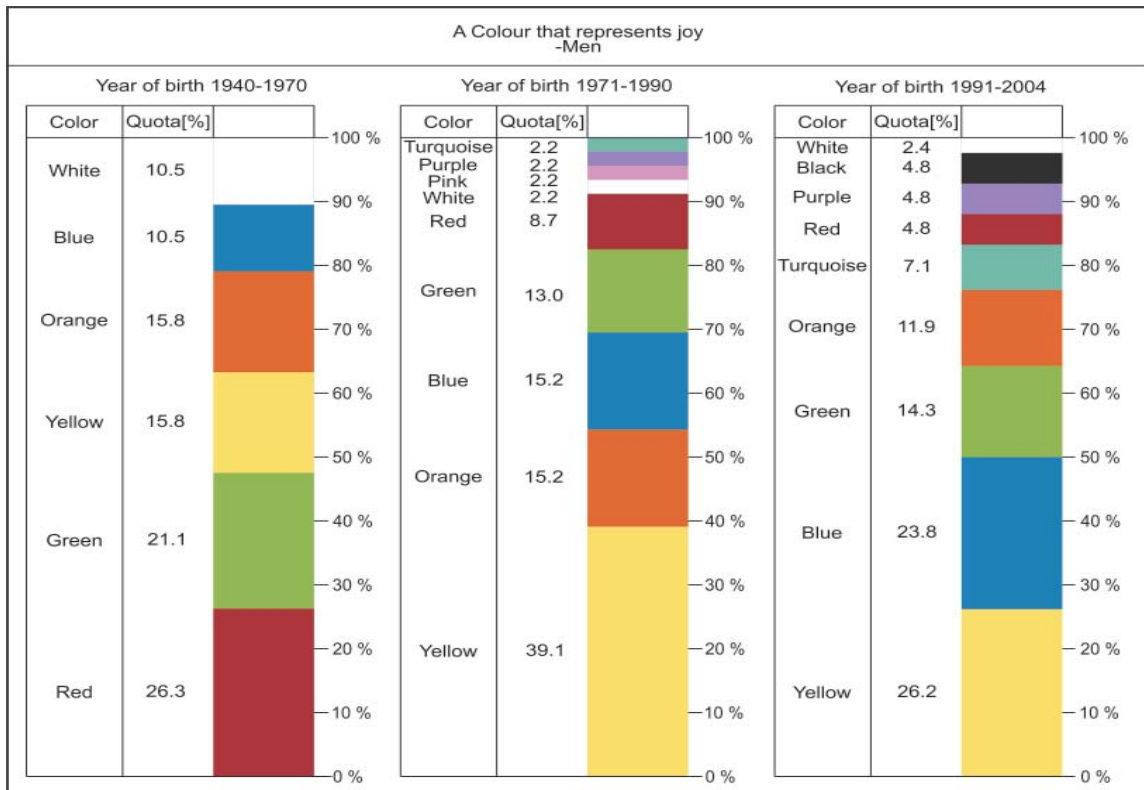


Figure 6: Colours of joy for males



least popular pink (up to 29.3%), and indifferent colours were orange, grey and yellow, with percentage differences between ages.

If we compare both genders and all ages (cf. Figures 3 and 4), a relatively popular colour was blue, more for males (up to 34.5%), unpopular was brown, more by females (up to 40%), and indifferent was yellow. In addition, women prefer red and men green colour, and both declined pink (men to a higher extent than women).

The findings of the presented research were compared with other studies as follows. In 1994, Tušak [8] interviewed gymnasium students and students of secondary vocational schools, and found out that blue was the most popular colour for both genders and for all researched groups. The second most popular colour among boys was green (gymnasium) and red (secondary vocational schools). The second most popular colour among girls was purple (gymnasium) and black (secondary vocational schools). The most unpopular colour at boys was pink, followed by yellow and brown. The most unpopular colour among girls was yellow (gymnasium), followed by pink and brown (secondary vocational schools). If we compare the results with our studied group (1991–2004), which was wider, but also included tertiary level students, some similarities as well as differences could be found, i.e. blue was the most and pink the least popular colour among males in both studies. The biggest differences were between the (un)popularities of colours among females.

In addition, Tušak [9] conducted a survey of colour popularity in a group of people aged between 60 and 87 years, without division by gender, which could be compared with our group of participants born between 1926 and 1970. Blue turned out to be the most popular colour in both researches, followed by green (as in our research for males) and red (second most popular colour for females in our study). The most unpopular colour in Tušak's research was black, followed by yellow and brown, while in our research, the least preferred colour for females was brown, followed by black, and for males pink, followed by brown.

A recent study prepared by Guzelj et al [14] in 2016 examined the emotional response to colours in a sample of the female population in Slovenia, revealing whether a selected colour was perceived as pleasant or not. Similarities with our study could be seen in the popularity of colours by age. Elderly females

preferred red and blue, and declined black as a popular colour. Interestingly, in a survey [14], most women selected purple as the colour they like. In our study, purple was less popular among females, except in the group born between 1971 and 1990.

### 3.2 Colour of joy

Figures 5 and 6 present the colour of joy for females and males, regarding their year of birth.

From Figure 5, it can be noted that yellow represents joy for females of all tested ages. In the first group (year of birth 1940–1970) and third group (1991–2004), yellow was selected by 34.0% and 55.2%, respectively, followed by orange and pink. The middle-aged group preferred yellow (41.7%), followed by red, pink and orange. All the mentioned colours are the so-called warm colours, except for pink. The minority of females of all ages (1.7 up to 2.3%) selected turquoise and purple as the colour of joy.

Figure 6 presents a rather different perception of joy through colour for men compared to women. In the younger generation (1991–2004), two so-called cold colours, blue and green (following yellow), represented the colour of joy, revealing blue as a very important colour in everyday life. Contrarily, the generation of men between 1940 and 1970 favoured red (26.3%) as the colour of joy, followed by green (21.1%), and yellow and orange in the same percentages (15.8%). On the opposite side of joyful colours for men, there were white, purple, turquoise and black.

The study performed by Kovachev and Musek [15] got similar results as presented in our study. Their survey included mainly female students, who most often associate joy with the red colour, followed by yellow and orange. In our study, women quite often selected pink (8.9% up to 16.7%), which was not available in a comparative study [15].

From the physiological point of view, yellow is the strongest colour, and relates to emotions, self-esteem and creativity [4]. Yellow is thought of as joyful, outgoing, open and friendly. In colour-mood association studies, yellow is associated with comedy, happy mood and playfulness. It occupies the largest range in the visible spectrum and has a beneficial effect on the eye and nervous system [16].

### 3.3 Favourite colour of clothing

Figures 7 and 8 present favourite colours of clothes for women and men, respectively, regarding their year of birth.

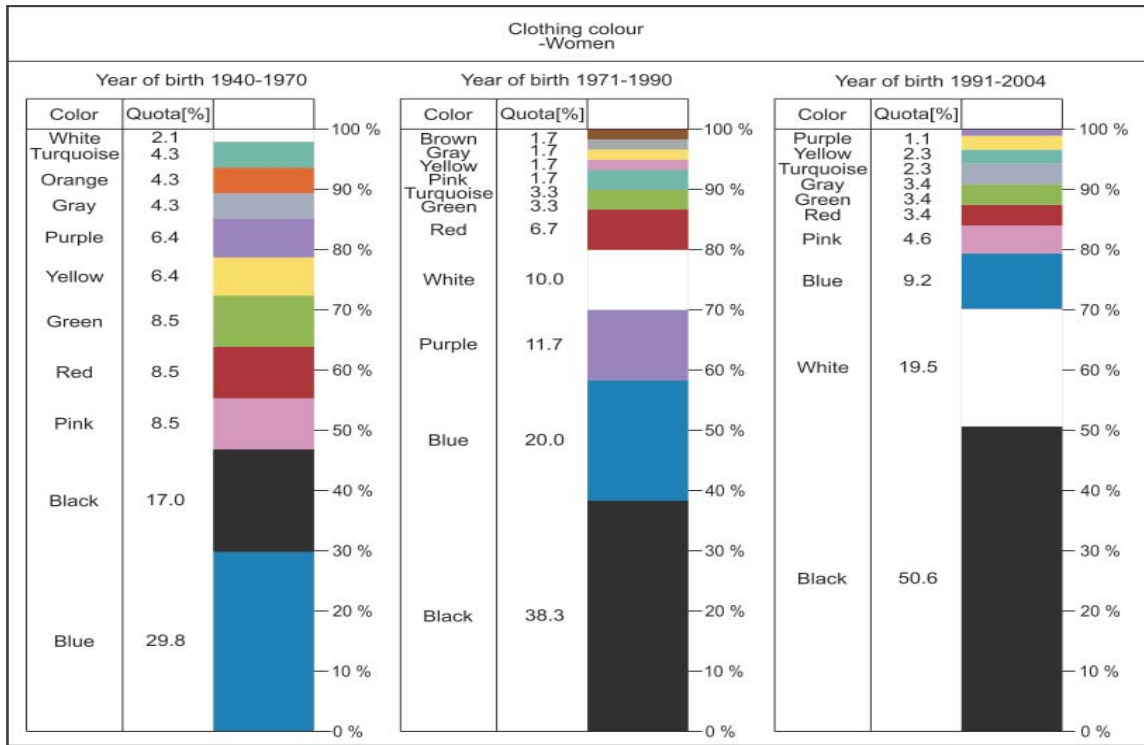


Figure 7: Favorite clothing colours among females

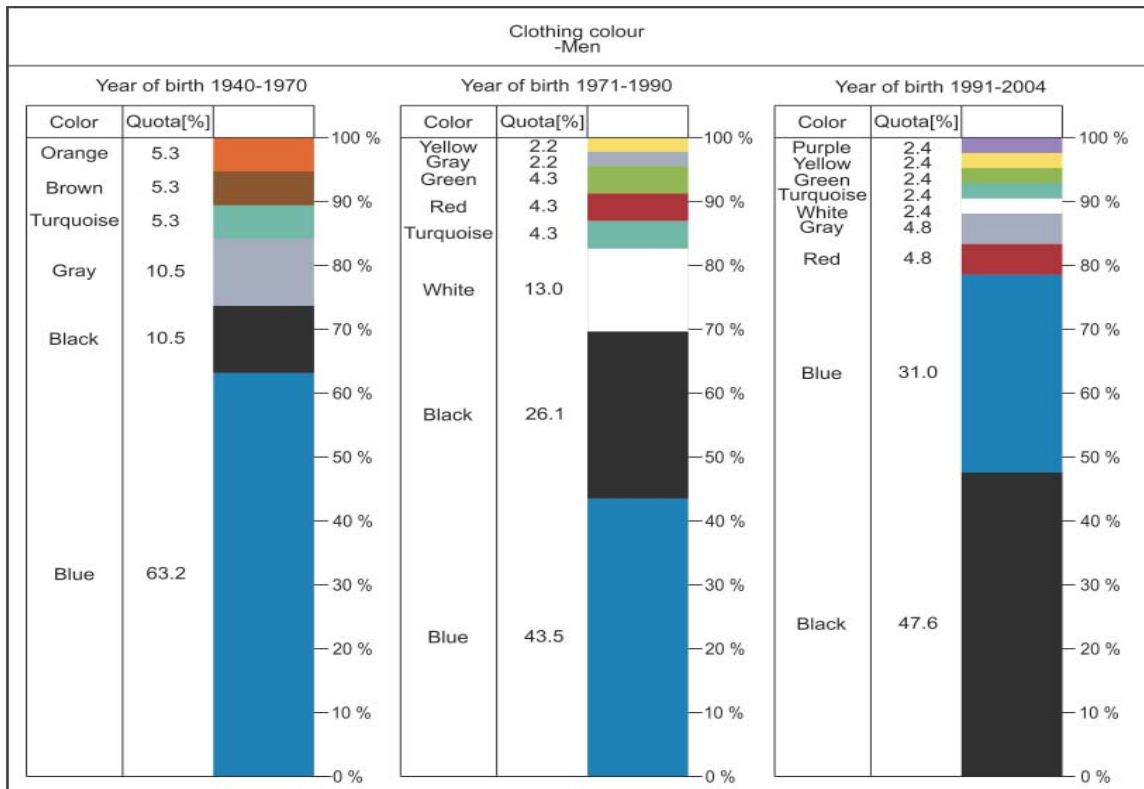


Figure 8: Favorite clothing colours among males

In Figure 7, minor differences can be observed among the favourite colours of female clothes regarding age. The oldest population (1940–1970) preferred blue (29.8%) over black (17.0%) and pink (8.5%), the population in their middle ages (1971–1990) black (38.3%) over blue (20.0%) and purple (11.7%), and the youngest ones (1991–2004) black (50.6%) over white (19.5%) and blue (9.2%). The minority of females preferred brown, purple, yellow and turquoise, with small differences between ages. It is not surprising that the black colour is the favourite colour for clothes, as it can be combined with all other colours, it is appropriate for all occasions, different subcultures, and can hide body's shortcomings.

The answers about the favourite colours for clothes among males (cf. Figure 8) were similar to those by females, but in different percentages. The eldest population (1940–1970) preferred blue (63.2.4%) over black (10.5%) and grey (10.5%). Then, the popularity of the blue colour diminished by lowering the age, on account of the black colour, i.e. in the population in their middle ages (1971–1990), black (43.5%) still dominated over blue (26.1%), and in the youngest population (1991–2004), black (47.6%) dominated over blue (31.0%).

If we compare the popularity of colours of garments by gender, it can be concluded that the trend is blue and black. The choice of black decreases with age, while the popularity of blue increases. Most men preferred cooler colours, while women selected some warm colours as their favourite ones. In some cases, women chose the pink colour that was not found in the men's answers. This can be linked to the colour popularity chart (cf. Figure 4), as pink was one of the undesirable colours according to men.

Trstenjak [10] investigated in 1996 the popularity of dress colours of persons aged 15 to 22 years, which could be compared with our 3<sup>rd</sup> study group (1991–2004). He found out that grey was the most popular colour for males, followed by blue; in our study, black was ahead of blue. The female population in Trstenjak's research preferred blue in a high percentage over red in a low percentage. The data obtained from both surveys for young female populations are not comparable at all. Two decades have passed since Trstenjak's survey and the above comparison shows that the popularity of certain colours has, as expected, changed over time since the colour of clothes (especially for women) is in close relation with fashion.

### 3.4 Colour of sleeping area

Figures 9 and 10 represent favourite colours of the sleeping area separately for women and men, regarding their year of birth.

From Figure 9, it can be observed that the white colour is the first choice for the sleeping area for females of all tested ages. Here, the similarities between groups stopped. In the first group (1940–1970), females also preferred yellow, green and grey, in this order, in the second group (1971–1990) they chose green, yellow and pink, and in the third group (1991–2004), blue, turquoise and orange. Women like cold colours in their sleeping area, e.g. white, blue, green and turquoise, although some also preferred warm colours, e.g. yellow and orange. In the youngest generation, 3.4% of females picked black as their favourite colour for their sleeping place. This colour was not favourite for other generations, from which it could be concluded that the younger generation follows the trends and changes colours more easily in indoor surroundings.

Elderly men and those in their middle ages were more traditional and favoured the white colour for their sleeping space in relatively high percentages (cf. Figure 10), i.e. 52.6% (1940–1970) and 58.7% (1971–1990). This trend changed with the youngest investigated group, where only 26.2% preferred white. Other popular colours were red and blue (1926–1970), green and blue (1971–1990), and blue and yellow (1991–2004). Similarly as in the youngest female generation (cf. Figure 9), 4.8% of males (cf. Figure 10) picked black as their favourite colour for their sleeping place.

We can conclude that white was the most popular colour for the sleeping surroundings irrespective of gender and age, whereas the popularity of other colours changed by age. Black became the perfect choice for the youngest males and females, although for the 2<sup>nd</sup> and 3<sup>rd</sup> groups, black was not even on the scale.

Van der Voordt et al [17] studied in 2017 the popularity of colours in different rooms. His research found that the most popular colour for the bedroom was white, as in our study, followed by red, blue and green, which is similar to our study, with the exception of red, which was not among the favourite colours with our participants. The reason for choosing white for the sleeping space could be that people want to have as much light in the room as possible. White is the colour that reflects the lightest and

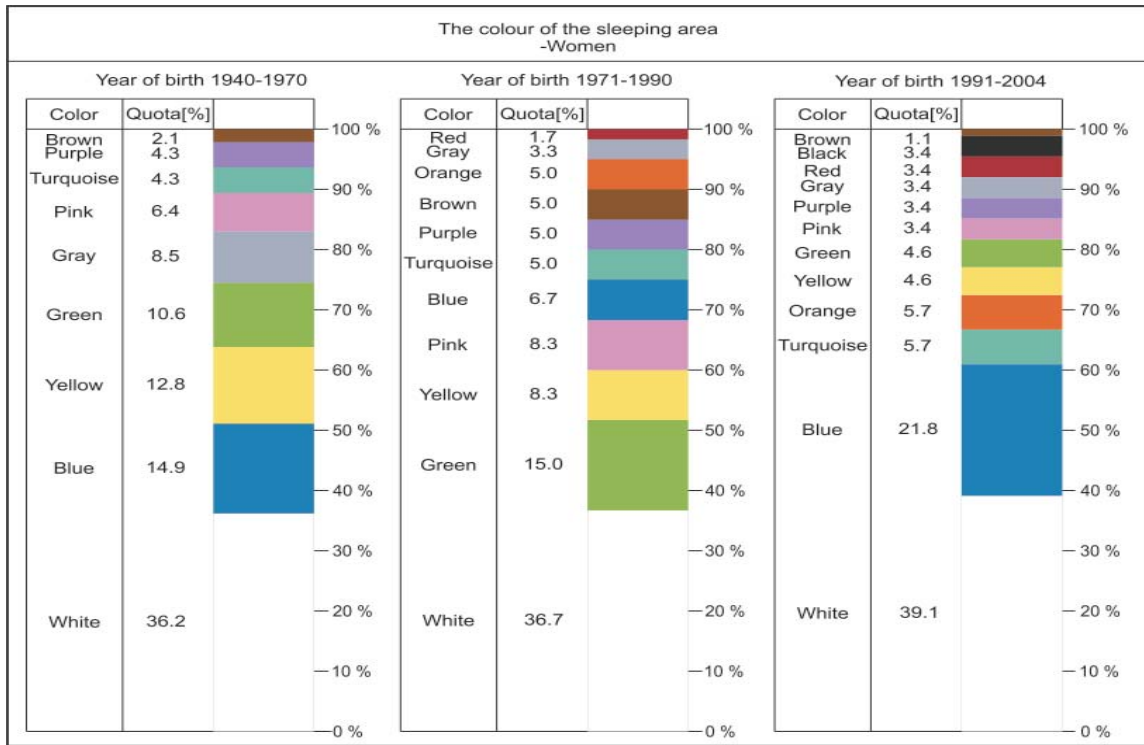


Figure 9: Females' favourite colours of sleeping area

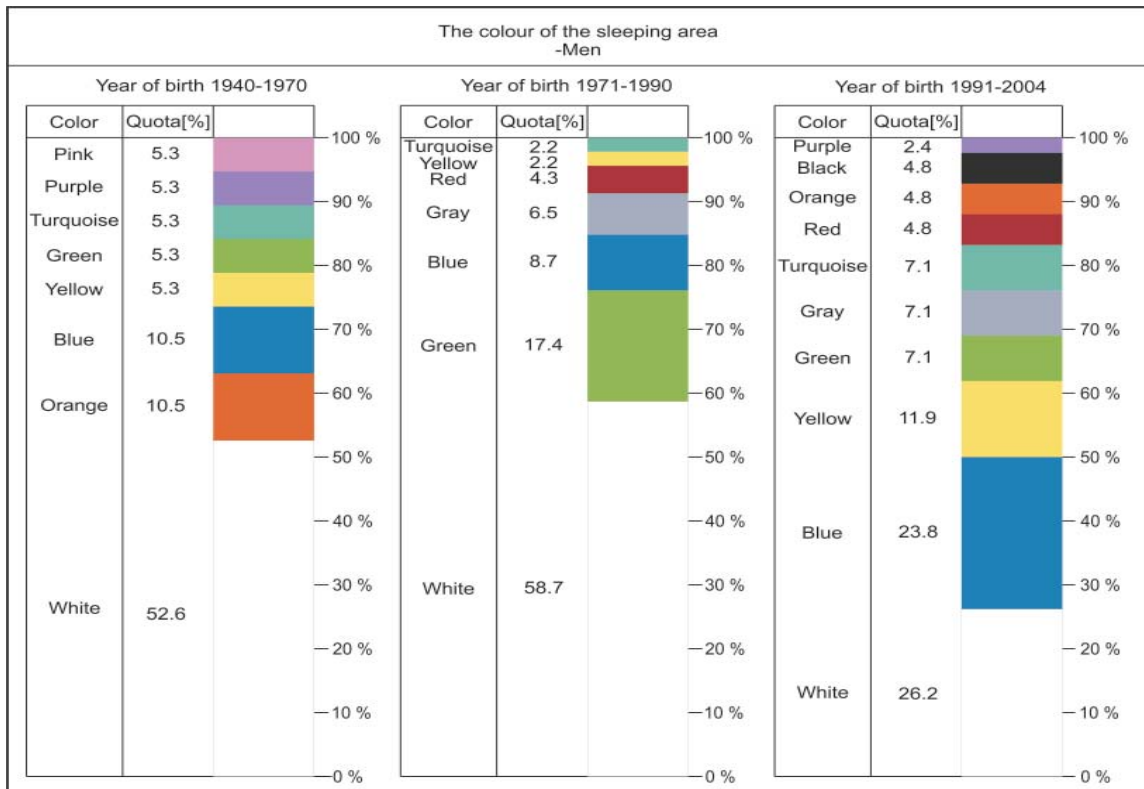


Figure 10: Males' favourite colours of sleeping area



therefore works as the brightest of all colours. The reason for its frequent choice could also be that white is considered as a safe choice and could be combined with all other shades in smaller proportions.

## 4 Conclusion

The purpose of the presented research was to investigate the perception of sensations through colour, regarding gender and year of birth, by preparing a survey together with 12 selected colours, representing the whole colour circle. The survey covered questions about the (un)popularity of colours, association of colours with joy, favourite colours of clothing and preferred colours of the sleeping space. We could find a symbolism in colours and establish that they can influence humans' well-being. Sometimes, we are unaware of their presence. The study gained a lot of data, providing a comprehensive view about the perception of colours. The presented research gave some general criteria of what we can expect from colours, while their perception still remains an individual choice. Colour perception is different by gender and age, although it is slowly changing with time, which could be a consequence of more aggressive propaganda of fashion/designers' industries through new (social) media and technologies. It would be interesting to perform a more detailed research within the individual sets of data obtained.

## References

1. KLANJŠEK GUNDE, Marta. Svetloba in barve – fizikalni vidik. V *Interdisciplinarnost barve. 1. del – v znanosti*. Edited by S. Jeler and M. Kumar. Maribor : Društvo koloristov Slovenije, 2001, 13–55.
2. MAYER, Linda and BHIKHA, Rashid, *The physiology and psychology of colour* [online]. Ibn Sina Institute of Tibb [cited 9. 12. 2019]. Available on World Wide Web: <<https://www.tibb.co.za/articles/Part-3-The-Physiology-and-Psychology-of-colour.pdf>>.
3. NASSAU, Kurt. *The perception of colour* [online]. Encyclopedia Britannica [accessed 9. 12. 2019]. Available on World Wide Web: <<https://www.britannica.com/science/color/The-perception-of-colour>>.
4. SEVINC, Kurt and KELECHI, Kingsley Osueke. The effects of color on the moods of college students. *SAGE Open*, 2014, 4(1), 1–12, doi: 10.1177/2158244014525423.
5. WITZEL, Christoph, VALKOVA, Hanna, HANSEN, Thorsten and GEGENFURTNER, Karl R. Object knowledge modulates colour appearance. *i-Perception*, 2011, 2(1), 13–49, doi: 10.1068/i0396.
6. BATAGODA, Muditha. *Understanding color psychology though culture, symbolism, and emotion* [online]. Medium [cited 9. 12. 2019]. Available on World Wide Web: <<https://uxplanet.org/understanding-color-psychology-though-culture-symbolism-and-emotion-215102347276>>.
7. The RAL DESIGN System [online]. TQC Sheen [cited 9. 12. 2019]. Available on World Wide Web: <<https://www.ral-shop.com/information-for-users/the-ral-design-system/>>.
8. TUŠAK, Maks. Psihologija barve. V *Interdisciplinarnost barve. 1. del – v znanosti*. Edited by S. Jeler and M. Kumar. Maribor : Društvo koloristov Slovenije, 2001, 87–118.
9. TUŠAK, Maks. Barvne preference, simbolika barv in osebnost. *Psihološka obzorja*, 1998, 7(4), 67–79.
10. TRSTENJAK, Anton. *Psihologija barv*. Ljubljana : Inštitut Antona Trstenjaka za psihologijo, logoterapijo in antropohigieno, 1996.
11. PFISTER, M. *Der Farbpentagon-test*. Bern : Hans Huber Verlag, 1951.
12. GIBSON, J.J. *The sexes considered as perceptual systems*. Boston : Houghton Mifflin, 1966.
13. FRIELING, H. *Der-Frieling Test*. Gottingen : Muster Schmidt, 1974.
14. GUZELJ, A., HLADNIK, Aleš and BRAČKO, Sabina. Examination of colour emotions on a sample of Slovenian female population. *Tekstilec*, 2016, 59(4), 311–320, doi: 10.14502/tekstilec2016.59.311-320.
15. KOVAČEV, A.N. and MUSEK, J. Grafična simbolizacija primarnih emocij. *Psihološka obzorja*, 1993, 2(3/4), 31–50.
16. ELLIOT, Andrew J. Color and psychological functioning: a review of theoretical and empirical work. *Frontiers in Psychology*, 2015, 6(368), 1–8, doi: 10.3389/fpsyg.2015.00368.
17. VAN DER VOORDT, Theo, BAKKER, Iris and DE BOON, Jan. Colour preferences for four different types of spaces. *Facilities*, 2017, 35(3/4), 155–169, doi: 10.1108/f-06-2015-0043.

## Prediction of Psychological Comfort Properties of 100% Cotton Plain Woven Fabrics made from Yarns with Different Parameters

*Napovedovanje psihološkega udobja 100-odstotnih bombažnih tkanin v vezavi platno, izdelanih iz prej z različnimi parametri*

Original scientific article/Izvirni znanstveni članek

Received/Prispelo 12-2019 • Accepted/Sprejeto 2-2020

---

### Abstract

The psychological satisfaction of the textile customer is the first criteria used to evaluate clothing and a lack of aesthetics, while fashionability and physical appearance contribute to the psychological discomfort of users. Either inherently or due to processing, cotton cloths demonstrate different psychological comfort behaviours. Manufacturers must therefore produce fabrics with optimum psychological comfort parameters. The objective of this research was to study the effect of cotton yarn parameters on the psychological comfort properties of woven fabrics. Four woven fabrics were produced from cotton yarns with different yarn twists, yarn counts, strengths and yarn elongations. Psychological comfort parameters such as wrinkle, drape, crease, bending modules and flexural rigidity were measured and analysed in accordance with the ES ISO 9867, ISO 9073-9, ES ISO 2313 and ASTM D1388-18 standards, respectively. Multiple regression equations were developed to predict the comfort properties of clothing in relation to yarn parameters. A statistical analysis showed that the wrinkle recovery and drapeability of fabrics were significantly affected by yarn twist, count and tenacity, and the elongation of yarns. However, yarn twist, count, tenacity and elongation had an insignificant effect on the crease recovery of woven samples at an F-value of 3.546 and a P-value of 0.069. The stiffness properties of the fabrics such as flexural rigidity and bending modules also showed insignificant difference between samples at  $F = 38487.969$ ,  $P = 0.057$  and  $F = 25.506$ ,  $P = 0.055$  respectively. A multiple regression analysis showed a positive correlation between yarn parameters (factors) and response, with Adj.  $R^2$  of 0.0998, Adj.  $R^2$  of 0.975 and Adj.  $R^2$  of 1 for crease recovery, wrinkle recovery and drape coefficient, respectively. The equations developed are helpful to fabric manufacturers in sourcing yarns with specific parameters to produce the desired comfort level in a fabric.

Keywords: yarn parameters, psychological comfort, cotton fabric, wrinkle, crease recovery, bending modules

### Izveček

*Psihološko zadovoljstvo kupca s tekstilijo je prvi kriterij ocenjevanja oblačila, pri čemer pomanjkanje estetike, modnosti in fizičnega videza vplivajo na psihološko neudobje uporabnika oblačila. Bombažna tekstilija izkazuje sama ali zaradi obdelav različne psihološke odzive. Proizvajalci morajo zato izdelovati tekstilije z optimalnimi parametri psihološkega udobja. Namen raziskave je bil preučiti vpliv parametrov bombažne preje na psihološke lastnosti udobja tkanin. Štiri tkanine so bile izdelane iz bombažnih prej z različnim vitjem, dolžinsko maso, trdnostjo in raztežkom. Parametri psihološkega udobja, kot so gube, drapiranje, zmečkanost, upogibni modul in upogibna togost, so bili izmerjeni in analizirani v skladu s standardi ES ISO 9867, ISO 9073-9, ES ISO 2313 in ASTM D1388-18.*

Razvite so bile regresijske enačbe za napovedovanje lastnosti udobnosti oblačil glede na parametre preje. Statistična analiza je pokazala, da so na izravnalne kote in drapiranje tkanin pomembno vplivali vitje, dolžinska masa, trdost in raztezek preje. Našteti parametri pa niso pomembno vplivali na izravnavanje gub (zmečkanin) tkanih vzorcev ( $F = 3,546$ ,  $P = 0,069$ ). Pri togosti tkanin, in sicer upogibni togosti in upogibnem modulu, med vzorci ni bilo statistično pomembnih razlik ( $F = 38487,969$ ,  $P = 0,057$ ;  $F = 25,506$ ,  $P = 0,055$ ). Večkratna regresijska analiza je pokazala pozitivno korelacijo med parametri preje (faktorji) in odzivom s prilagojenimi korelacijskimi koeficienti  $R^2 = 0,0998$  za izravnavanje gub,  $R^2 = 0,975$  za izravnalne kote in  $R^2 = 1$  za drapiranje. Razvite enačbe so v pomoč proizvajalcem tkanin pri nabavi preje z določenimi parametri za izdelavo tkanin z želenim udobjem.

Ključne besede: parametri preje, psihološko udobje, bombažna tkanina, gube, zravnava gub, upogibni modul

## 1 Introduction

Psychological comfort has received attention from manufacturers in recent years due to consumers' demands for aesthetic value, fashionability and good clothing appearance, as factors considered in the purchase process. To produce a comfortable garment, comfort properties should be considered during manufacturing and garment design [1]. Clothing with poor wrinkle, low drapeability and crease recovery properties will decrease wearers' psychological satisfaction. Natural fibres have better comfort properties than synthetic fibres. Even though they have several advantages, they also have some disadvantages, such as the quick wrinkling of cotton fabric during wear [2]. Yarn parameters are very important in producing suitable fabric with optimised performance for a specific end use. Several researchers have shown that yarn properties affect the properties of clothing. Gong studied cotton fabrics using five control factors in order to examine their effects on yarn cross-sectional shape changes along the yarn path. The factors studied were fibre type, yarn linear density and twist factor, and warp and weft cover factors. The study focused on the cross-sectional structure and its influence on woven fabric [3]. Pattanayak and Luximo pointed out that there are many factors that influence the aesthetic appearance of a fabric and the outstanding effect on the actual beauty of the cloth [4]. Drape is one of the critical factors affecting psychological comfort. The drape or drapeability of a fabric refers to the manner in which the fabric falls, shapes, gathers or flows with gravity on a model form or on a human body. Fabric drape has attracted the attention of many researchers in recent years because of the attempt to create a clothing CAD system by introducing fabric material properties in which drape is the key element [5]. Pattanayak and Luximo stated that fabric drape is an important parameter for

the selection and development of textile materials for apparel industries. Predictions of the drape property of cotton woven fabrics were developed using multiple regression methods [4]. Another researcher investigated the improvement of the crease recovery of cotton fabrics. Reactive dyed fabrics were treated with dimethylol dihydroxy ethylene urea (DMDHEU) resin in order to improve their crease recovery characteristics. Two types of treatments were carried out: conventional thermal curing and gamma irradiation. Finally, the effect of treatments on crease recovery, and the mechanical and thermal properties of fabrics were studied. They found that the finishing of cotton fabrics with gamma irradiation demonstrated better crease recovery [6]. The effect of yarn twist has also been studied. It was observed that the crease recovery of cotton fabrics decreases as yarn twist increases [7]. Similarly, Liu et al. investigated the impact of mechanical action on the wrinkling of cotton fabrics in a drum washer [8]. They observed that the spinning speed and wash load were the main factors influencing the smoothness of cotton fabrics. As the wash load increased, the free motion region decreased and the ratio of the passive motion region increased, resulting in the severe wrinkling of cotton fabric.

Hala [9] studied the effect of yarn twist direction on the drapability of fabrics and observed that twist direction does indeed have an effect on drape property. The bending and drape properties of woven fabrics, and the effect of weft density, weft yarn count and warp tension on these properties were also investigated by Süle [10]. It was reported that woven fabrics with thicker weft yarns and higher weft densities had a higher bending rigidity. In addition, the bending rigidities of the fabrics in the warp directions increased as warp tension increased. King and Johnston [11] studied the effect of stiffness, shear, extensibility, thickness and density on the drape coefficient

of fabrics. A multiple regressions analysis equation was developed to determine drape coefficient based on stiffness, shear, extensibility and density. They concluded that the drapability characteristics of a fabric are affected, to some extent, by fibre stiffness [12]. Multiple regression models were built based on factors such as bending, shear, tensile, compression and aerial density. It was found that tensile and compression factors have little effect on the drape property of fabrics. It was observed that bending, shear and aerial density affect drape characteristics [2, 4]. The effect of yarn parameters on the mechanical properties (at low-stress) of woven fabrics, tensile strength, compression, bending and shear property were studied by the authors of this work [13]. Though many researchers have studied the effect of yarn parameters such as count and twist on tactile comfort, and on drape, tensile and stiffness properties, most of the studies were done at the grey fabric level. The effect of yarn properties on fabric wrinkle resistance have not been thoroughly addressed. The effects of yarn parameters such as yarn count, twist, strength and elongation on the psychological comfort properties of half-bleached woven fabrics were studied in this work. A multiple regression analysis was carried out to predict stiffness, wrinkle recovery, crease recovery and the drape properties of fabrics.

## 2 Materials and methods

### 2.1 Materials

Four types of cotton yarns were manufactured by Bahir Dar Textile S.C. using a C-60 IDF (Integrated Draw frame) machine and a rotor spinning system (RIETER- R 923). The yarns were selected randomly from daily production when the count and twist were changed by spinners on the same machine. All yarns samples were produced from the same fibre mix with a micronaire value of 4.02, maturity of 0.85, upper half mean length (UHML) of 30.16 mm, uniformity

index (UI) of 83.8%, short fibre content of 6.9, strength of 29.8 g/tex, elongation of 7.6% and trash grade three. Trash grade is known as TrGrd in USTER HVI 1000 machine and this value is measured by the trash module and consist of 1 up to 4 alphanumeric characters. Yarn twist, yarn count, strength and elongation were evaluated according to ASTM D1422, ES ISO 2060 and ES ISO 2062 testing standard methods, respectively, and are shown in Table 1.

A Statimat Me+ instrument was used to evaluate yarn strength and elongation. Table 2 shows the actual thread density and thickness of the fabrics, as well as nominal yarn count and twist. All woven fabrics were produced on the same air jet loom (PICANOL- OMP 800-2-P) at a speed of 350 min<sup>-1</sup> (350 rpm) by Bahir Dar Textile S.C. Machine speed, warp yarn property, thread density (warp = 20 cm<sup>-1</sup> and weft 18 cm<sup>-1</sup>) and fabric structure (plain) were kept constant (see Tables 1 and 2) during fabric production. The only variation was the use of different weft yarns. The produced fabric samples were treated using a half-bleach combined treatment system on a Jigger machine. The fabric and water solution were prepared at a material liquor ratio (MLR) of 1:5, H<sub>2</sub>O<sub>2</sub> 4% of fabric weight, NaOH 3% of fabric weight and Na<sub>2</sub>SiO<sub>3</sub> 2% of fabric weight, and a wetting agent of 0.5% of fabric weight. Each sample was treated at a temperature of 95 °C for 1.5 hours, with a machine working speed of 40 m/minute.

### 2.2 Test methods

Specimens were conditioned at a relatively humidity of (65 ± 2)% and a temperature of (20 ± 1) °C before each test.

### Structural properties

The structural parameters of the developed fabrics such as thread density and fabric weight were evaluated according to ESISO 7211-2 and ES ISO 3801 test methods, respectively. The nominal thread density

Table 1: Yarn characteristics

| Yarn code | Yarn count [tex] | Twist [turns/m] | Tenacity [cN/tex] | Elongation [%] |
|-----------|------------------|-----------------|-------------------|----------------|
| Y1        | 21.5             | 937.2           | 14                | 6.29           |
| Y2        | 22.9             | 916.7           | 5.74              | 4.43           |
| Y3        | 24.1             | 876.7           | 11.22             | 5.10           |
| Y4        | 36.4             | 843.5           | 8.78              | 5.04           |
| Warp yarn | 20               | 920             | 15                | 6.42           |



(set at loom) of the fabric and the actual thread density (after manufacturing) are presented in Table 2.

### Stiffness test

Fabric stiffness is the resistance of a fabric to bending. This test measures the bending stiffness of a fabric by allowing a narrow strip of the fabric to bend to a fixed angle under its own weight. The length of the fabric required to bend to this angle is measured and is known as the bending length.

A cantilever stiffness test system is often used as a measure of a fabric's stiffness, as it is an easy test to perform. During testing, a horizontal strip of fabric is clamped at one end and the rest of the strip allowed to hang under its own weight as shown in Figure 1.

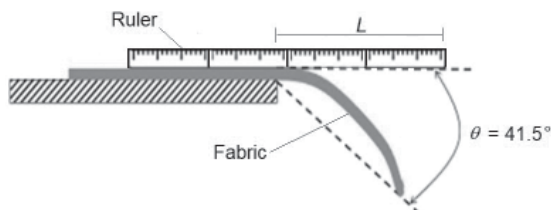


Figure 1: cantilever fabric stiffness test method  
*L* – length of projecting fabric,  $\Theta$  – angle to which fabric bends, *M* – fabric mass per unit area

Test specimens measuring 25 mm in width and 200 mm in length were cut in a lengthwise direction. Five tests were carried out on each sample in the warp and weft direction according to the ASTM D1388-18 standard. A fabric stiffness analysis, including parameters such as flexural rigidity, bending modulus and bending length, was also performed. The bending length was measured, and the bending modulus and flexural rigidity calculated according to equations 1 and 2:

$$\text{Flexural rigidity} = MC^3 \quad (1),$$

$$\text{Bending modulus} = \frac{G}{\text{Thickness (mm)}} \quad (2),$$

where *M* is the weight of a fabric in g/m<sup>2</sup>, *C* is the bending length, *G* is flexural rigidity and *T* is fabric thickness.

### Drapeability test

Drape is the degree of fabric deformation when it is allowed to hang freely under its own weight. It is quantitatively expressed as a drape coefficient [11]. The drape coefficient is defined as the percentage of

the area of the annular ring of fabric obtained by vertically projecting the shadow of the draped specimen. This test is used as an indication of garment appearance properties when a fabric orients itself into folds in more than one plane under its own weight. In this study, 30 cm diameter circles samples were used for testing on a Cusick drape tester in order to assess the drape of the fabric. Five tests were carried out on each sample in accordance with the ISO 9073-9 test method. The samples were positioned over a horizontally placed circular rigid disk of 18 centimetres in diameter. The fabric was deformed into a series of folds around the disk. The paper ring containing the shadow image of the draped configuration represents the weight (*W*<sub>1</sub>). The shadow image cut from the paper ring is weighed and marked as *W*<sub>2</sub>. Finally, the drape coefficient (*DC*) is calculated using equation 3:

$$DC\% = \frac{W_2}{W_1} \times 100 \quad (3),$$

where *W*<sub>2</sub> is the mass of the shaded area and *W*<sub>1</sub> is the total mass of the paper ring.

### Wrinkle property

Cotton fabric wrinkles easily and is therefore prone to shrinking, which decreases the wearer's psychological acceptance. A wrinkle may be explained as a rhytide, fold, ridge or crease in a cloth or garment. To test the wrinkling behaviour of the samples, their appearance was evaluated after crushing. The fabric sample was crushed and maintained at a specified pressure and time under standard atmospheric conditions in a wrinkle tester. The sample was then removed and its appearance visually compared to a reference sample and rated according to the ES ISO 9867 tests standard.

### Crease recovery

Creasing of a fabric during wear has a significant influence on the wearer's psychological satisfaction and on viewer acceptance. Thus, all clothing must have good crease recovery properties. Crease recovery is the ability of a fabric to return from a collapsed deformed state. In this investigation, crease recovery was measured quantitatively in terms of the crease recovery angle.

Textiles used in clothing must have the ability to crease and fold in order to conform to body shapes, and thus ensure improved comfort during wear. To retain their appearance, however, they must be able

to eliminate creases that occur in wear and laundering. When a fibre bends, cross-links may break and be formed in a new position, restricting recovery. Otherwise, they will merely stretch and recover when the load is removed. The M003A Shirley crease recovery tester was used for evaluation purposes. For the crease recovery test, 50 mm × 25 mm rectangular specimens were conditioned at a relative humidity of  $65 \pm 2\%$  and a temperature of  $20 \pm 1\text{ }^\circ\text{C}$  for 24 hours then folded for five minutes under a 2-kg load as per the ES ISO 2313 test standard method. This creasing load was then removed and the specimen allowed to recover for another five minutes in the crease recovery tester and the crease recovery angle recorded.

### 3 Results and discussion

#### 3.1 Structural properties

As observed in Table 2, the samples had the same fabric structure, thread density and loom settings. Nominal and actual thread densities were slightly different, as shown in Table 2.

#### Stiffness of fabrics

Table 3 shows that fabric stiffness, expressed as flexural rigidity and bending modulus, did not change significantly. The effects of yarn count, yarn twist, strength and elongation on woven fabrics were insignificant at an F-value of 38487.969 and Sig-value (P-value) of 0.057 on flexural rigidity, and an F-value of

Table 2: Woven fabric characteristics

| Sample code | Type of weave | Nominal warp/weft density [threads/cm] | Actual warp/weft density [threads/cm] | Thickness [cm] | Mass per unit area [ $\text{g}/\text{m}^2$ ] |
|-------------|---------------|--|---------------------------------------|----------------|--|
| F1          | Plain         | 26/18                                  | 27/20                                 | 0.37           | 168  |
| F2          | Plain         | 26/18                                  | 26/17                                 | 0.38           | 140  |
| F3          | Plain         | 26/18                                  | 27/18                                 | 0.35           | 145  |
| F4          | Plain         | 26/18                                  | 26/16                                 | 0.4            | 160  |

Table 3: Statistical descriptions of fabric properties

| Properties fabrics           |    | Mean      | Std. deviation | Std. error | Minimum | Maximum |
|------------------------------|----|-----------|----------------|------------|---------|---------|
| Crease recovery of fabrics   | F1 | 102.6000  | 4.77493        | 2.13542    | 97.00   | 109.00  |
|                              | F2 | 99.6000   | 6.18870        | 2.76767    | 95.00   | 110.00  |
|                              | F3 | 110.6000  | 9.58123        | 4.28486    | 98.00   | 120.00  |
|                              | F4 | 111.8000  | 6.97854        | 3.12090    | 104.00  | 120.00  |
| Wrinkle recovery of fabrics  | F1 | 4.4000    | .54772         | .24495     | 4.00    | 5.00    |
|                              | F2 | 2.4000    | .54772         | .24495     | 2.00    | 3.00    |
|                              | F3 | 2.2000    | .44721         | .20000     | 2.00    | 3.00    |
|                              | F4 | 2.0000    | .00000         | .00000     | 2.00    | 2.00    |
| Drape coefficient of fabrics | F1 | 73.3220   | .83527         | .37354     | 72.25   | 74.35   |
|                              | F2 | 66.1060   | .60455         | .27036     | 65.25   | 66.91   |
|                              | F3 | 72.7300   | .45645         | .20413     | 72.12   | 73.21   |
|                              | F4 | 74.8000   | 1.15972        | .51864     | 73.00   | 76.12   |
| Flexural rigidity            | F1 | 2014.2000 | 1.78885        | .80000     | 2012.00 | 2016.00 |
|                              | F2 | 1398.0000 | 5.70088        | 2.54951    | 1390.00 | 1405.00 |
|                              | F3 | 1596.6000 | 2.30217        | 1.02956    | 1595.00 | 1600.00 |
|                              | F4 | 2238.4000 | 5.94138        | 2.65707    | 2230.00 | 2245.00 |
| Bending modulus              | F1 | 5439.6000 | 11.32696       | 5.06557    | 5425.00 | 5450.00 |
|                              | F2 | 3664.4000 | 16.75709       | 7.49400    | 3648.00 | 3684.00 |
|                              | F3 | 4430.2000 | 813.02380      | 363.59530  | 3680.00 | 5650.00 |
|                              | F4 | 5636.4000 | 33.42604       | 14.94858   | 5600.00 | 5665.00 |

25.506 and Sig-value of 0.055 on bending modulus. As evident from the statistical analysis, the fabrics made from Y1 (21 tex) to Y4 (36 tex) showed no significant difference in flexural rigidity and bending modulus. This is because fabric flexural properties and handle are primarily influenced by the thickness and density of the fabric. For the tested samples, the two properties shown in Table 2 were not significantly different. Fabric thickness influences bending resistance, or rigidity, and may vary significantly, depending on the structure and texture, while mass per surface area, or GSM, in itself is not an expressive property concerning fabric flexibility in the absence of information on fabric thickness [14].

**Drapeability of fabrics**

As evident in Table 5, the produced woven fabrics showed a high significant change in drape coefficient with an F-value of 113.610 and P-value of 0.000. Drape coefficient is the inverse of drapeability. As mentioned earlier, drape is the extent to which a fabric will distort when it is permitted to droop under its own weight. It is correlated with a fabric’s mechanical properties. The most significant factors include bending, shear, formability, fabric weight and thickness. Drape depends on a fabric’s parameters, including structure, yarn type and fibre content, as well as finishing treatments [14].

Table 4 shows a multiple linear regression equation of the fabrics’ properties. These equations would be useful in predicting crease and wrinkle recovery, as well as the drape coefficient of the fabrics. The adjusted R<sup>2</sup> value is an indication of the correlation of yarn properties (factors) and fabric characteristics (responses). When the adjusted R<sup>2</sup> value increases or decreases to 1 or -1, this indicates a strong correlation between them. In this study, the correlation of stiffness and yarn parameters was low (Adj. R<sup>2</sup> = 0.231 for flexural rigidity and Adj. R<sup>2</sup> = 0.125 for bending modulus). However, crease recovery, wrinkle recovery and the drape coefficient showed a very good correlation with the studied yarn parameters, with values

of Adj. R<sup>2</sup> = 0.0998, Adj. R<sup>2</sup> = 0.975 and Adj. R<sup>2</sup> = 1, respectively. The rigidity (high drape coefficient) of woven fabric F<sub>1</sub> with a coarser count was higher, while fabrics with 36.4 tex had a higher drape coefficient (rigidity) of 74.8%. This indicated that the rigidity of fabrics increased proportionally with an increase in the yarn count (tex). In the case of a coarser count, the number of fibres is high in the yarn cross section and leads to a high drape coefficient, making them less comfortable during wear. Because of its high drape coefficient, the fabric demonstrated less drapeability and flexibility. It was observed that fabric thickness and weight also affected the drapeability of woven fabrics. Fabrics F<sub>2</sub> and F<sub>3</sub>, with a low thickness and low weight, demonstrated a better drapeability of 66.1% and 72.7%, respectively. A similar concept was also reported in earlier research [14]. Süle reported that woven fabrics with thicker weft yarns and higher weft densities had a higher rigidity [10].

**Wrinkle recovery**

The wrinkle recovery of woven fabrics made from four types of yarns with different properties demonstrated a significant change at an F-value of 30.917 and P-value of 0.000 (see Table 5). As the results show, wrinkle recovery was significantly affected by yarn count, twist, elongation and the tenacity of yarns, respectively. A high level of wrinkling was observed in fabric F<sub>4</sub> made from a low twist, coarser count, and low elongation and tenacity of yarn. This was because when a load was applied on the fabric, it became compressed and deformed. When the applied load was removed, the tendency to recover to the original position was very low because the structure of low twisted yarns tends to be distorted. The individual correlation of yarn parameters was analysed using linear regression. The results showed that yarn elongation and tenacity were highly correlated to wrinkle recovery at Adj. R<sup>2</sup> of 0.928 and Adj. R<sup>2</sup> of 0.924, respectively. Yarn twist also had good correlation at Adj. R<sup>2</sup> of 0.879, but was low for yarn count at Adj. R<sup>2</sup> of 0.596.

Table 4: Multiple linear regression equation of fabric properties

| Properties               | Multiple linear regression equation   | Adj. R <sup>2</sup> |
|--------------------------|---|---------------------|
| Crease recovery in angle | 169.89411 + 0.39761 × X <sub>1</sub> - 0.06034 × X <sub>2</sub> + 2.54839 × X <sub>3</sub> - 8.73989 × X <sub>4</sub> | 0.998               |
| Wrinkle recovery (grade) | -22.94906 + 0.05257 × X <sub>1</sub> + 0.02249 × X <sub>2</sub> + 0.02214 × X <sub>3</sub> + 0.76871 × X <sub>4</sub> | 0.975               |
| Drape coefficient        | 86.12092 + 0.22059 × X <sub>1</sub> - 0.03755 × X <sub>2</sub> + 0.7464 × X <sub>3</sub> + 1.14481 × X <sub>4</sub>   | 1                   |

X<sub>1</sub> = yarn count, X<sub>2</sub> = yarn twist, X<sub>3</sub> = tenacity, X<sub>4</sub> = elongation

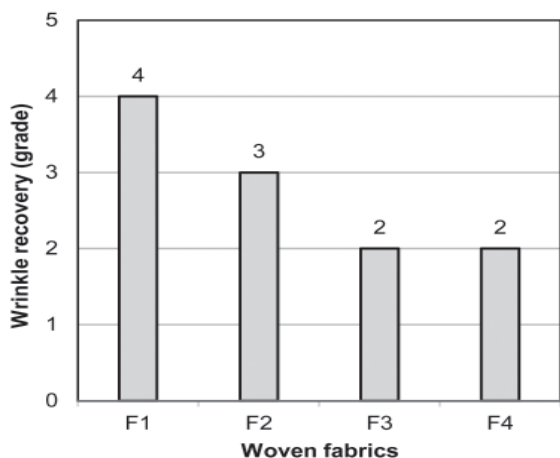


Figure 2: Wrinkle recovery

Figure 2 shows the average grade of wrinkle recovery of developed fabrics. Grade 4 mean very good wrinkle recovery, grade 3 means moderate recovery, grade 2 means low recovery or high wrinkling and grade 1 means poor recovery (formation of extreme wrinkles). The wrinkle recovery grade was thus reduced from fabric F<sub>1</sub>, F<sub>2</sub>, F<sub>3</sub> to F<sub>4</sub>, respectively. This indicated that fabrics F<sub>3</sub> and F<sub>4</sub> with less twist yarns demonstrated poor recovery due to loose yarns in the fabric, which are easily damaged when a load is applied and the tendency of recovery to the original position is lower. However, woven fabric F<sub>1</sub> with a higher yarn twist and fine count demonstrated very good wrinkle recovery. This is because of the higher number of turns per meter, which contributes to resistance to the applied load (undamaged) and easier recovery. This result is confirmed by a previous similar report on the recoverability of knitted fabrics [15] and the bending properties of woven fabrics [13].

Table 5: Analysis of variance of fabric properties

| Properties Fabrics |                | Sum of squares | df | Mean square | F         | Sig.  |
|--------------------|----------------|----------------|----|-------------|-----------|-------|
| Crease recovery    | Between groups | 536.150        | 3  | 178.717     | 3.546     | 0.069 |
|                    | Within groups  | 806.400        | 16 | 50.400      |           |       |
| Wrinkle recovery   | Between groups | 18.550         | 3  | 6.183       | 30.917    | 0.000 |
|                    | Within groups  | 3.200          | 16 | 0.200       |           |       |
| Drape coefficient  | Between groups | 222.942        | 3  | 74.314      | 113.610   | 0.000 |
|                    | Within groups  | 10.466         | 16 | 0.654       |           |       |
| Flexural rigidity  | Between groups | 2202474.000    | 3  | 734158.000  | 38487.969 | 0.057 |
|                    | Within groups  | 305.200        | 16 | 19.075      |           |       |
| Bending modules    | Between groups | 12673882.150   | 3  | 4224627.383 | 25.506    | 0.055 |
|                    | Within groups  | 2650136.400    | 16 | 165633.525  |           |       |

### Crease recovery

As evident in Table 5, the four types of woven fabrics made from yarns with different properties demonstrated no significant change in terms of the statistical value of the F-value of 3.546 and P-value of 0.069. A P-value is  $\geq 0.05$  indicates that there is no difference between samples. As seen in Figure 3, the crease recovery of the F<sub>3</sub> and F<sub>4</sub> samples seems to have greater value. However, that value was statistically insignificant. To predict the crease recovery of fabrics, a multiple regression equation was developed and is presented in Table 4. All factors together had an Adj. R<sup>2</sup> of 0.998. In addition, linear regression was also performed to show the relation of a single factor and response (crease recovery). Yarn twist (Adj. R<sup>2</sup> of 0.991) elongation (Adj. R<sup>2</sup> of 0.973), yarn count (Adj. R<sup>2</sup> of 0.955) and tenacity of yarn (Adj. R<sup>2</sup> of 0.854) were correlated with the crease recovery of fabrics. The Adj. R<sup>2</sup> value was used to analyse individual factors, while the remaining yarn parameters were taken as constants.

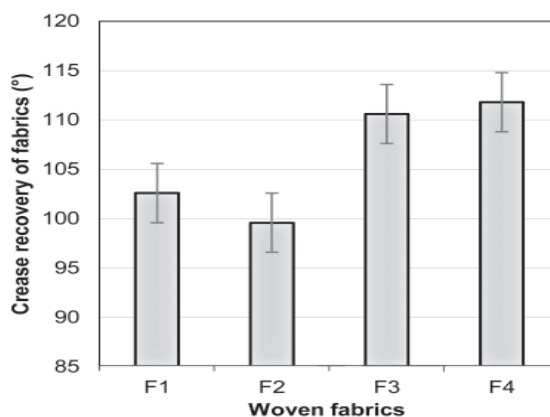


Figure 3: Crease recovery of fabrics



## 4 Conclusion

In this study, four types of woven fabrics were produced from yarns with different properties by varying the weft yarn count, twist, strength and elongation. In all woven fabrics, the same warp yarn properties were applied, with the only variation in weft direction due to different weft yarn properties. The effect of these yarn properties on the psychological comfort of woven fabrics was studied and analysed statistically. To predict the value of crease recovery, wrinkle and the drape coefficient of fabrics, an equation was developed using multiple regression. A statistical analysis showed that yarn twist, count, tenacity and elongation demonstrated insignificant changes at an F-value of 3.546 and Sig-value (P-value) of 0.069 on the crease recovery of fabrics. The stiffness of fabrics, expressed as flexural rigidity and bending modulus, also showed an insignificant difference between the samples at an F-value of 38487.969, Sig-value of 0.057 and an F-value of 25.506, Sig-value of 0.055, respectively. However, the wrinkle properties and drapability of fabrics were significantly affected by yarn twist, count, tenacity and elongation. Woven fabrics  $F_3$  and  $F_4$  with less twist yarns had poor recovery properties due to loose yarns in the fabric, which were easily damaged when loaded, while woven fabric  $F_1$  with a higher yarn twist ( $937.4 \text{ m}^{-1}$ ) and fine count (21.5 tex) had very good wrinkle recovery properties. Due to a coarser yarn count, a high drape coefficient (poor drapability) was observed because the number of fibres is high in the yarn cross section, thus making them less comfortable.

## References

- JEVŠNIK, S., YI, L., HU, J., XIAO, H., XINXING, W., PRIMENTAS, A. Thermal-mechanical sensory properties of hot-air welded textile transmission lines. *Tekstilec*, 2016, **59**(2), 126–131, doi: 10.14502/Tekstilec2016.59.126-131.
- XIAO, H.F., YAN, K.L., JI, B.L. Improvement of anti-wrinkle properties of cotton fabrics treated with additives of neutral salts. *Fibers Polym.*, 2018, **19**(7), 1576–1583, doi: 10.1007/s12221-018-7954-0.
- GONG, R.H., OZGEN, B., SOLEIMANI, M. Modeling of yarn cross-section in plain woven fabric. *Text. Res. J.*, 2009, **79**(11), 1014–1020, doi: 10.1177/0040517508101799.
- PATTANAYAK, A.K., LUXIMON, A., KHANDUAL, A. Prediction of drape profile of cotton woven fabrics using artificial neural network and multiple regression method. *Text. Res. J.*, 2011, **81**(6), 559–566, doi: 10.1177/0040517510380783.
- HU, J.L., CHAN, Y.F. Effect of fabric mechanical properties on drape. *Text. Res. J.*, 1998, **68**(1), 57–64, doi: 10.1177/004051759806800107.
- HASSAN, M.S. Crease recovery properties of cotton fabrics modified by urea resins under the effect of gamma irradiation. *Radiat. Phys. Chem.*, 2009, **78**(5), 333–337, doi: 10.1016/j.radphyschem.2009.01.009.
- STEELE, R. The effect of yarn twist on fabric crease recovery. *Text. Res. J.*, 1956, **26**(10), 739–744, doi: 10.1177/004051755602601001.
- LIU, H., GONG, H., XU, P., DING, X., WU, X., The mechanism of wrinkling of cotton fabric in a front-loading washer : the effect of mechanical action. *Text. Res. J.*, 2019, **89**(18), 3802–3810, doi: 10.1177/0040517518821909.
- AL-GAADI, B., GOKTEPE, F., HALASZ, M.A. A new method in fabric drape measurement and analysis of the drape formation process. *Text. Res. J.*, 2012, **82**(5), 502–512, doi: 10.1177/0040517511420760.
- SÜLE, G. Investigation of bending and drape properties of woven fabrics and the effects of fabric constructional parameters and warp tension on these properties. *Text. Res. J.*, 2012, **82**(8), 810–819, doi: 10.1177/0040517511433152.
- GAUCHER, M.L., KING, M.W., JOHNSTON, B. Predicting the drape coefficient of knitted fabrics. *Text. Res. J.*, 1983, **53**(5), 297–303, doi: 10.1177/004051758305300506.
- RUPPENICKER, G.F., BROWN, J.J. Properties of fabrics produced from three extra long staple cottons. *Text. Res. J.*, 1959, **29**(7), 567–573, doi: 10.1177/004051755902900707.
- ATALIE, D., FEREDÉ, A., ROTICH, G.K. Effect of weft yarn twist level on mechanical and sensorial comfort of 100% woven cotton fabrics. *Fash. Text.*, 2019, **6**(3), 1–12, doi: 10.1186/s40691-018-0169-6.
- OMEROGLU, S., KARACA, E., BECERIR, B. Comparison of bending, drapability and crease recovery behaviors of woven fabrics produced from polyester fibers having different cross-sectional shapes. *Text. Res. J.*, 2010, **80**(12), 1180–1190, doi: 10.1177/0040517509355351.
- ATALIE, D., GIDEON, R. K., FEREDÉ, A., TESINOVA, P., LENFELDOVA, I. Tactile comfort and low-stress mechanical properties of half-bleached knitted fabrics made from cotton yarns with different parameters. *J. Nat. Fibers*, in press, 1–13, doi: 10.1080/15440478.2019.1697989.

Sukhvir Singh<sup>1</sup>, Niranjan Bhowmick<sup>1</sup>, Anand Vaz<sup>2</sup>

<sup>1</sup> Dr. B. R. Ambedkar National Institute of Technology, Department of Textile Technology, Jalandhar-144011, Punjab, India

<sup>2</sup> Dr. B. R. Ambedkar National Institute of Technology, Department of Mechanical Engineering, Jalandhar-144011, Punjab, India

# Theoretical Modelling of Can-spring Mechanism Using Bond Graph

*Teoretično modeliranje mehanizma vzmeti v loncu z uporabo veznega grafa*

Original scientific article/Izvirni znanstveni članek

Received/Prispelo 11-2019 • Accepted/Sprejeto 2-2020

## Abstract

Helical compression springs are extensively used for the combed cotton sliver handling system in spinning preparatory sections in the textile industry. Storage can-spring stiffness decreases with time due to prolonged fatigue loading. It has been found that older storage can-springs of reduced spring stiffness deform non-uniformly during combed sliver deposition and withdrawal. In order to produce consistent quality of an intermediate delicate product like combed sliver, sliver stresses should be monitored meticulously at the time of sliver deposition and withdrawal from storage cans. The present research is an attempt to study the dynamics of the can-spring mechanism used for sliver storage through the bond graph approach. The paper records the first stage of the work, which is concerned with establishing the relationship between spring stiffness and sliver forces. Bond graph modelling of the can-spring mechanism is one of the best-suited approaches to study the present research problem due to its characteristic features.

Keywords: bond graph, combed cotton sliver, can-spring stiffness, storage can

## Izvleček

Vijačne tlačne vzmeti se pogosto uporabljajo v tekstilni industriji pri rokovanju s česanim bombažnim pramenom pri pripravi na predenje. Togost vzmeti v loncih se lahko ob dolgotrajnih obremenitvah sčasoma zmanjša zaradi utrujenosti. Ugotovljeno je bilo, da se starejše vzmeti z zmanjšano togostjo med odlaganjem česanega pramena v lonce in vlečenjem iz loncev neenakomerno deformirajo. Da bi dosegli stalno kakovost tako zelo občutljivega polizdelka, kot je česani pramen, je potrebno skrbno nadzirati napetost pramena v času odlaganja v lonec in vlečenja pramena iz lonca. Raziskava predstavlja primer uporabe veznega grafa za študij dinamike mehanizma vzmeti, ki se uporablja v loncih za shranjevanje pramena. V članku je predstavljena prva faza raziskav, tj. vzpostavljanje odvisnosti med togostjo vzmeti in silami, ki delujejo na pramen. Modeliranje veznega grafa za mehanizem vzmeti v loncu je zaradi njegovih značilnosti eden najprimernejših pristopov k preučevanju predstavljenega raziskovalnega problema.

Ključne besede: vezni graf, česan bombažni pramen, togost vzmeti v loncu, lonec

## 1 Introduction

In the process of making short-staple yarn from fibres in the spinning industry, circular metallic containers called cans, with closed coil helical compression

springs inside, are used for laying down the fibre strand [1–2]. These cans are transported and used to feed the material from one machine to another in the process sequence. The closed coil helical compression spring is an imperative element of a can

Corresponding author/Korespondenčni avtor:

Sukhvir Singh

E-mail: sukh7911@gmail.com

*Tekstilec*, 2020, **63**(1), 68-76

DOI: 10.14502/Tekstilec2020.63.68-76

used for a uniform deposition and withdrawal of sliver to avoid any undue stretching of sliver, which is very weak. Combed cotton drafted sliver is a rope-like structure and most of the fibres are oriented parallel to the sliver axis. Due to very low inter-fibre cohesion, the combed sliver is susceptible to undesirable stretching at the time of sliver deposition at the draw-frame and during sliver withdrawal in subsequent machine processes.

The can-springs used for sliver storage are subjected to repeated reversals of loading over a prolonged period of time resulting in their degradation due to fatigue; consequently, with the passage of time, their stiffness reduces [3–4]. Therefore, an older can-spring will deflect more in comparison to a newer one made of the same material, against the same applied load. In the case of low can-spring stiffness, there are chances of sliver stretching due to its own weight in the unsupported region, as shown in Figure 1. ( $L + L_1$ ) is the sliver length contributing in sliver stretching during processing. In consequence, the combed sliver, roving and resultant combed yarn quality characteristics are found significantly influenced [5–8]. The optimum storage can-spring pressure should be maintained for smoother operations [9].

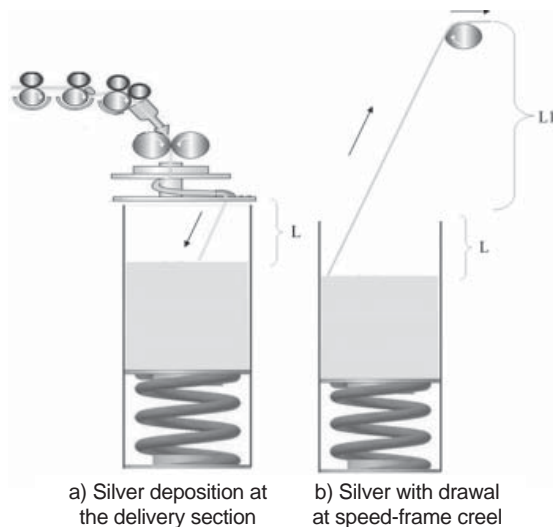


Figure 1: Combed sliver deposition and withdrawal from older storage can: a) sliver deposition at delivery section; b) sliver withdrawal at speed-frame creel

The non-uniform deformation of a can-spring may severely influence sliver quality at the time of deposition and withdrawal of sliver on subsequent machine passages. Modelling the dynamics of the can-spring

sliver deposition/withdrawal system is necessary to develop the understanding of the system and to study the effects of variation of can-spring stiffness, rate of deposition and withdrawal of sliver, etc. on the quality of sliver and yarn. The variation of mass on the top plate due to the deposition or withdrawal of sliver makes the task of developing the model relatively challenging. A review of the literature reveals that modelling such a system with variation in its inertia has not been carried out yet.

## 2 Materials and methods

Combed cotton sliver of 14.22 ktex produced from an extra-long variety MCU-5 from the south Indian states was used for this study. A bond graph model for the can-spring sliver deposition/withdrawal system was developed systematically from first principles. The model explains the transactions of power and understanding of the *cause-effect* relationships between the interacting subsystems. The model facilitates the study of the effect of sliver can-spring stiffness and the rate of sliver deposition or withdrawal on the forces experienced by the combed sliver and top plate through simulations and analysis.

### 2.1 Brief introduction of bond graph technique

A bond graph is a unified approach to the modelling of physical system dynamics. The bond graph approach was originally developed and presented by H. M. Paynter at MIT in 1959. Bond graph is a pictorial or graphical representation of the dynamics of a physical system based on power transactions between component elements and subsystems [10–12]. The cause and effect relationships, or *causality*, are represented elegantly through the *causal strokes* on the bonds. The bond graph approach has numerous advantages over conventional simulation. It provides a graphical representation of the model of dynamics and systematic extraction of system equations algorithmically [11].

In a physical system, only the exchange and conversion of energy in different forms take place. Power ( $P$ ) is the change in energy ( $E$ ) with respect to time ( $t$ ) and can be expressed as:

$$P = \frac{dE}{dt} \quad (1).$$

The power transacted using bonds through the parts of a bond graph can be expressed as the product of effort ( $e$ ) and flow ( $f$ ) variables which are functions of time ( $t$ ):

$$P = e(t) \cdot f(t) \tag{2}$$

2.2 System elements used in bond graph modelling approach

The bond graph elements are categorised as Sources (or active elements), Passive elements, Converters and Junctions [10].

2.2.1 Source elements

In the bond graph approach, there are two kinds of source elements, i.e. a source of effort and a source of flow. The source of effort ( $S_e$ ) imposes an effort on the system irrespective of the flow in return which is decided by the system, as shown in Figure 2a. In the same way, the source of flow ( $S_f$ ) imposes a flow on the system irrespective of the returning effort which is decided by the system, as shown in Figure 2b. The cause and effect relationship in terms of causality remains fixed for source elements, as shown below in Figure 2. For a power bond connecting two subsystems, if effort is decided by the subsystem at one end, the flow will be decided by the subsystem at the other end. Both the effort and flow associated with a bond cannot be determined by the system at any end. The assignment of causality is an algorithmic process. In a bond graph representation, a causal stroke is placed on the bond at the effort receiving end. The other end of the bond automatically receives the flow.

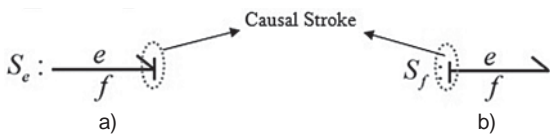


Figure 2: Source elements: a) source of effort; b) source of flow

2.2.2 Junction elements

There are two junction elements which connect different parts in a bond graph. These are the 0-junction and 1-junction. The 0-junction is an effort equalising junction; thus, efforts in all the bonds connected to it remain the same, as depicted in Figure 3a. The flow relationship can be expressed as given below:

$$f_1 = f_2 + f_3 + f_4 \tag{3}$$

In the case of the 1-junction, the flow remains the same in all the bonds connected to it. It acts as a flow equalising junction, as shown in Figure 3b. The efforts summing at this junction can be expressed with equation 4:

$$e_1 = e_2 + e_3 + e_4 \tag{4}$$

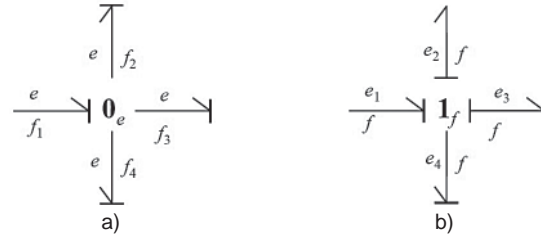


Figure 3: Junction elements: a) 0-junction; b) 1-junction

2.2.3 Compliance element

In natural or integral causality, the C-element receives the flow from the system and gives back effort to the system, as shown in Figure 4. The variable  $q$  associated with the C-element is the generalised displacement.  $K$  represents the stiffness associated with it.

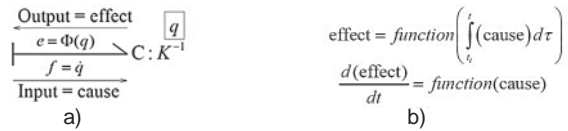


Figure 4: Compliance element: a) representation of output and input; 4b) cause and effect relationship for integrally causalled C-element

The output of the C-element is effort, which is a function of its state variable  $q$ , given as:

$$e(t) = \Phi(q) = K \cdot q = K \int_{t_1}^t q \dot{q} d\tau = K \int_{t_1}^t f(\tau) d\tau \tag{5}$$

2.2.4 Inertia element

In its natural or integral causality, the I-element receives effort from the system and gives back the flow to the system, as shown in Figure 5. The state variable

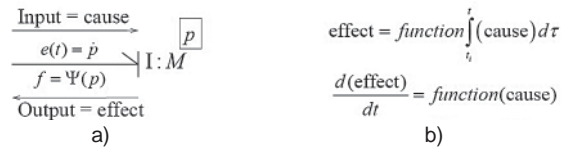


Figure 5: Inertia element: a) representation of output and input; b) cause and effect relationship of I-element



associated with the I-element is the generalised momentum  $p$ .  $M$  is the mass associated with the I-element.

The output of the I-element is flow, which is a function of its state variable  $p$ :

$$f(t) = \Psi(p) = \frac{P}{M} = \frac{1}{M} \int_{t_1}^t \dot{p} d\tau = \frac{1}{M} \int_{t_1}^t e(\tau) d\tau \quad (6).$$

2.2.5 Resistive element

The R-element is used to represent dissipation. It can be causalised in both ways, depending on the invertibility exhibited by the phenomenon. The two types of causality in the case of the R-element are shown in Figure 6.

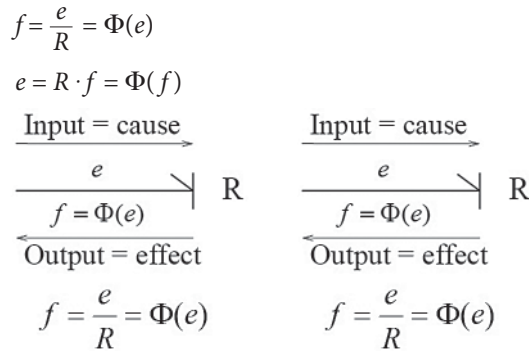


Figure 6: Causality for R-element

2.2.6 Transformer element

TF represents the transformer element in a bond graph. It can relate an input flow to the output flow, and an input effort to the output effort, as shown in Figure 7. This flow to flow or effort to effort relationship is established through the transformation modulus  $\mu$ .

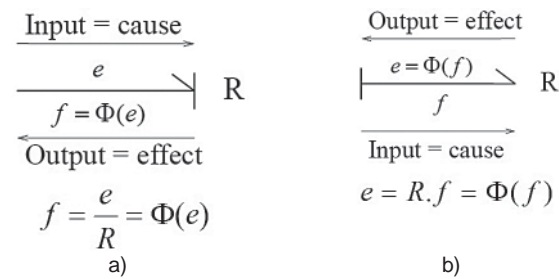


Figure 7: Flow to flow and effort to effort relationship at transformer

2.2.7 Gyrator element

The GY-element represents the gyrator in a bond graph. It relates the input flow to the output effort, and vice-versa. This flow to effort and effort to flow

relationship is established using the modulus  $\mu$ , as shown in Figure 8.

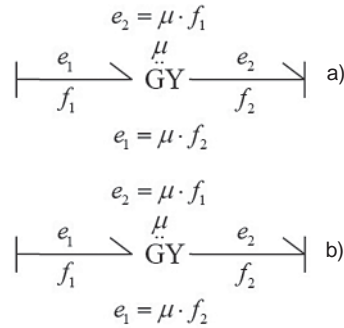


Figure 8: Flow to effort and effort to flow relationship represented by gyrator

Using the power bond and the nine elements of the bond graph, the dynamics of the physical system in any energy domain or a combination of energy domains can be modelled.

2.3 Theoretical modelling of can-spring mechanism using bond graph

An attempt was made to study the dynamics of the can-spring mechanism used at the finisher draw-frame stage for sliver storage. It was presumed that the combed cotton sliver deposited over the top plate has uniform linear density or fineness and that the weight of sliver deposited per second over the top plate remains constant. For an accurate prediction of the can-spring mechanism, real values of independent variables based on industrial experience were considered for evaluation. Also, an in-depth study of sliver quality characteristics was conducted while selecting sliver linear density, inter-fibre cohesion and lengthwise sliver uniformity. The schematic diagram of the can-spring mechanism is shown in Figure 9.

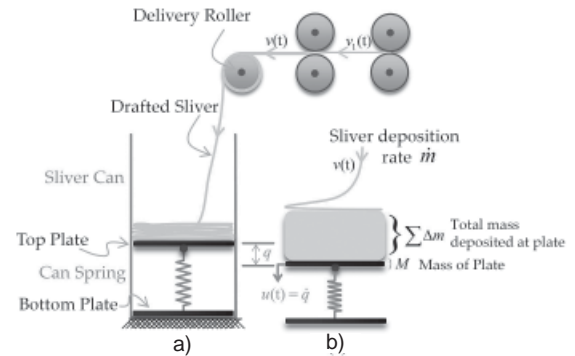


Figure 9: (a) Sliver storage at draw-frame delivery, (b) can-spring mechanisms at draw-frame

The following nomenclature was adopted:

$M$  = initial mass of the top plate before sliver deposition takes place.

$\Delta m$  = increment in mass of deposited sliver on the top plate in the time duration  $\Delta t$ .

$u$  = velocity of the top plate at time  $t$ .

$v$  = flow velocity of sliver at time  $t$ , before depositing on the top plate.

$q(t)$  = deformation in can-spring due to applied load of deposited sliver at time  $t$ .

$g$  = acceleration due to gravity

$(\Sigma\Delta m + \Delta m)$  = total weight on the top plate at an instance due to small increment of combed sliver weight.

The linear momentum of the top plate, along with deposited sliver on it at time  $t$  can be expressed as

$$p(t) = M \cdot u(t) + (\Sigma\Delta m) \cdot u(t) + \Delta m \cdot v(t) \quad (7).$$

Considering that the deposited sliver moves with the same velocity as that of the top plate, after the sliver deposition  $(u + \Delta u)$  is equivalent to  $(v + \Delta v)$ . The flow velocity of sliver  $v(t)$  is equal to  $u(t)$  after the sliver deposition and will follow the velocity of the top plate. The linear momentum of the top plate at time  $(t + \Delta t)$  can be expressed as

$$p(t + \Delta t) = M \cdot (u + \Delta u) + (\Sigma\Delta m) \cdot (u + \Delta u) + \Delta m \cdot (u + \Delta u) \quad (8).$$

On subtracting equation (7) from equation (8), and on dividing both sides by  $\Delta t$ , we get

$$\lim_{\Delta t \rightarrow 0} \left( \frac{p(t + \Delta t) - p(t)}{\Delta t} \right) = \lim_{\Delta t \rightarrow 0} \left( M \frac{\Delta u}{\Delta t} + (\Sigma\Delta m) \frac{\Delta u}{\Delta t} + \frac{\Delta m \Delta u}{\Delta t} \right) + \frac{\Delta m}{\Delta t} u(t) - \frac{\Delta m}{\Delta t} v(t) \quad (9),$$

$$\therefore \lim_{\Delta t \rightarrow 0} \left( \frac{\Delta m \Delta u}{\Delta t} \right) = 0,$$

$$\frac{dp}{dt} = M \frac{du}{dt} + \lim_{\Delta t \rightarrow 0} \left( \frac{(\Sigma\Delta m) \cdot \Delta u}{\Delta t} \cdot \left( \frac{\Delta t}{\Delta t} \right) \right) - \dot{m}v(t) + \dot{m}u(t) \quad (10),$$

$$\frac{dp}{dt} = M \frac{du}{dt} + \left( \int^t \frac{dm}{d\tau} d\tau \right) \cdot \frac{du}{dt} - \dot{m}v(t) + \dot{m}u(t) \quad (11),$$

$$\frac{dp}{dt} = \frac{d}{dt} \left[ \left( M + \int^t \dot{m} \cdot d\tau \right) \cdot u \right] - \dot{m}v(t) \quad (12).$$

The rate of change of the linear momentum of the top plate is caused by the forces acting on it and can also be expressed as given in (13)

$$\frac{dp}{dt} = - \left[ M + \frac{(\Sigma\Delta m + \Delta m) \cdot \Delta t}{\Delta t} \right] \cdot g - F_K(q) - F_R(u) \quad (13),$$

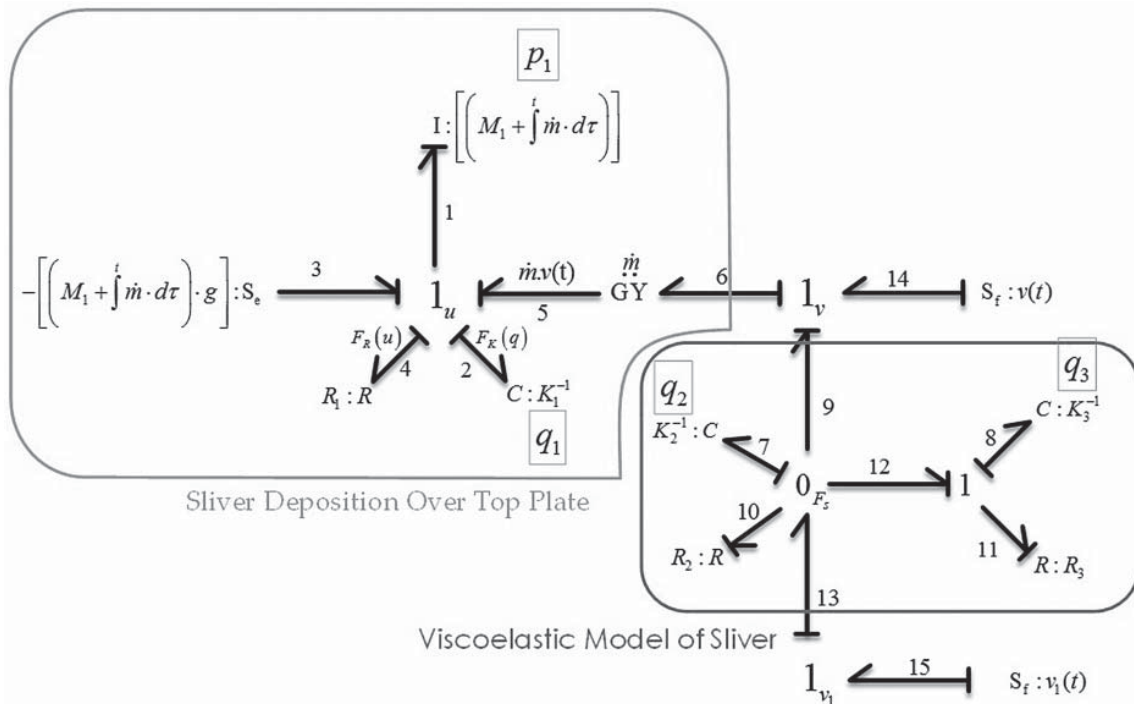


Figure 10: Bond graph model of sliver deposition at draw-frame delivery

where

$$F_K = K \cdot q(t) \quad (14)$$

and

$$F_R = \dot{m} \cdot \dot{q} = \dot{m} \cdot u(t) \quad (15),$$

$$\frac{dp}{dt} = - \left[ M + \int \frac{dm}{dt} \cdot dt \right] \cdot g - F_K(q) - F_R(u) \quad (16).$$

By comparing (16) with (12),

$$\begin{aligned} \frac{d}{dt} &= [(M + \int \dot{m} \cdot dt) \cdot u] = \\ &= - [M + \int \dot{m} \cdot dt] \cdot g - F_K(q) - F_R(u) + \dot{m}v(t) \end{aligned} \quad (17).$$

This represents the formulation of dynamics for the can-spring system.

Equation (17) is represented graphically as outlined in green in the bond graph of Figure 10.

#### 2.4 Viscoelastic representation of sliver

For the purpose of modelling, the Kelvin-Voigt model, the Maxwell model and the standard model were studied initially. The standard model consists of two springs and a dashpot. It is the simplest model that describes both creep and stress relation behaviour of a viscoelastic material. Based on the observed behaviour of the combed sliver, the widely accepted Kelvin representation of the standard model was used. A minor modification was made in the Kelvin representation of the standard model by considering a permanent deformation due to  $R_2$  in the viscous region which appears to be a more suitable representation of the viscoelastic nature of combed sliver, as shown in Figure 11. This viscoelastic behaviour was already modelled in the bond graph of Figure 10.

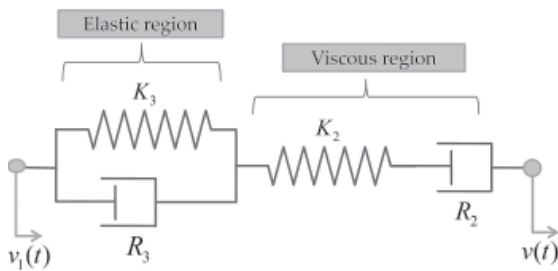


Figure 11: Representation of viscoelastic behaviour of sliver

#### 2.5 Deriving system equations from bond graph

System equations can be derived algorithmically from the bond graph model as a set of the first order differential equations, using the following two equations:

What do the elements give to the system?

$$Se = e_3 = -[(M_1 + \int \dot{m} \cdot dt)] \quad (18)$$

$$f_1 = \frac{P_1}{(M_1 + \int \dot{m} \cdot dt)} \therefore f_1 = f_3 = f_4 = f_2 = f_5 \quad (19)$$

$$e_4 = R_1 \cdot f_4 = R_1 \cdot \frac{P_1}{(M_1 + \int \dot{m} \cdot dt)} \quad (20)$$

$$e_2 = K_1 \cdot q_1 \quad (21)$$

$$S_{f_{14}} = f_{14} = v(t) \quad (22)$$

$$S_{f_{15}} = f_{15} = v_1(t) \quad (23)$$

$$e_8 = K_3 \cdot q_3 \quad (24)$$

$$e_7 = K_2 \cdot q_2 \therefore e_7 = e_9 = e_{10} = e_{13} = e_{12} \quad (25)$$

$$f_{11} = \frac{e_{11}}{R_3} = \frac{e_{12} - e_8}{R_3} = \frac{K_2 \cdot q_2 - K_3 \cdot q_3}{R_3} \quad (26)$$

$$f_{10} = \frac{K_2 \cdot q_2}{R_2} \quad (27)$$

$$e_5 = \dot{m} \cdot f_6 = \dot{m} \cdot f_{14} = \dot{m} \cdot v(t) \quad (28)$$

$$e_6 = \dot{m} \cdot f_5 = \dot{m} \cdot f_1 = \dot{m} \cdot \frac{P_1}{(M_1 + \int \dot{m} \cdot dt)} \quad (29)$$

What do the integrally caused storage elements receive from the system?

$$\dot{p}_1 = e_1 = e_3 + e_5 - e_2 - e_4 \quad (30)$$

$$\begin{aligned} \dot{p}_1 &= -(M_1 + \int \dot{m} \cdot dt) \cdot g + \dot{m} \cdot v(t) - \\ &- K_1 \cdot q_1 - R_1 \cdot \frac{P_1}{(M_1 + \int \dot{m} \cdot dt)} \end{aligned} \quad (31)$$

$$\dot{q}_1 = f_2 = f_1 = \frac{P_1}{[(M_1 + \int \dot{m} \cdot dt)]} \quad (32)$$

$$\begin{aligned} \dot{q}_3 &= f_8 = f_{12} = f_{11} = f_{11} = \\ &= \frac{e_{11}}{R_3} = \frac{e_{12} - e_8}{R_3} = \frac{K_2 \cdot q_2 - K_3 \cdot q_3}{R_3} \end{aligned} \quad (33)$$

$$\dot{q}_2 = f_7 = f_{13} - f_9 - f_{12} - f_{10} \quad (34)$$

$$\dot{q}_2 = f_7 = f_{13} - f_9 - f_{12} - f_{10} = f_{15} - f_{14} - f_{11} - f_{10} \quad (35)$$

$$\dot{q}_2 = v_1(t) - v(t) = \frac{K_2 \cdot q_2 - K_3 \cdot q_3}{R_3} - \frac{K_2 \cdot q_2}{R_2} \quad (36)$$

The first order equations obtained from the bond graph model can be conveniently simulated numerically using solvers for ordinary differential equations provided by any of the available computational programming software such as Matlab, Scilab etc.

### 3 Results and discussion

In order to study the simulated behaviour of the can-spring mechanism, some initial conditions were presumed considering the realistic values of parameters during sliver storage and are mentioned in Table 1. The linear momentum and displacement of the top plate built up with time and direction was considered as negative. This was due to the energy build up in the storage spring through compression, as shown in Figure 12. Similarly, it was observed that after a sudden initial impact of the sliver on the top plate, the velocity of the top plate remained almost

Table 1: Initial conditions/input data used in simulation

| Parameter   | Unit             | Value  |
|---|------------------|--------|
| Initial mass of top plate ( $M$ )                   | kg               | 0.250  |
| Can-spring stiffness ( $K$ )                        | N/m              | 163.3  |
| Flow velocity of sliver at time ( $t$ )             | m/s              | 5      |
| Acceleration due to gravity ( $g$ )                 | m/s <sup>2</sup> | 9.81   |
| Rate of change of mass over top plate ( $\dot{m}$ ) | kg/s             | 0.0255 |
| Time span (s)                                       | s                | 750    |

constant with a small decrease over time. Furthermore, the mass deposited over the top plate increased with time depending on the sliver deposition rate, as shown in Figure 12.

Linear stretching remained due to the viscoelastic part of the model  $q_7$  almost unchanged with the passage of time, and the sliver deformation in the elastic region  $q_8$  experienced a sudden increase within a short time. After that, it remained constant, as shown in Figure 13. Moreover, the force experienced by the can-spring increased with an increase in its deformation, as shown in Figure 14. The latter agrees with the deformation of the can-spring as

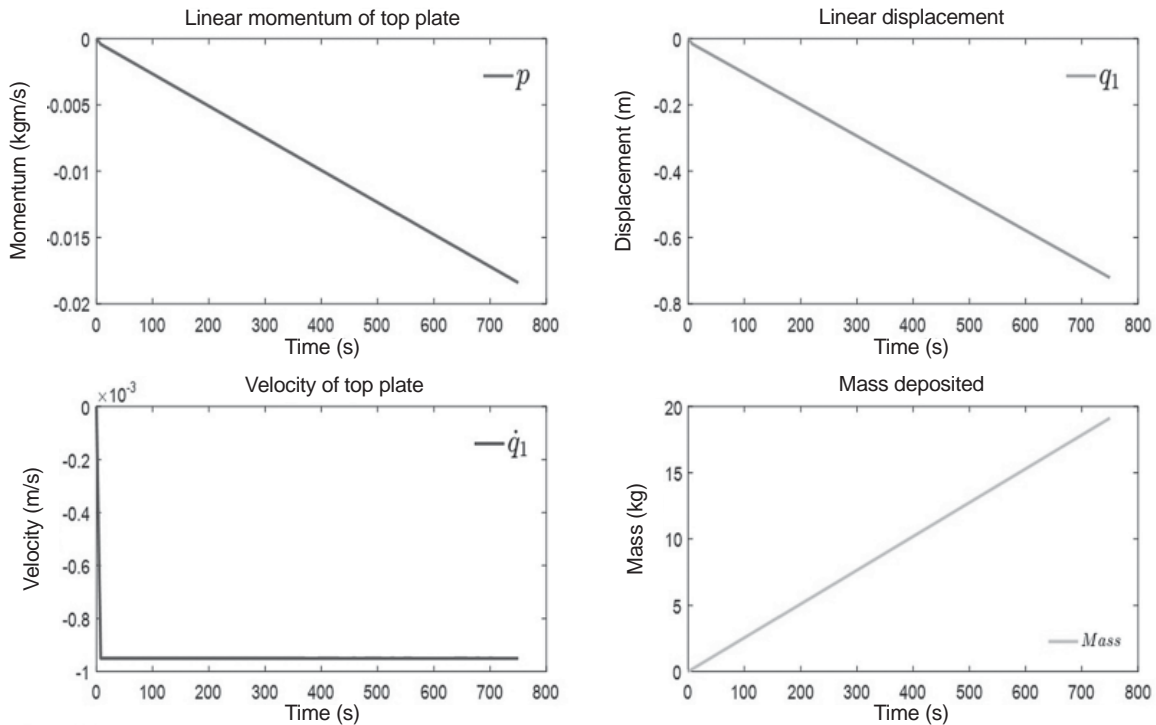


Figure 12: Linear momentum, displacement, velocity and mass responses with time



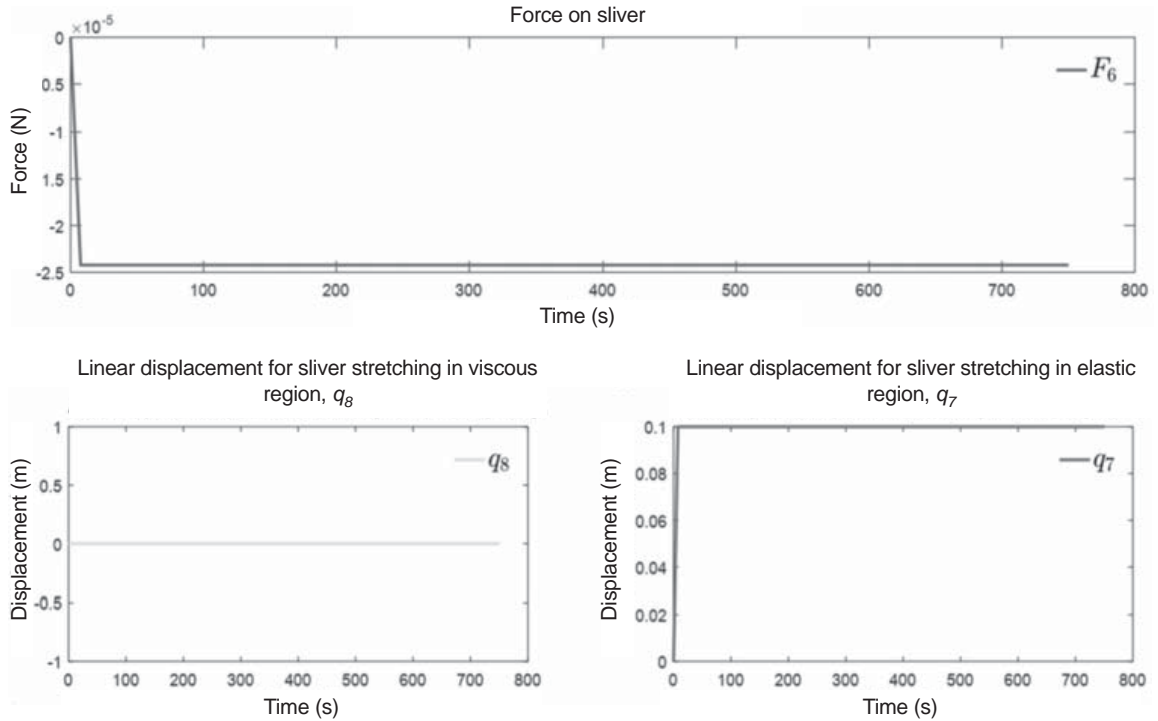


Figure 13: Force on sliver and sliver stretching in viscoelastic region with time

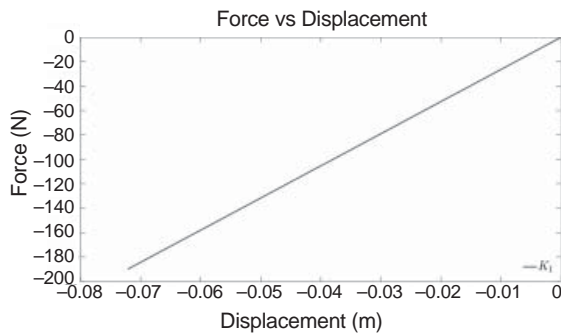


Figure 14: Force experienced by storage spring versus displacement

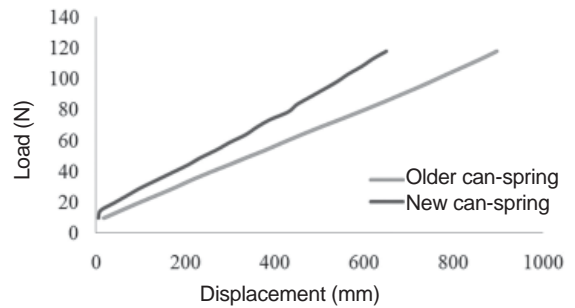


Figure 15: Load versus displacement curve for new and older can-spring

observed from the experimental work shown in Figure 15. It is found that the force on the can-spring built up in the negative direction due to compression of the can-spring since the deposited sliver mass increased with time, as shown in Figure 14. In the case of sliver withdrawal from storage cans, the force experienced by the can-spring gradually reduced due to the decrease in the amount of sliver mass over the top plate with time during sliver withdrawn, as shown in Figure 15.

#### 4 Conclusion

In order to study the dynamics of the can-spring mechanism, a bond graph model was developed. It was established that sliver deformation in the elastic region  $q_8$  experienced a sudden increase within a short time and after that remained constant whereas  $q_7$  remained unchanged. The mass deposited over the top plate increased with the increase in time. It was found out that the linear momentum of the top

plate and its displacement increased with time. The velocity of the top plate showed a peak in short time initially during sliver deposition and remained unchanged afterwards. The force experienced by the storage can-spring also built up as a result of the can-spring compression due to the increase in the deposited sliver mass with time. The force experienced by the sliver showed an initial sudden increment followed by a downfall and then remained unchanged. It can be inferred that a small undesirable deflection can deteriorate the sliver structure and can alter the sliver configuration during drafting operation. It was found that the linear momentum of the top plate increased in the negative direction over time depending on sliver linear density and sliver deposition rate. However, a more rigorous study is required to study the accurate dynamics of such precise systems as the force and stresses experienced by the sliver are too low due to very low inter-fibre cohesion. The current bond graph model can be used for a further investigation for a more accurate prediction based on the dynamics of the can-spring-sliver system behaviour used for combed sliver handling.

## References

1. ARORA, V., SINHA, S. K. Sliver cans – an influencing factor of yarn quality. *Textile Trends*, 1998, **41**, 27–30.
2. RIMTEX Sliver handling systems [online]. RIMTEX Industries [accessed 27 .2. 2020]. Available on World Wide Web: <<https://www.rimtex.com/>>.
3. UGURAL, Ansel C. *Mechanical design of machine components*. 2nd ed. Boca Raton, New York, London : CRC Press, Taylor & Francis, 2016, 652–683.
4. CHESLEY, James C. *Handbook of reliability prediction procedures for mechanical equipment*. West Bethesda, Maryland : NSWC Carderock Division, 2011, 4.1–4.41.
5. SINGH, Sukhvir, BHOWMICK, Niranjana, VAZ, Anand. Effect of finisher draw frame variables on combed cotton yarn quality. *Tekstilec*, 2018, **61**(4), 245–253, doi: 10.14502/Tekstilec2018.61.245–253.
6. SINGH, Sukhvir, BHOWMICK, Niranjana and VAZ, Anand. Influence of can-spring stiffness, deliver rate and sliver coils position on unevenness. *Journal of Textile and Apparel, Technology and Management*, 2019, **11**(1), 1–12.
7. SINGH, Sukhvir, BHOWMICK, Niranjana, VAZ, Anand. Effect of can-storage parameters of finisher draw-frame on combed ring-spun yarn quality. *Research Journal of Textile and Apparel*, 2019, **23**(2), 153–167, doi: 10.1108/RJTA-06-2018-0040.
8. SINGH, Sukhvir, BHOWMICK, Niranjana, VAZ, Anand. Impact of finisher draw-frame storage variables on combed yarn quality. *Tekstilec*, 2019, **62**(2), 110–123, doi: 10.14502/Tekstilec2019.62.110-123.
9. GHOSH, A., MAJUMDAR, A. Process control in drawing, combing and speedframe operations. In *Process Control in Textile Manufacturing*. 1st ed. Edited by V. Kothari, R. Alagirusamy, A. Das and A. Majumdar. New Delhi : Woodhead Publishing, 2013, 158–190.
10. KARNOPP, D. C., MARGOLIS, D. L., ROSENBERG, R. C. *System dynamics, modeling and simulation of mechatronic systems*. New York : John Wiley & Sons, 2000.
11. MUKHERJEE, A., KARMAKAR, R., SAMANTARAY, A. K. *Bond graph in modeling, simulation and fault identification*. 2<sup>nd</sup> ed. Boca Raton : CRC Press, 2006.
12. BORUTZKY, W. *Bond graphs : a methodology for modelling multidisciplinary dynamic systems*. San Diego : SCS Publishing House, 2004.

# SHORT INSTRUCTIONS FOR AUTHORS OF SCIENTIFIC ARTICLES

## Scientific articles categories:

- **Original scientific article** is the first publication of original research results in such a form that the research can be repeated and conclusions verified. Scientific information must be demonstrated in such a way that the results are obtained with the same accuracy or within the limits of experimental errors as stated by the author, and that the accuracy of analyses the results are based on can be verified. An original scientific article is designed according to the IMRAD scheme (Introduction, Methods, Results and Discussion) for experimental research or in a descriptive way for descriptive scientific fields, where observations are given in a simple chronological order.
- **Review article** presents an overview of most recent works in a specific field with the purpose of summarizing, analysing, evaluating or synthesizing information that has already been published. This type of article brings new syntheses, new ideas and theories, and even new scientific examples. No scheme is prescribed for review article.
- **Short scientific article** is original scientific article where some elements of the IMRAD scheme have been omitted. It is a short report about finished original scientific work or work which is still in progress. Letters to the editor of scientific journals and short scientific notes are included in this category as well.

**Language:** The manuscript of submitted articles should be written in UK English and it is the authors responsibility to ensure the quality of the language.

**Manuscript length:** The manuscript should not exceed 30,000 characters without spacing.

**Article submission:** The texts should be submitted only in their electronic form in the format \*.doc (or \*.docx) and in the format \*.pdf (made in the computer program Adobe Acrobat) to the address: [tekstilec@a.ntf.uni-lj.si](mailto:tekstilec@a.ntf.uni-lj.si). The name of the document should contain the date (year-month-day) and the surname of the corresponding author, e.g. 20140125Novak.docx. The articles proposed for a review need to have their figures and tables included

in the text. The article can also be submitted through a cloud-based file transfer service, e.g. "WeTransfer" ([www.wetransfer.com](http://www.wetransfer.com)).

**Publication requirements:** All submitted articles are professionally, terminologically and editorially reviewed in accordance with the general professional and journalistic standards of the journal Tekstilec. Articles are reviewed by one or more reviewers and are accepted for publication on the basis of a positive review. If reviewers are not unanimous, the editorial board decides on further proceedings. The authors can propose to the editorial board the names of reviewers, whereas the editorial board then accepts or rejects the proposal. The reviewers' comments are sent to authors for them to complete and correct their manuscripts. The author is held fully responsible for the content of their work. Before the author sends their work for publication, they need to settle the issue on the content publication in line with the rules of the business or institution, respectively, they work at. When submitting the article, the authors have to fill in and sign the Copyright Statement ([www.tekstilec.si](http://www.tekstilec.si)), and send a copy to the editors by e-mail. They should keep the original for their own personal reference. The author commits themselves in the Copyright Statement that the manuscript they are submitting for publication in Tekstilec was not sent to any other journal for publication. When the work is going to be published depends on whether the manuscript meets the publication requirements and on the time reference the author is going to return the required changes or corrections to the editors.

**Copyright corrections:** The editors are going to send computer printouts for proofreading and correcting. It is the author's responsibility to proofread the article and send corrections as soon as possible. However, no greater changes or amendments to the text are allowed at this point.

**Colour print:** Colour print is performed only when this is necessary from the viewpoint of information comprehension, and upon agreement with the author and the editorial board.

**More information on:** [www.tekstilec.si](http://www.tekstilec.si)

